AD-770 089

AN INVESTIGATION OF THE CORROSION CHARACTERISTICS OF DENTAL ALLOYS

Terry J. Rickard

Air Force Institute of Technology
Wright-Patterson Air Force Base, Ohio

June 1971

DISTRIBUTED BY:

NTIS

National Technical Information Service
U. S. DEPARTMENT OF COMMERCE
5285 Port Royal Road, Springfield Va. 22151

Unclassified
Security Classification

AD 720089

DOCUMENT CONTROL DATA - R & D

(Security classification of title, body of abstract and indexing annotation must be entered when the overall report is classified)

1. ORIGINATING ACTIVITY (Corporate author) Air Force Institute of Technology Wright-Patterson AFB, Ohio 45433	2a. REPORT SECURITY CLASSIFICATION Unclassified 2b. GROUP

3. REPORT TITLE

An Investigation of the Corrosion Characteristics of Dental Alloys

4. DESCRIPTIVE NOTES (Type of report and inclusive dates)

AFIT Thesis

5. AUTHOR(S) (First name, middle initial, last name)

Terry J. Rickard
Captain USAF

6. REPORT DATE	7a. TOTAL NO. OF PAGES	7b. NO. OF REFS
June 1971	~~91~~ 106	24

8a. CONTRACT OR GRANT NO.	9a. ORIGINATOR'S REPORT NUMBER(S)
b. PROJECT NO.	GAW/MC/71-11
c.	9b. OTHER REPORT NO(S) (Any other numbers that may be assigned this report)
d.	

10. DISTRIBUTION STATEMENT

Approved for public release, distribution unlimited.

11. SUPPLEMENTARY NOTES	12. SPONSORING MILITARY ACTIVITY
Approved for public release; IAW AFR 190-17 JERRY C. HIX, Captain, USAF Director of Information	Air Force Institute of Technology Wright-Patterson Air Force Base, Ohio

13. ABSTRACT

Cathodic linear polarization behavior of six commercially-available dental alloys was investigated galvanostatically in an aerated synthetic saliva electrolyte, at 22±1°C. Each alloy was investigated with three different surface finishes; obtained by grinding with 4/0 emery paper, polishing with dental pumice, and polishing with dental tin-oxide powder. Complete potentiostatic polarization tests were also conducted and anodic Tafel slopes were obtained for these six dental alloys. Due to the effects of concentration polarization, cathodic Tafel slopes were not obtained.

Corrosion rate calculations were performed on an IBM 1620 digital computer with a Fortran program written specifically for linear-polarization studies.

In general, the corrosion rates of all of the dental alloys were very low; ranging from approximately 4 to 200 microns/yr. The gold alloys had the lowest corrosion rates while the amalgams had the highest. All corrosion rates reached steady-state values within 48 to 96 hours. Corrosion rates of each of the alloys decreased as the smoothness of the surface finish increased; the corrosion rates of the amalgams showed the greatest dependence on surface finish.

Reproduced by
NATIONAL TECHNICAL
INFORMATION SERVICE
U S Department of Commerce
Springfield VA 22151

DD FORM 1 NOV 68 1473

12

Unclassified
Security Classification

14. KEY WORDS	LINK A		LINK B		LINK C	
	ROLE	WT	ROLE	WT	ROLE	WT
Corrosion						
Linear-Polarization Technique						
Polarization Resistance						
Dental Alloys						

GAW/MC/71-11

AN INVESTIGATION OF THE CORROSION CHARACTERISTICS OF DENTAL ALLOYS

THESIS

GAW/MC/71-11 Terry J. Rickard
Captain USAF

DDC
RECEIVED
NOV 27 1973
B

Approved for public release; distribution unlimited

GAW/MC/71-11

AN INVESTIGATION OF THE CORROSION CHARACTERISTICS OF DENTAL ALLOYS

THESIS

Presented to the Faculty of the School of Engineering
of the Air Force Institute of Technology
Air University
in Partial Fulfillment of the
Requirements for the Degree of
Master of Science

by

Terry J. Rickard
CAPT USAF

Graduate Aerospace Engineering (Air Weapons)

Approved for public release; distribution unlimited

Preface

Since there are numerous types of relatively noble alloys used in the dental profession, the polarization-resistance method with its many advantages was chosen for this corrosion investigation. With this method, I was able to acquire more data and subsequent results in the time alloted than with other methods that are available.

The theoretical aspects of polarization as applied to corrosion are not given extensive treatment in this thesis. The theory has been discussed elsewhere and the bibliography of this thesis can serve as a guide to the more theory-oriented reader. The experimental apparatus, procedure, and interpretation of polarization data has been given the most emphasis in this study.

Another advantage of choosing the polarization-resistance method was that I had available for consultation one of the most knowledgable men in galvanostatic and potentiostatic polarization research. I refer to Dr. James R. Myers, my thesis advisor, to whom I am deeply indebted for his timely advice and encouragement in this investigation. I would also like to thank Mr. S. G. Lee and Capt. W. B. Crow for their patience and guidance throughout this study.

Terry J. Rickard

Contents

		Page
Preface		ii
List of Figures		v
List of Tables		ix
Abstract		x
I.	Introduction	1
	Purpose	1
	Background and Theory	3
	Obtaining Quantitative Corrosion Data	6
II.	Experimental Apparatus	13
	Electrical Circuitry	13
	Polarization Test Cell	16
	Salt Bridge	16
	Reference Electrode	18
	Auxiliary Electrode	19
	Specimen Holder	19
	Aerator Assembly	19
	Electrolyte	21
	Specimens	22
	Test Apparatus for Potentiostatic Polarization Studies	22
III.	Experimental Procedure	25
	Test Cell Preparation	25
	Specimen Activation	27
	Open-Circuit Potential	27
	Galvanostatic Polarization Tests	28
	Potentiostatic Polarization Studies	29
IV.	Results and Discussion	31
	Criteria Observed	31
	Metallurgy of Materials Tested	31
	Silver-Tin Amalgam	31
	Copper Amalgam	32
	Gold-Silver-Copper Alloy	33
	Gold-Palladium-Silver Alloy	34
	Nickel-Chromium-Molybdenum Alloy	34
	Nickel-Chromium-Palladium-Cobalt Alloy	34
	Open-Circuit Corrosion Potentials	35

Page

Linear-Polarization Curves 37
Corrosion Rates 60
Comparison of Results 64
Anodic and Cathodic Polarization Curves . . 65

V. Conclusions and Recommendations 81

Conclusions 81
Recommendations 82

Bibliography 84

Appendix A: Development of Computer Program for Determining Corrosion Rates from Linear-Polarization Data 86

Vita 91

List of Figures

Figure		Page
1.	Galvanic Cell with Reference Electrode	4
2.	Combined Polarization Curve. Activation and Concentration Polarization	5
3.	Typical Anodic Polarization Curve of an Active-Passive Metal	7
4.	Generalized Anodic and Cathodic Polarization Curve	9
5.	Linear Polarization Curve	10
6.	Electrical Circuitry Used for Galvanostatic Determination of Polarization Curves	14
7.	Electrical Circuitry of π - Filter	15
8.	Galvanostatic Polarization Test Equipment . . .	15
9.	Polarization Test Cell	17
10.	Working Electrode Assembly	20
11.	Potentiostatic Polarization Test Apparatus . .	24
12.	Phase Diagram of the Ag-Sn Alloys	33
13.	Phase Diagram of the Au-Cu Alloys	35
14.	Ternary Diagram of Au-Pd-Hg Alloy Showing Vickers Hardness as Function of Composition . .	36
15.	Effect of Time on the Galvanostatic Cathodic Linear-Polarization Curves for Au-13Ag-9Cu Dental Alloy in Aerated Synthetic Saliva at 22°C. Surface Finished with 4/0 Emery Paper .	39
16.	Effect of Time on the Galvanostatic Cathodic Linear-Polarization Curves for Au-13Ag-9Cu Dental Alloy in Aerated Synthetic Saliva at 22°C. Surface Finished with Dental Pumice . .	40
17.	Effect of Time on the Galvanostatic Cathodic Linear-Polarization Curves for Au-13Ag-9Cu Dental Alloy in Aerated Synthetic Saliva at 22°C. Surface Finished with Dental Tin-Oxide .	41

Figure		Page
18.	Effect of Time on the Galvanostatic Cathodic Linear-Polarization Curves for Au-5Pd-1Ag Dental Alloy in Aerated Synthetic Saliva at 22°C. Surface finished with 4/0 Emery Paper .	42
19.	Effect of Time on the Galvanostatic Cathodic Linear-Polarization Curves for Au-5Pd-1Ag Dental Alloy in Aerated Synthetic Saliva at 22°C. Surface Finished with Dental Pumice . .	43
20.	Effect of Time on the Galvanostatic Cathodic Linear-Polarization Curves for Au-5Pd-1Ag Dental Alloy in Aerated Synthetic Saliva at 22°C. Surface Finished with Dental Tin-Oxide .	44
21.	Effect of Time on the Galvanostatic Cathodic Linear-Polarization Curves for Ni-16.5Cr-2.5Mo Dental Alloy in Aerated Synthetic Saliva at 22°C. Surface Finished with 4/0 Emery Paper .	45
22.	Effect of Time on the Galvanostatic Cathodic Linear-Polarization Curves for Ni-16.5Cr-2.5Mo Dental Alloy in Aerated Synthetic Saliva at 22°C. Surface Finished with Dental Pumice . .	46
23.	Effect of Time on the Galvanostatic Cathodic Linear-Polarization Curves for Ni-16.5Cr-2.5Mo Dental Alloy in Aerated Synthetic Saliva at 22°C. Surface Finished with Dental Tin-Oxide .	47
24.	Effect of Time on the Galvanostatic Cathodic Linear-Polarization Curves for Hg-30Ag-12Sn-2Zn Dental Alloy in Aerated Synthetic Saliva at 22°C. Surface Finished with 4/0 Emery Paper .	48
25.	Effect of Time on the Galvanostatic Cathodic Linear-Polarization Curves for Hg-30Ag-12Sn-2Zn Dental Alloy in Aerated Synthetic Saliva at 22°C. Surface Finished with Dental Pumice . .	49
26.	Effect of Time on the Galvanostatic Cathodic Linear-Polarization Curves for Hg-30Ag-12Sn-2Zn Dental Alloy in Aerated Synthetic Saliva at 22°C. Surface Finished with Dental Tin-Oxide .	50
27.	Effect of Time on the Galvanostatic Cathodic Linear-Polarization Curves for Hg-34.5Cu Dental Alloy in Aerated Synthetic Saliva at 22°C. Surface Finished with 4/0 Emery Paper .	51

Figure		Page
28.	Effect of Time on the Galvanostatic Cathodic Linear-Polarization Curves for Hg-34.5Cu Dental Alloy in Aerated Synthetic Saliva at 22°C. Surface Finished with Dental Pumice . .	52
29.	Effect of Time on the Galvanostatic Cathodic Linear-Polarization Curves for Hg-34.5Cu Dental Alloy in Aerated Synthetic Saliva at 22°C. Surface Finished with Dental Tin-Oxide .	53
30.	Effect of Time on the Galvanostatic Cathodic Linear-Polarization Curves for Ni-24.5Cr-24.5Pd-10.5Co Dental Alloy in Aerated Synthetic Saliva at 22°C. Surface Finished with 4/0 Emery Paper	54
31.	Effect of Time on the Galvanostatic Cathodic Linear-Polarization Curves for Ni-24.5Cr-24.5Pd-10.5Co Dental Alloy in Aerated Synthetic Saliva at 22°C. Surface Finished with Dental Pumice .	55
32.	Effect of Time on the Galvanostatic Cathodic Linear-Polarization Curves for Ni-24.5Cr-24.5Pd-10.5Co Dental Alloy in Aerated Synthetic Saliva at 22°C. Surface Finished with Dental Tin-Oxide	56
33.	Limits Within Which the Relation Between Corrosion-Current Density and Polarization Resistance Applies for Most Real Systems . . .	65
34.	Potentiostatic Anodic Polarization Curve for Au-13Ag-9Cu Dental Alloy in Aerated Synthetic Saliva at 22°C	66
35.	Potentiostatic Anodic Polarization Curve for Au-5Pd-1Ag Dental Alloy in Aerated Synthetic Saliva at 22°C	67
36.	Potentiostatic Anodic Polarization Curve for Ni-16.5Cr-2.5Mo Dental Alloy in Aerated Synthetic Saliva at 22°C	68
37.	Potentiostatic Anodic Polarization Curve for Hg-30Ag-12Sn-2Zn Dental Alloy in Aerated Synthetic Saliva at 22°C	69
38.	Potentiostatic Anodic Polarization Curve for Hg-34.5Cu Dental Alloy in Aerated Synthetic Saliva at 22°C	70

Figure | Page

39. Potentiostatic Anodic Polarization Curve for Ni-24.5Cr-24.5Pd-10.5Co Dental Alloy in Aerated Synthetic Saliva at 22°C 71

40. Potentiostatic Cathodic Polarization Curve for Au-13Ag-9Cu Dental Alloy in Aerated Synthetic Saliva at 22°C 72

41. Potentiostatic Cathodic Polarization Curve for Au-5Pd-1Ag Dental Alloy in Aerated Synthetic Saliva at 22°C 73

42. Potentiostatic Cathodic Polarization Curve for Ni-16.5Cr-2.5Mo Dental Alloy in Aerated Synthetic Saliva at 22°C 74

43. Potentiostatic Cathodic Polarization Curve for Hg-30Ag-12Sn-2Zn Dental Alloy in Aerated Synthetic Saliva at 22°C 75

44. Potentiostatic Cathodic Polarization Curve for Hg-34.5Cu Dental Alloy in Aerated Synthetic Saliva at 22°C 76

45. Potentiostatic Cathodic Polarization Curve for Ni-24.5Cr-24.5Pd-10.5Co Dental Alloy in Aerated Synthetic Saliva at 22°C 77

A-1 Computer Program for Calculating Corrosion Rates from Linear-Polarization Data 89

List of Tables

Table		Page
I.	Composition of Synthetic Saliva Solution	21
II.	Dental Alloy Specimen Compositions	23
III.	Effect of Time on Open-Circuit Corrosion Potentials (Volt vs. S.C.E.) for Dental Alloys in Aerated Synthetic Saliva	38
IV.	Effect of Time and Surface Finish on Corrosion-Current Densities (ma/cm^2) for Dental Alloys in Aerated Synthetic Saliva at 22°C	57
V.	Effect of Time and Surface Finish on Corrosion Rates (microns per year) for Dental Alloys in Aerated Synthetic Saliva at 22°C	61
VI.	Tafel Slopes for Anodic Dissolution of Six Dental Alloys in Aerated Synthetic Saliva at 22°C	79

Abstract

Cathodic linear-polarization behavior of six commercially-available dental alloys was investigated galvanostatically in an aerated synthetic saliva electrolyte. Polarization measurements were obtained within 15 millivolts of the open-circuit potential every 24 hours until steady-state polarizaion resistance was achieved. Each alloy was investigated with three different surface finishes; obtained by grinding with 4/0 emery paper, polishing with dental pumice, and polishing with dental tin-oxide powder. All measurements were obtained at 22 $\pm$ 1°C (72°F)with two of the alloys additionally tested at 98.6°F (human body temperature) to determine the effect of this more elevated temperature. This small increase in temperature seemed to have a negligible effect on the corrosion rates of the alloys tested.

Complete potentiostatic polarization tests were also conducted and anodic Tafel slopes were obtained for these six dental alloys. Due to the effects of concentration polarization, cathodic Tafel slopes were not obtained.

Corrosion rates were determined from the linear-polarization data and the Stern-Geary relationship for corrosion processes controlled by concentration polarization. The actual corrosion rate calculations were performed on an IBM 1620 digital computer with a computer program written specifically for linear-polarization studies.

In general, the corrosion rates of all of the dental alloys were low; the gold alloys having the lowest corrosion rates and the amalgams having the highest. All corrosion rates reached steady-state values within 48 to 96 hours.

The corrosion rates of each of the alloys decreased as the smoothness of the surface finish increased. The alloys whose corrosion rates showed the greatest dependence on surface finish were the amalgams. Corrosion rates of the Ag-Sn amalgam by the linear-polarization technique compared well with rates obtained by other investigators using the Tafel slope-extrapolation technique.

GAW/MC/71-11

AN INVESTIGATION OF THE CORROSION CHARACTERISTICS OF DENTAL ALLOYS

I. Introduction

Purpose

Clinical evidence has shown that corrosion is one of the four most common causes of failure in dental amalgam restorations. The warm, humid environment of the mouth coupled with the rapidly fluctuating pH of saliva and large biting stresses produce conditions conducive to corrosion. This corrosion is particularly evident in amalgams and dental alloys containing less than 75% precious metal[1]. In addition to general deterioration, corrosion of dental restorations can be affected by surface and stress conditions. At crevices in the tooth-restoration interface, differences in oxygen concentration exist. A corrosion cell is produced with surface areas containing the least oxygen being preferentially attacked. When the surface stress is inhomogeneous; a galvanic cell composed of stressed metal, saliva, and unstressed metal is formed with the stressed area being attacked preferentially[1,12].

With the advent of future space flights of long duration and internment of aircrew members in enemy prisons, a requirement for knowledge of the corrosion resistance characteristics of available dental alloys has become

necessary. Proper selection of materials can minimize the probability of premature failures of restorations at times when dental care is not readily available.

The need to study the corrosion characteristics of dental alloys in a limited amount of time dictated that the polarization resistance method would be the most feasible testing method. Hence, the purpose of this investigation was to obtain galvanostatic polarization data within ± 15 mv of the corrosion potential of six commonly-used dental alloys. The electrolyte for this investigation was aerated synthetic saliva at 22°C[2,3]. The linear-polarization data and the Stern-Geary[4] relationship were used to determine the general corrosion rates of the alloys investigated. Concurrently, the corrosion rates of the alloys with surface finishes obtained by grinding with 4/0 emery paper, polishing with dental pumice, and polishing with dental tin-oxide were investigated. It was considered beyond the scope of this investigation to study the effects of localized attack (ie, galvanic corrosion, crevice corrosion) on the deterioration of dental restorations.

Although not an initial objective of this study, complete potentiostatic anodic and cathodic polarization curves were obtained for the six alloys. In addition, the effect of raising the electrolyte temperature to human body temperature was investigated on the most noble and the most active of the six alloys.

Background and Theory

Corrosion may be defined as the destruction or deterioration of a material because of a reaction with its environment[5]. Since this reaction involves a chemical change which produces an electrical current, the reaction is an electrochemical process. The extent of this electrochemical change, measured in volts, is called polarization [6,7]. To further clarify the concept of polarization, consider a galvanic cell with reference electrode as shown in Figure 1. There is a measureable potential difference, in volts, between each of these two electrodes and the reference electrode when the circuit is open. The open-circuit potential of the metal being investigated (Fe in this case) with respect to the reference electrode is designated E_{corr}. If the circuit is closed, current flows and the potential changes from the original E_{corr}. The amount that the potential of the metal electrode changes from the original E_{corr} is referred to as the overvoltage, η. This overvoltage is a measure of the polarization of the electrode. In other words, polarization can be defined as the displacement of the electrode potential from the original E_{corr} resulting from a net current flow[5]. If an external current were applied to the cell such that it opposed the normal closed-circuit current, the direction of the net current will determine which metal electrode will gain or lose electrons. If a metal loses electrons, by definition it is called an anode. If the impressed current causes the metal being

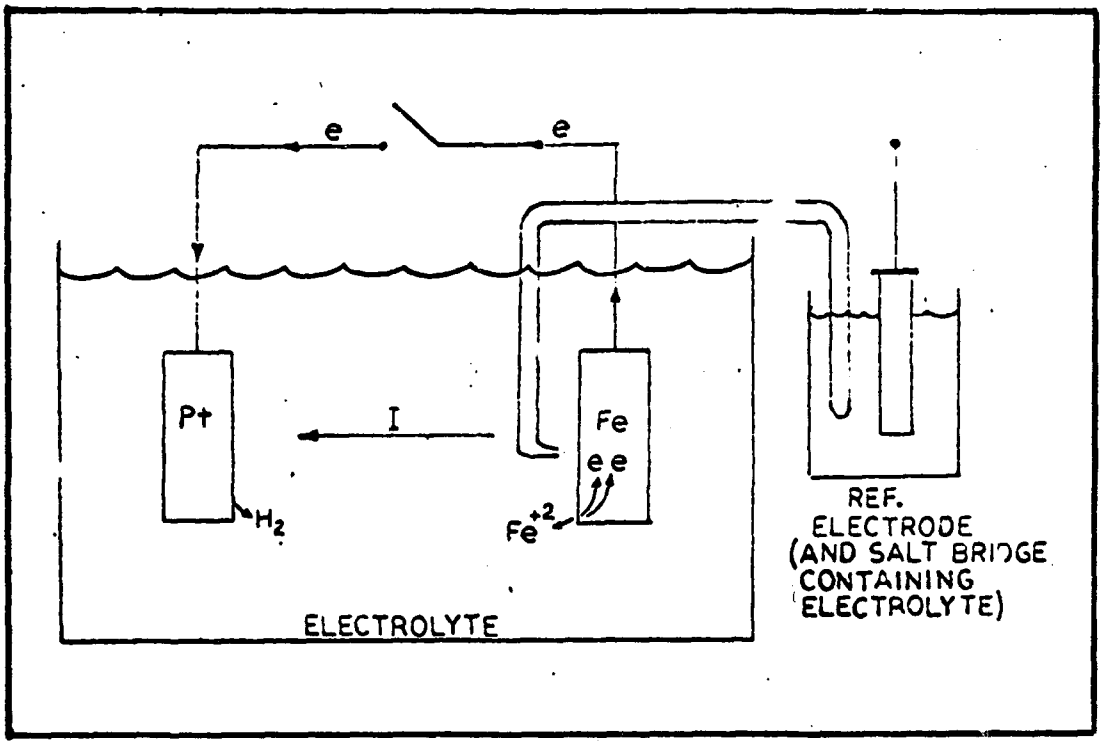

Figure 1. Galvanic Cell
with Reference Electrode

investigated to gain electrons, the metal becomes the cathode and its overvoltage is a measure of its cathodic polarization[8].

Each type of polarization, anodic and cathodic, can be further subdivided and classified depending on the controlling phenomenon of the electrochemical process near the electrode surface. Activation polarization refers to an electrochemical reaction which is controlled by the slowest step in the reaction sequence at the metal-electrolyte interface[5]. For example, in Figure 1 the slowest step at the platinum electrode might be the formation of hydrogen molecules from monatomic hydrogen.

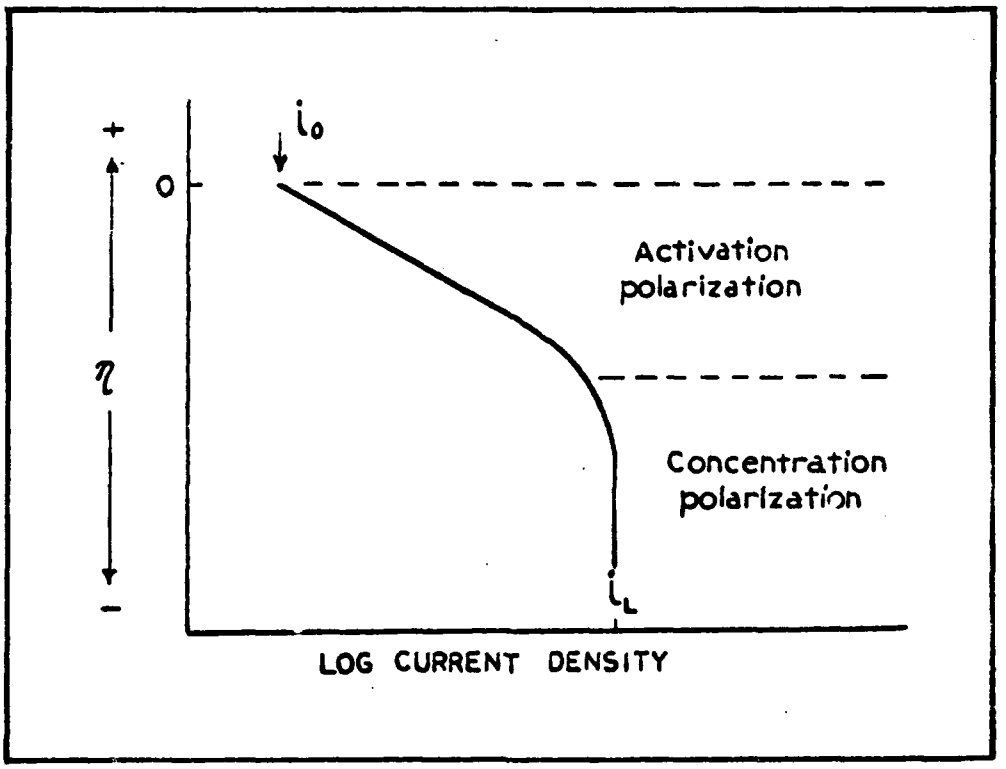

Figure 2. Combined Polarization Curve. Activation and Concentration Polarization (Ref 5)

Activation polarization results in a sloping straight line on a polarization curve as shown in Figure 2. Concentration polarization refers to electrochemical reactions which are controlled by the diffusion of ions in the electrolyte near the metal-electrolyte interface[5]. Cathodic polarization occurs when one of the reactants is consumed at the electrode faster than it can diffuse through the electrolyte to the electrode[8,9]; similarily, polarization at the anode can occur when the diffusion of the metal ions away from the metal surface is the rate-controlling process. Concentration polarization does not have an appreciable affect on metal dissolution until high current densities are present. The

current density where concentration polarization begins to limit further applied current is called the limiting applied diffusion current density, i_L [8]. The effect of concentration polarization and i_L on a polarization curve is shown in Figure 2. Concentration polarization usually is the controlling factor when the concentration of reducible species is small (e.g., dilute acids, aerated basic solutions) while activation polarization generally predominates in concentrated acids[5].

Obtaining Quantitative Corrosion Data Electrochemically

The shortcomings of the conventional weight-loss technique promoted the early attempts to relate electrochemical properties of metals to their corrosion rates. The weight-loss technique involves exposing a specimen to a corrosive environment for a given period of time and then measuring the specimen weight loss. In addition to requiring considerable time, the technique gives only an average corrosion rate. This information is not always useful if the corrosion rate varies with time.

To obtain quantitative corrosion data from electrochemical properties of a metal, a current must be forced to flow through the metal while the metal is in a particular corrosive environment. This involves polarizing the specimen, as described earlier, so as to obtain polarization data that will yield a corrosion current. There are two basic methods for obtaining these polarization data.

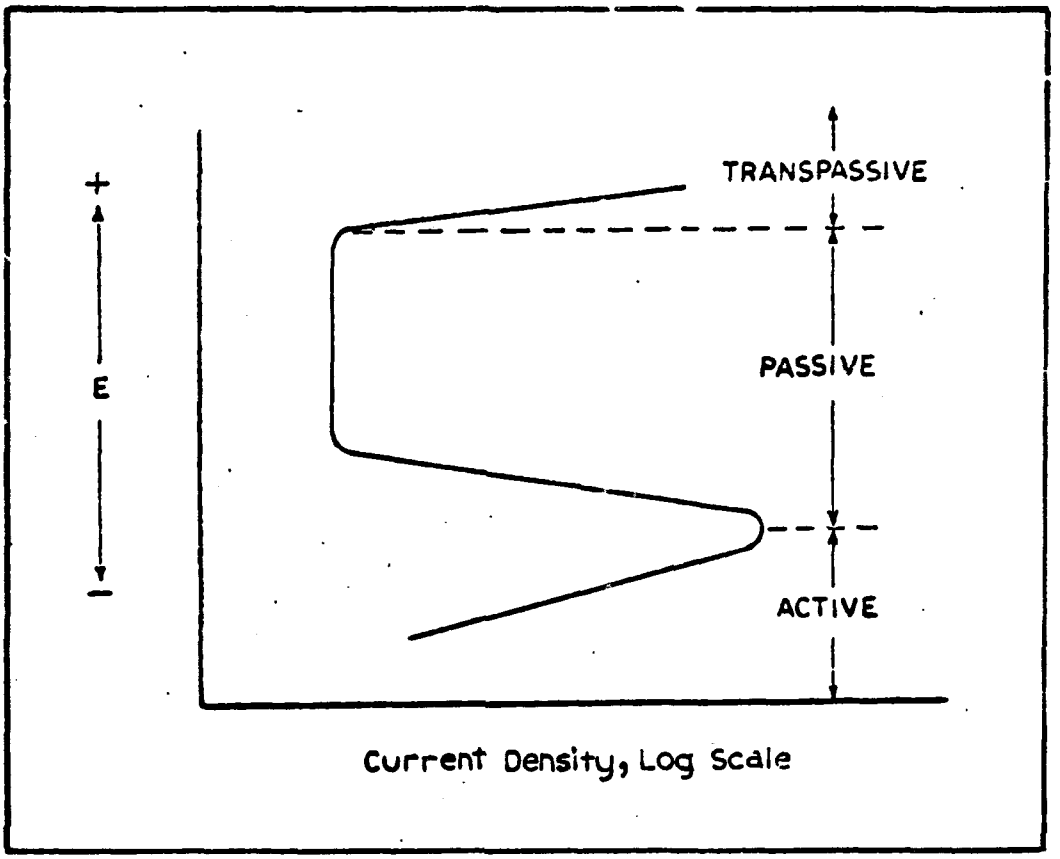

Figure 3. Typical Anodic Polarization Curve of an Active-Passive Metal (Ref 5)

The first is the potentiostatic method which involves changing the potential between the specimen and an auxiliary electrode in the cell (Figure 1) and measuring the resulting current. The advantage of the potentiostatic method is that it can be used to examine metals which exhibit active-passive transitions (Figure 3). The second method is the galvanostatic method in which a current is impressed on the cell and the change in potential (overvoltage) is measured. This method has the advantage of providing very accurate information about the polarization behavior of a metal near its open-circuit potential (E_{corr}).

The data gathered in either the potentiostatic or galvanostatic polarization studies can be analyzed to predict corrosion rates by the Tafel Slope-Extrapolation Technique or the Linear-Polarization Technique.

If the potential of a metal immersed in an electrolyte is plotted against the logarithm of applied current density, a polarization curve such as Figure 4 might be obtained. Within 50 to 200 mv more active or noble than the corrosion potential, the curve becomes linear. The linear region is called the Tafel region and metals that have polarization curves such as this are said to exhibit Tafel behavior[5]. To obtain the corrosion current density (i_{corr}) from this curve, the Tafel region is extrapolated until it crosses a horizontal line drawn from the corrosion potential, E_{corr}. The point of intersection designates a point on the abscissa which is i_{corr}. This corrosion current density can then be used with Faraday's Law to obtain the corrosion rate of the metal. Corrosion rates can be determined from either anodic or cathodic polarization curves. The Tafel region should extend over a current range of at least 1 order of magnitude to obtain sufficient accuracy when obtaining corrosion rates by this method. This range cannot usually be obtained in corroding systems that have more than one reduction-oxidation process occurring. Thus, while the Tafel extrapolation technique is accurate and faster than the weight-loss technique, its application is restricted to a limited number of corroding systems[8].

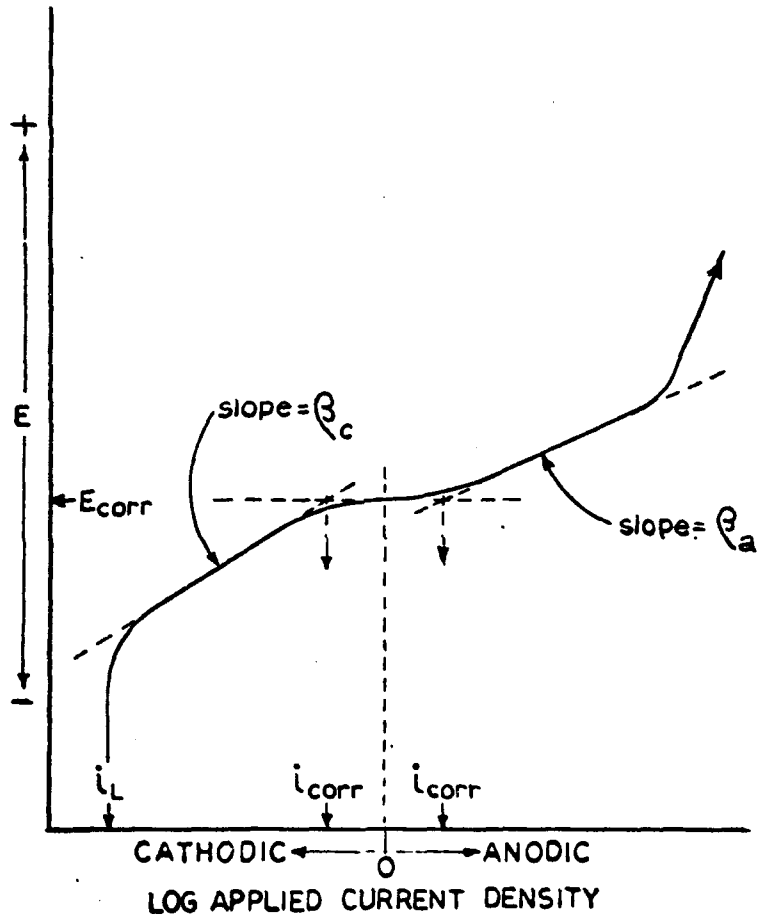

Figure 4. Generalized Anodic and Cathodic Polarization Curve (Ref 8)

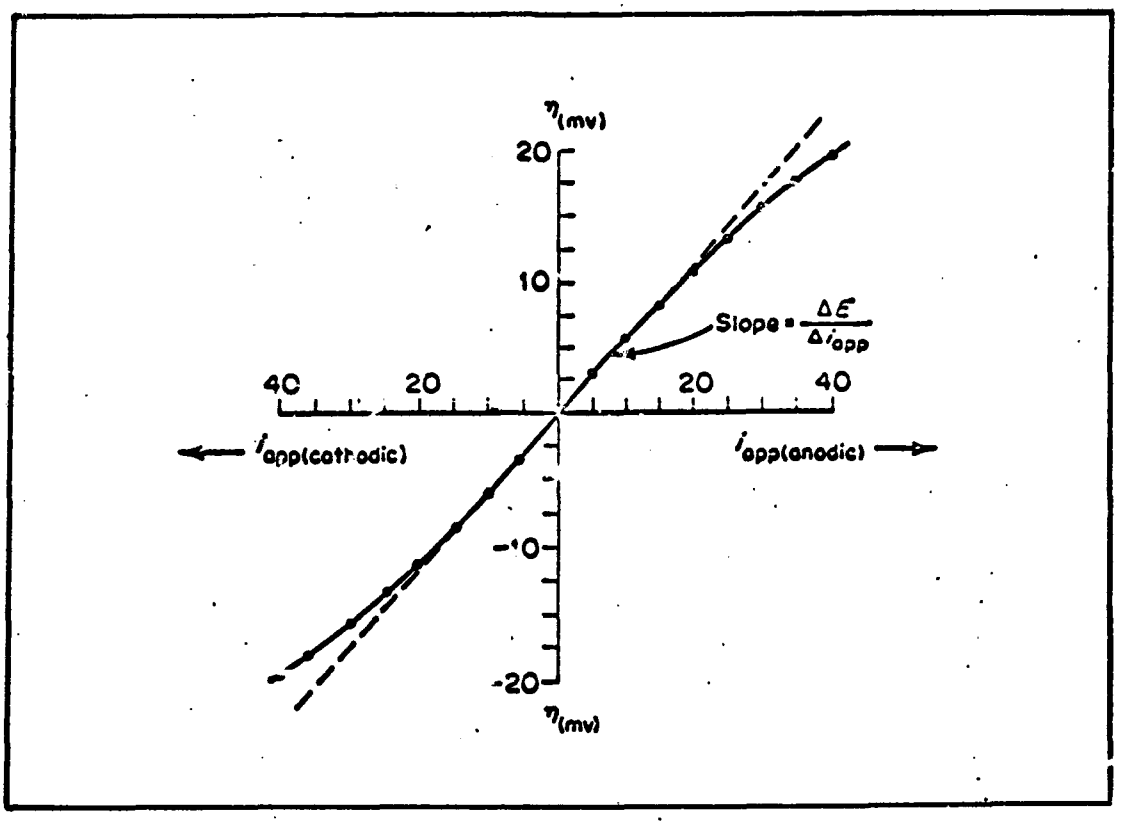

Figure 5. Linear Polarization Curve (Ref 5)

The linear-polarization technique is not limited in application like the Tafel extrapolation technique. It has been shown that at potentials near the corrosion potential, the polarization curve of a corroding system is linear as in Figure 5. Stern and Geary[4] found that for corroding systems controlled by activation polarization, the slope of this straight line, $\Delta E/\Delta i$, was inversely proportional to the corrosion current density. They derived the following equation for these conditions and it has come to be known as the Stern-Geary equation:

$$\frac{\Delta E}{\Delta i} = \frac{\beta_a \beta_c}{2.3(i_{corr})(\beta_a+\beta_c)} \qquad (1)$$

where β_a and β_c are the Tafel slopes of the anodic and cathodic polarization curves respectively (Figure 4). In other words, the Stern-Geary equation states that within 10 mv more active or more noble than the corrosion potential, E_{corr}, the electrode potential is a linear function of the applied current density. If a corroding specimen is polarized using the galvanostatic method, a plot of overvoltage versus applied current density similar to Figure 5 is obtained.

The original Stern-Geary equation, equation (1) considered only the case of activation polarization. Stern[10] showed in a later paper that a corroding electrode controlled by concentration polarization also produces a linear-polarization curve. However, in this case β_c becomes effectively infinite and equation (1) becomes:

$$\frac{\Delta E}{\Delta i} = \frac{\beta_a}{2.3(i_{corr})} \qquad (2)$$

Corroding electrodes exposed to aerated or oxygenated electrolytes are thought to be controlled by concentration polarization[5]. In such cases, equation (2) has been found to be a useful relationship in linear-polarization studies.

The linear-polarization technique for determining corrosion rates has the following important advantages:

1. The technique is fast enough to obtain a large number of corrosion rate determinations in a relatively short period of time. These determinations can be quite accurate if the values of β_a and β_c are known.

2. Even if the beta values are unknown, corrosion rates of most metals can be estimated within a factor of two if beta values between 0.06 to 0.12 volt/decade are used[4,11].

3. The corroding system is investigated so close to the corrosion potential, that the system is not greatly disturbed from equilibrium conditions. Thus, there are very few systems to which this technique cannot be applied[4,14].

4. The technique can be used to obtain very low corrosion rates with accuracy [13].

5. The technique has been used successfully to obtain corrosion rates of surgical implants in living animals (in vivo)[15,16].

Because of the many advantages of the linear-polarization technique, and in particular the advantage of being able to obtain very low corrosion rates, the corrosion rates of six commonly used dental alloys were determined by this technique. These corrosion rates were determined for three different surface finishes. In order to insure accuracy, beta values of these materials were obtained using the potentiostatic polarization method.

II. Experimental Apparatus

Electrical Circuitry

The electrical circuitry used for the galvanostatic determination of linear-polarization curves is shown in Figure 6. The circuitry is similar to that described by Haugen[8]; however, a π - filter (Figure 7) was added in parallel to the regulated D.C. power supply in order to filter out undesirable noise encountered at very low currents (less than 1.0μamp).

The constant-current source consisted basically of a regulated D.C. power source (Heathkit Model PS-4), a π - filter, a decade resistor bank, and a double-pole-double-throw (DPDT) switch.

For selecting the desired constant current, a decade resistor bank with rotary selector switch (S-1) and 12 resistors: 1K, 3K, 10K, 30K, 100K, 330K, 1M, 3.3M, 10M, 33M, 50M, and 500M ohms (R-12) was used. By the position of switch S-2, the direction of current could be controlled so that the working electrode could be made to act as an anode or a cathode. Thus, both anodic and cathodic polarization curves could be obtained with this electrical circuitry.

A high impedance (10^{10} ohms) digital voltmeter (Hewlett-Packard model 3440A) was used in the circuit to measure both cell current and potential of the working electrode. The potential was measured directly off one side of the DPDT switch (S-3) while the current was

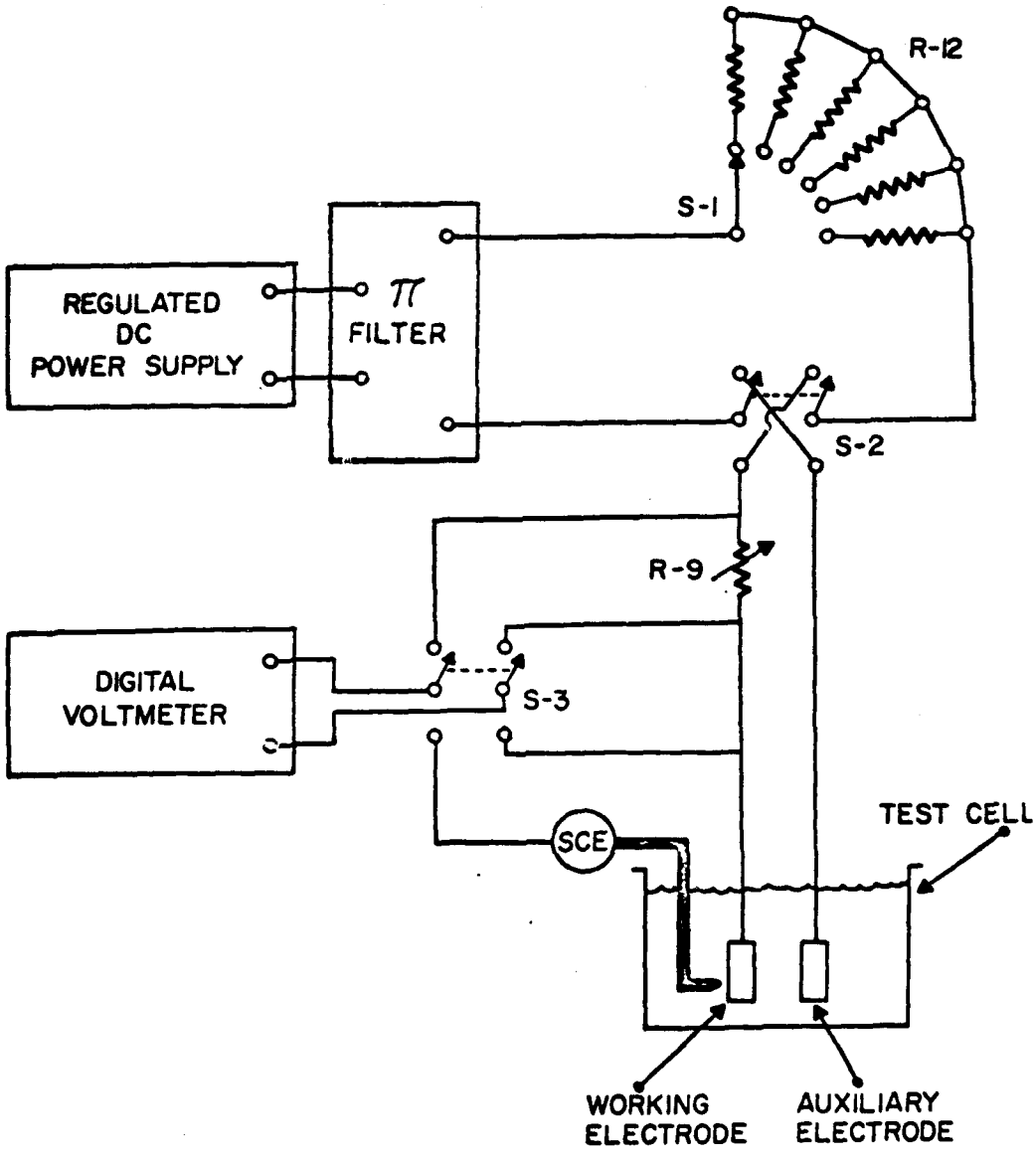

Figure 6. Electrical Circuitry Used for Galvanostatic Determination of Polarization Curves

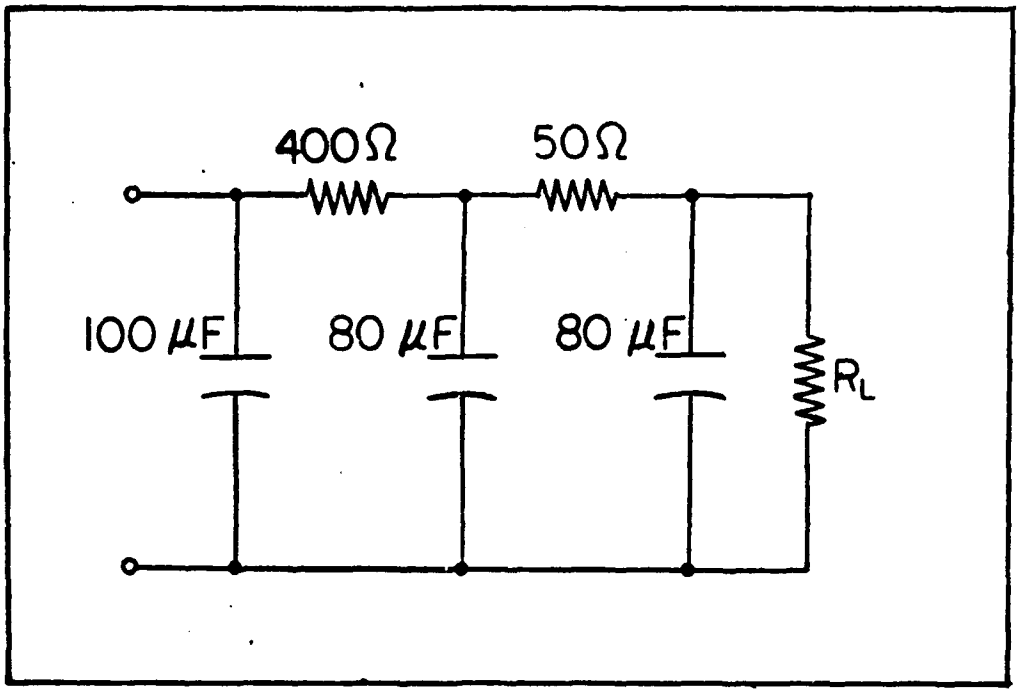

Figure 7. Electrical Circuitry of π -Filter Used in Circuit Shown in Figure 6

Figure 8. Galvanostatic Polarization Test Equipment Showing Components of Circuitry Illustrated in Figure 6

measured off the other side of S-3 (i.e., by using Ohm's law and the voltage drop across resistance R-9). The resistance, R-9, was a decade resistor bank consisting of 9 precision (1%) resistors: 0.1, 1, 10, 100, 1K, 10K, 100K, 1M, and 5M ohms.

Polarization Test Cell

The polarization test cell (Figure 8) was similar to that used by Haugen[8] and Smulczenski[17]. Basically, it was a specially constructed 2-liter beaker with a gas-tight fluorocarbon lid. This lid was fitted with two ground-glass receptacles to accomodate the aerator assembly and thermometer. In addition, the lid contained three O-ring fittings for the working electrode, auxiliary electrode, and Luggin probe. The specimen (working electrode) was positioned in the cell so that its surface could be observed during testing.

Salt Bridge. The potential between the working electrode and the reference electrode was measured with a digital voltmeter. This could be accomplished because of the electrolytic connection between the two electrodes provided by a salt bridge having a Luggin probe and a Haber capillary tip[18] which was immersed in a beaker containing electrolyte and the reference electrode.

The salt bridge was constructed in two parts for ease of assembly. A fluorocarbon sleeve was used to connect the exterior portion of the salt bridge (left side of Figure 8) to the glass-tube portion of the Luggin probe which extended through the test-cell lid.

Reproduced from best available copy.

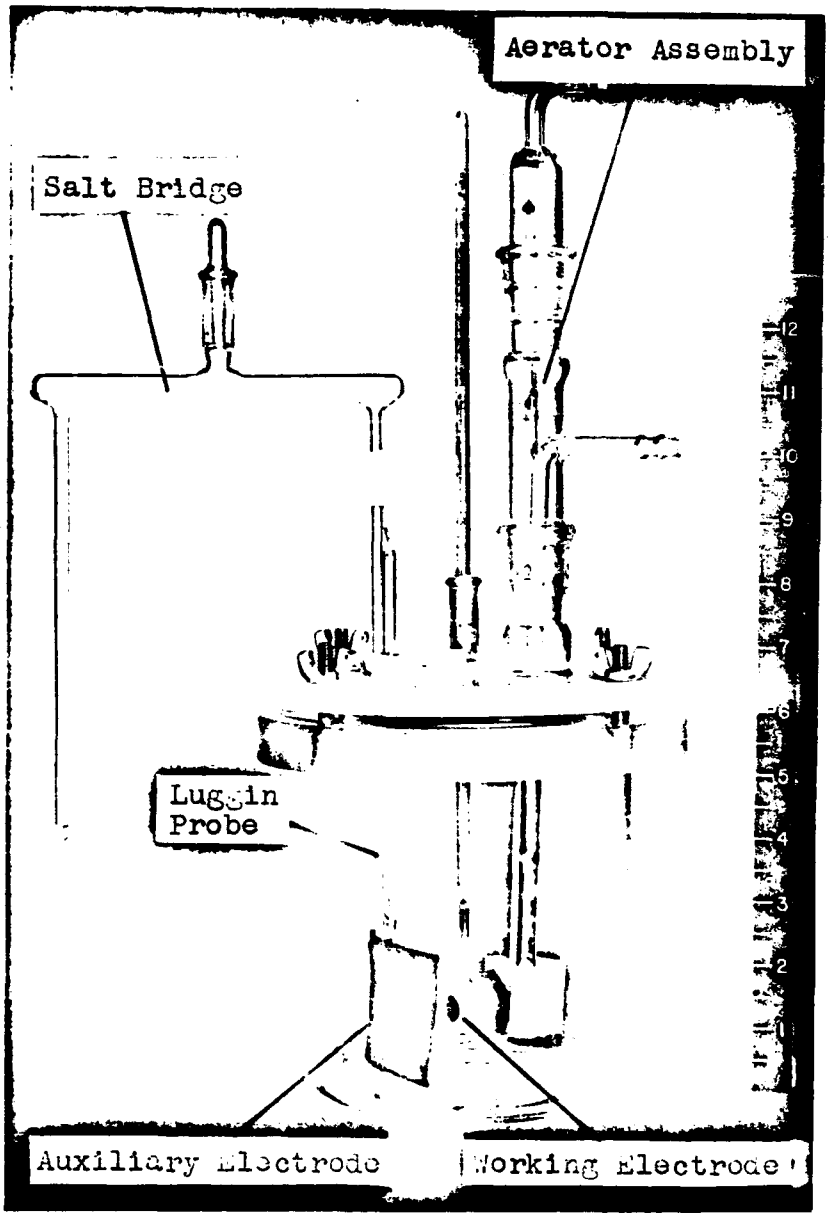

Figure 9. Polarization Test Cell

In accordance with Barnartt[19], a 1 mm (o.d.) Luggin probe was placed 2 mm from the face of the working electrode. The Haber capillary tip on the bottom outside leg of the salt bridge contained a small perforation which would allow one drop of electrolyte to flow in approximately 30 minutes. This permitted the electrolytic contact between the working electrode and the reference electrode when the salt bridge was filled with electrolyte. A ground-glass joint at the top of the bridge aided in filling the bridge with electrolyte (i.e., the electrolyte was drawn into the bridge by a suction device used at the joint).

During testing at constant current, movement of the Luggin probe to various distances further from, and across, the face of the working electrode showed negligible changes in potential. Thus, IR drop in the electrolyte between the working and reference electrodes was believed to be negligible. In addition, since potential did not change across the specimen surface, a backside capillary was not considered necessary for this investigation[20].

For a given several-day test, pH of the electrolyte did vary from one 24-hour test period to another; however, the pH was adjusted to the desired range[3] and the salt bridge was refilled prior to each test. Change in concentration of the electrolyte during polarization testing was negligible.

Reference Electrode. A saturated calomel half-cell (SCE) reference electrode was used in this investigation. This electrode maintains a relatively-constant potential in a wide range of environments.

The specific calomel reference electrode used was a fibrous-membrane type (Leeds and Northrup Standard 1199-3). The electrode was placed in a 100 ml beaker filled with approximately 80 ml of electrolyte. This electrolyte completed the circuit between the reference electrode, the external leg of the salt bridge, and the working electrode.

Auxiliary Electrode. The auxiliary electrode consisted of a 2 x 2½ inch platinum screen. The screen was spot-welded to a platinum wire which was supported by a glass tube. The glass tube extended vertically through the cell lid where it made an air-tight seal. The platinum wire protruded through the glass tube above the cell lid to provide a terminal for electrical connection.

Specimen Holder. The working-electrode assembly (specimen holder) is shown in Figure 9. The specimen holder used in this investigation was similar to the one described in detail by Myers[21]; however, the polycarbonate cover was modified so that the exposed area of the specimen was 0.1 cm^2. This allowed tests to be conducted on smaller specimens (large specimens of the precious metals used in dentistry are difficult to obtain).

The oblique entry design of the specimen holder was retained to eliminate crevice effects, prevent accumulation of corrosion products on specimen surface, and permit the escape of gases formed.

Aerator Assembly. Filtered air was bubbled through the electrolyte with the use of a glass assembly that was designed

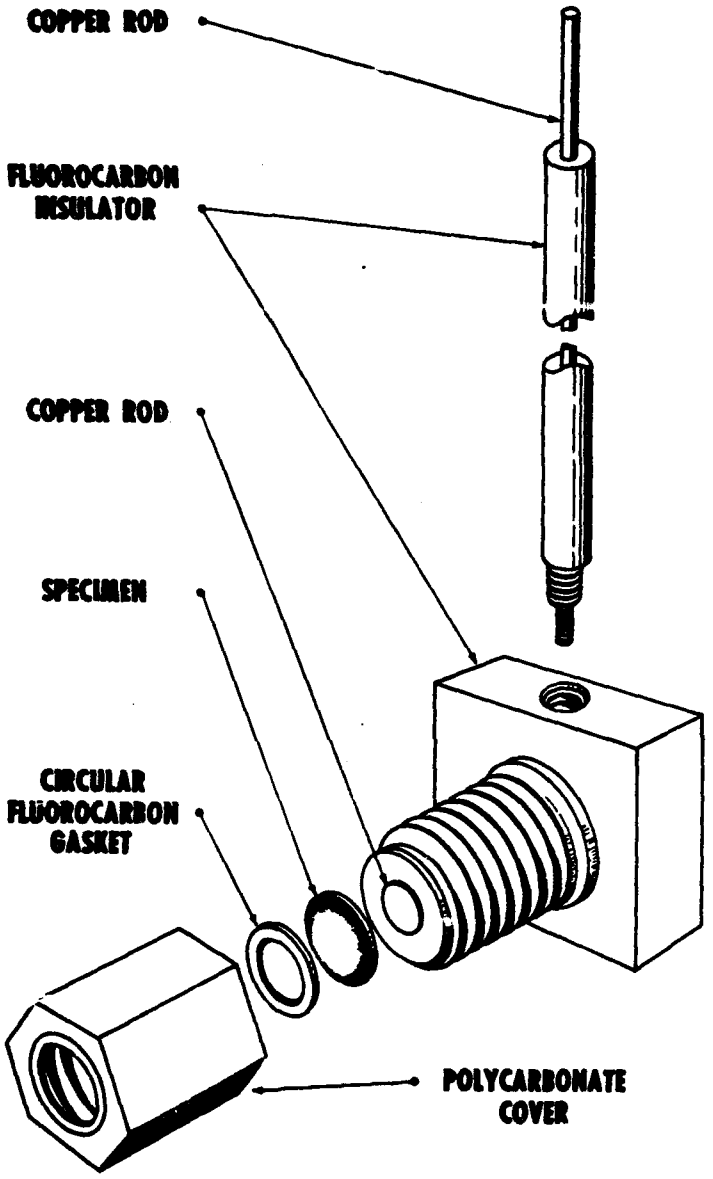

Figure 10. Working Electrode Assembly (Specimen Holder, not to scale) (Ref 21)

to fit into one of the ground-glass necks in the test cell lid. Air entered the electrolyte thru a fritted glass tube which extended into the electrolyte to within approximately 1 inch of the bottom of the cell. Expended air was vented thru a tube in the top of the aerator assembly.

Electrolyte

The electrolyte used in this investigation was aerated synthetic saliva[2,3] with no attempt made to reproduce the bacteriological constituents. Upon consultation with several members of the dental profession, it was concluded that aeration would best simulate the conditions of the human mouth in preference to other gases considered.

Table I

Composition of Synthetic Saliva Solution

Chemical Name	Chemical Formula	Weight
Dipotassium hydrogen phosphate	K_2HPO_4	0.200 g
Calcium phosphate (tribasic)	$Ca_3(PO_4)_2$	0.300 g
Potassium thiocyanate	KSCN	0.330 g
Sodium bicarbonate	$NaHCO_3$	1.500 g
Sodium chloride	NaCl	0.700 g
Potassium chloride	KCl	1.200 g
Urea	$(NH_2)_2CO$	0.130 g
Distilled Water	H_2O	1 liter

(From Ref 2)

The composition of this saliva is shown in Table I. The pH of the electrolyte was maintained between 6.5 and 7.0 (pH range of the mouth) for each test by additions of small amounts of hydrochloric acid when necessary.

Specimens

Six commercially-available dental alloys (Table II) were investigated. These alloys were supplied by the Wright-Patterson AFB Dental Clinic and Dr. Edgar White of Dayton, Ohio. All of the alloys with the exception of the amalgams were supplied in shapes that could be easily adapted to the specimen holder.

A Lucite mold was made to obtain the desired shape of the Ag-Sn amalgam. This amalgam was then condensed into the mold by dental personnel of Wright-Patterson AFB. Twenty-four hours after condensation, the Lucite mold was cut away from the amalgam and the resulting specimen (a right-circular cylinder, 1.52 cm in diameter and 1 cm thick) could then be mounted in the specimen holder.

The copper amalgam was supplied in the cylindrical-pellet form and tested after grinding to proper shape. No attempt was made to heat and condense this amalgam; thus, the Hg content was slightly higher than would be encountered in actual use.

Test Apparatus for Potentiostatic Polarization Studies

In addition to the apparatus already described, some potentiostatic data-determination equipment was used to obtain complete anodic and cathodic polarization curves.

Table II

Dental Alloy Specimen Compositions

(Weight Percent)

Type of Dental Alloy and Nominal Composition	Analyzed Composition											
	Au	Ag	Cu	Pd	Ni	Cr	Mo	Hg	Sn	Co	Zn	Ti
Dental Gold Au-13Ag-9Cu	78.0	13.25	9.28	1.91	-	-	-	-	-	-	-	-
Dental Gold Au-5Pd-1Ag	94.0	0.95	0.02	5.0	-	-	-	-	-	-	-	-
Dental Ag-Sn Amalgam Hg-30Ag-12Sn-2Zn	-	30.22	-	-	-	-	-	57.5	12.0	-	0.28	-
Dental Cu Amalgam Hg-34.5Cu	-	-	34.5	-	-	-	-	65.4	-	-	-	-
Dental Casting Alloy Ni-16.5Cr-2.5Mo	-	-	-	-	80.96	16.5	2.52	-	-	.01	-	.01
Dental Casting Alloy Ni-24.5Cr-24.5Pd-10.5Co	-	-	-	24.5	40.0	24.5	-	-	-	10.5	-	-

Reproduced from best available copy.

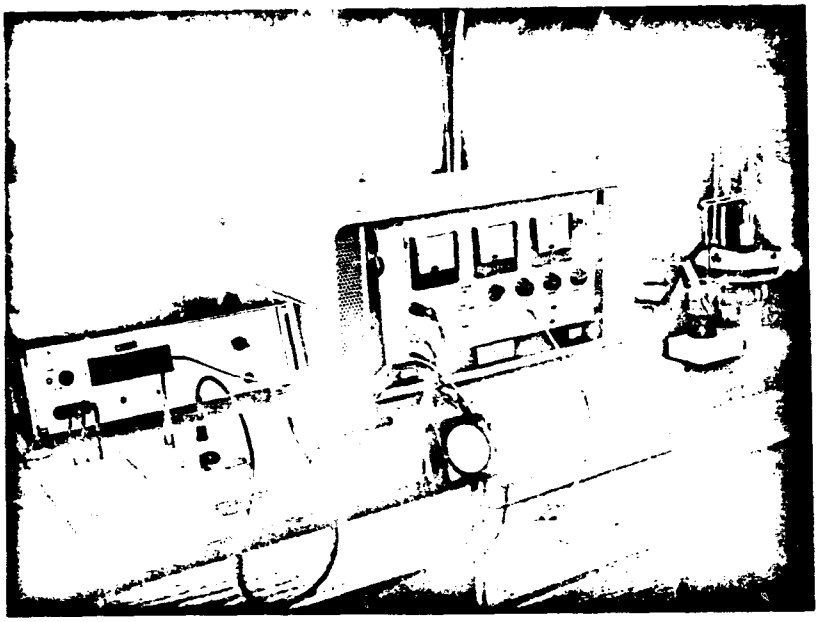

Figure 11. Potentiostatic Polarization Test Apparatus Showing Digital Voltmeter, Potentiostat, and Test Cell

Basically, only three major components of apparatus were used for this phase of the investigation: the electronic potentiostat (Anotrol Model 4100), the digital voltmeter, and the test cell as shown in Figure 10.

The equipment was connected in such a way that the potentiostat could apply the desired voltage (read on the digital voltmeter) between the test specimen and the reference electrode. A corresponding current was determined for each test potential by measuring the potential drop across a precision resistor with a digital voltmeter and calculating the current using Ohm's Law.

III. Experimental Procedure

Test Cell Preparation

All test cell components were cleaned, rinsed in distilled water, and dried prior to each test. The test cell was filled with approximately 1400 ml of electrolyte. The test cell lid with Luggin probe, thermometer, and aerator assembly was then installed. Holes in the lid for the working and auxiliary electrodes were plugged. Air, filtered through a cartridge-type air filter, was then bubbled through the electrolyte for approximately 2 hours. At the same time that aeration was initiated, the digital voltmeter and regulated D.C. power supply were turned on to insure that transient conditions were not present in the electrical components during polarization tests. The 2-hour aeration time was decided upon because it was observed that the open-circuit potentials of both working and auxiliary electrodes reached stable values within 1 hour. The additional 1 hour was used to insure complete aeration of the electrolyte.

During the aeration period, the working and auxiliary electrodes were prepared. One side of the test specimen was ground with 4/0 emery paper, dental pumice, or dental tin oxide depending upon which surface finish was being tested. Each specimen (with the exception of the amalgams) was degreased in boiling benzene for approximately 3 minutes, rinsed in triple-distilled water, and air dried. It was found that boiling benzene attacked the grain boundaries of the amalgam specimens making them unsuitable for testing.

Therefore, the amalgam specimens were not degreased, but were rinsed in triple-distilled water and air-dried like the other specimens. The dried specimen was then mounted in the working-electrode assembly (specimen holder). The auxiliary electrode was cleaned by boiling in aqua regia for approximately 5 minutes and then rinsed in triple-distilled water. Also during the aeration period, the pH of the electrolyte in the cell was measured with a pH Meter (Beckman, Zeromatic II). If necessary, the pH was adjusted to the range 6.5 to 7.0 with small amounts of hydrochloric acid.

After 2 hours of aeration, the test cell lid was removed and the working electrode and auxiliary electrode were installed in the lid. With the lid off, approximately 80 ml of electrolyte was removed from the test cell and put into the 100 ml beaker which contained the saturated calomel electrode. The test cell lid was then replaced and the external portion of the salt bridge was inserted into the fluorocarbon sleeve at the top of the Luggin probe. The external leg of the salt bridge was then placed in the beaker containing the saturated calomel electrode. The liquid level of this small beaker was adjusted (using shim spacers under the base of the beaker) so that it was slightly lower than the liquid level in the test cell. Thus, electrolyte would not be siphoned from the small beaker into the test cell. The salt bridge was then filled with electrolyte with the use of a suction device at the ground-glass joint in the top of the bridge.

Aeration was continued at a slower, but constant, rate during all polarization testing. All testing was conducted at 22°±1°C; however, two of the samples were additionally tested at 37°±1°C (98.6°F) by placing the test cell in a thermostatically controlled water bath.

Specimen Activation

Each specimen was cathodically activated in the test cell to remove any surface film that might have formed after grinding. The positive terminal of a 1.5 volt dry cell battery was connected to the auxiliary electrode and the negative terminal was connected to the working electrode. Three minutes of cathodic activation was found to be sufficient for all specimens. However, it was observed that if the gold alloys were activated for more than 30 seconds, a period of approximately 45 minutes was necessary for the open-circuit potential to shift back to a steady-state value. Thus, the gold alloys were cathodically activated for only 15 seconds.

Open-Circuit Potential

The open-circuit potential of each specimen was measured by connecting the digital voltmeter between the working electrode and the saturated calomel electrode (SCE). This open-circuit potential was monitored on the voltmeter until a steady-state value was obtained. The steady-state value was defined as that potential which showed a change of less than 1 mv over a 10 minute period. This steady-state open-circuit potential was recorded as E_{corr} of the sample.

Galvanostatic Polarization Tests

After E_{corr} was established and recorded, cathodic polarization data were obtained within 15 mv of E_{corr}. The polarization data were obtained by applying a cathodic current between the working electrode (specimen) and the auxiliary electrode by means of the regulated D.C. power source (Figure 6). This power source was initially set at a value of 20 volts and the applied current was adjusted to the desired range by the decade resistor bank, R-12. Applied currents in this investigation varied between 5×10^{-9} and 4×10^{-5} amps. These applied currents were measured by observing the potential drop across precision resistance, R-9. The potential of the working electrode was measured with respect to a reference electrode (SCE).

The current range of interest for each specimen was obtained by initially setting the applied current density at 10^{-8} amp/cm^2 and increasing it slowly by means of the regulated D.C. power source and the resistance R-12. This current was increased until a 1 mv change in potential from E_{corr} was observed. That value of current was recorded and the current was increased until another mv change in potential occurred. The change in current from the first value gave an indication of the size of the current "steps" needed for testing of the specimen. The time of 1 minute between steps (i.e., between establishing a constant current and obtaining a stable potential) was found to be adequate for all specimens tested.

After obtaining the first set of polarization data, the specimen was left in the test cell and aeration was continued; after 24 hours had elapsed, a new E_{corr} was established and another set of polarization data were obtained. Polarization curves were obtained by plotting the applied current density, Δi, versus the change in potential, ΔE. This procedure of obtaining polarization data and polarization curves was repeated every 24 hours until a steady-state slope, $\Delta E/\Delta i$, was obtained. This steady-state slope established the steady-state corrosion current density (i_{corr}) in accordance with the Stern-Geary relationship (Equation 2). Corrosion rates were determined from the values of i_{corr} and the following version of Faraday's Law:

$$\text{Corrosion Rate} = \frac{(i_{corr})(GMW)(V)(3.15)(10)^{11}}{(F)(Z)} \quad \frac{\text{microns}}{\text{yr}} \quad (3)$$

where, i_{corr} = corrosion current density, amps/cm^2

GMW = molecular weight of the metal, gms/mole

V = specific volume of the metal, cm^3/gm

F = Faraday's Constant = 96500 amp-sec/equivalent

Z = # of equivalents/mole

Initially, to gain familiarity with the equipment and to insure equipment was operating properly, several calibration runs were made on one of the metals studied by previous investigators[8].

Potentiostatic Polarization Studies

After completing galvanostatic polarization testing on a specimen, the test cell was connected to the terminals of

the potentiostat (Figure 11) which had been previously left on "standby" for approximately 1 hour to allow electronic components to stabilize.

The value of the established E_{corr} was set into the potentiostat by means of the voltage adjustment dial and observed on the digital voltmeter. The potentiostat was then switched from "standby" to "operate".

For anodic polarization tests, the potential was increased initially by steps of 5 mv in the noble (anodic) direction. Three minutes after setting in each potential step, the voltmeter selector switch was moved from the "voltage" to the "current" position. The voltage drop through a known resistance was displayed on the voltmeter and recorded as current. Polarization curves were obtained by plotting the applied potential and the corresponding value of current density (the recorded current divided by the exposed surface area of the specimen). After 200 mv of polarization away from E_{corr} the potential steps were increased to 20 mv and after 500 mv to 50 mv. Polarization was continued to the potential limit of the potentiostat (+5.4 volts).

For the cathodic polarization tests, the potential was increased initially by 10 mv steps in the active (cathodic) direction. At -200 mv the steps were increased to 50 mv and at -500 mv to 100 mv. Again, polarization was continued to the limit of the potentiostat (-5.4 volts).

IV. Results and Discussion

Criteria Observed

The following criteria are applicable to the discussion of the results of this investigation:

1. The Stockholm sign convention is used for electrode potentials (i.e., noble potentials are positive; active potentials are negative).
2. All potentials are referenced to the saturated calomel electrode (S.C.E.).
3. Current densities (ma/cm^2) are calculated using the original exposed surface area of the specimen.
4. Compositions of the alloys are given in weight percent (w/o).
5. Corrosion rates are expressed in microns per year (microns/yr).

Metallurgy of Materials Tested

The following sections present a discussion of the metallurgical aspects and uses of the dental alloys that were investigated.

Silver-Tin Amalgam. The first material tested was a Ag-Sn amalgam which had an approximate composition of Hg-30Ag-12Sn-2Zn. It is estimated that 80% of all dental restorations are made using this material[1]. The Ag-Sn alloy is usually supplied to the dentist in the form of filings. These filings are mixed (triturated) with liquid Hg such that the mix composition is approximately 52% Hg by

weight. The resulting "plastic-mass" is compacted into a prepared cavity in the tooth by a process called condensation.

From a dental standpoint, the only phase of the Ag-Sn alloy which is of interest is the γ-phase (Figure 12). The γ-phase when triturated with the proper amount of Hg will expand upon solidification, resulting in a tight interface between the tooth and the restoration. This phase is an intermediate compound (Ag_3Sn) having a composition of approximately 73% Ag and 27% Sn. When γ-phase is triturated with Hg a reaction occurs which produces two new solid phases, $\gamma_1(Ag_2Hg_3)$ and $\gamma_2(Sn_7Hg)$. Since the excess (unreacted) Hg is squeezed out during condensation, microstructure of the amalgam consists of γ-phase with continuous phases of γ_1 and γ_2. Visual solidification of the amalgam occurs in approximately 3 minutes. A period of 24 hours should elapse before surface polishing of the restoration because heat produced during polishing will release Hg from the γ_1 and γ_2 phases and cause a weakening of the grain boundaries.

Copper Amalgam. Copper amalgam has an approximate composition of 65%-70% Hg and a balance of Cu. The amalgam is mixed and solidified at the manufacturer's facility and supplied to the dentist in the form of pellets. In preparation for a restoration, these pellets are heated in a crucible by the dentist until droplets of Hg appear. The softened mass is then triturated and condensed in the usual manner. Since condensation removes some of the excess Hg,

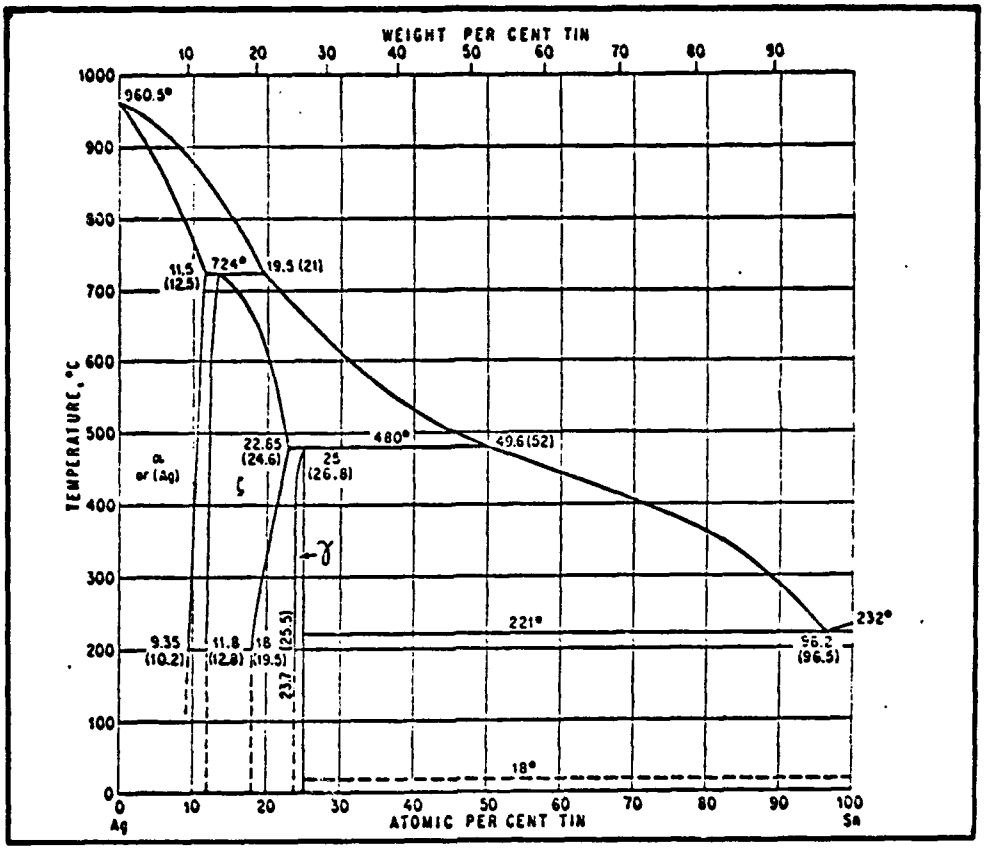

Figure 12. Phase Diagram of the Ag-Sn Alloys (Ref 22)

the resulting restoration has an Hg content of approximately 60 to 65 w/o. No attempt was made to heat, triturate, or condense the Cu amalgam used in this investigation. Thus, the Hg content (64.5 w/o) was slightly higher than would have been expected for the same amalgam in a restoration.

It has been reported that Cu amalgams corrode considerably in mouth fluids[1]. As a result, their use in recent years has been largely replaced by Ag-Sn amalgams.

Gold-Silver-Copper Alloy. This alloy is used in dentistry in the form of wrought plate, wire, castings, and solders. It is casted for making inlays, crowns, bridges,

and partial dentures. The casting characteristics are excellent and it has been reported that certain compositions of this alloy have corrosion resistance characteristics that are adequate for use in the mouth[23].

In the Cu-Au phase diagram (Figure 13) the alloy composition of dental interest is approximately 75 w/o Au. It has been clinically demonstrated that the order-hardened δ-phase has both the required strength and corrosion resistance for dental use[1].

Gold-Palladium-Silver Alloy. This alloy system is single-phase with no solid-state transformations. The corrosion resistance properties of this alloy are very good[23]. In addition to corrosion resistance, the relatively-low hardness and malleability of these alloys make them suitable for dental applications. The Vickers hardness of the various compositions is given in Figure 14. The alloy tested in this investigation had an approximate composition of 94Au-5Pd-1Ag.

Nickel-Chromium- Molybdenum Alloy. This alloy is used for dental castings and orthodontic wires. The alloy can be welded without fear of carbide-precipitation in the grain boundaries because it has an extremely-low carbon content. Tensile strengths of these alloys, in wire form, vary between 95,000 psi (annealed wire) and 220,000 psi (as-drawn wire)[1]. The alloy used in this investigation had an approximate composition of Ni-16.5Cr-2.5Mo.

Nickel-Chromium-Palladium-Cobalt Alloy. This family of alloys is used mainly for casting appliances such as

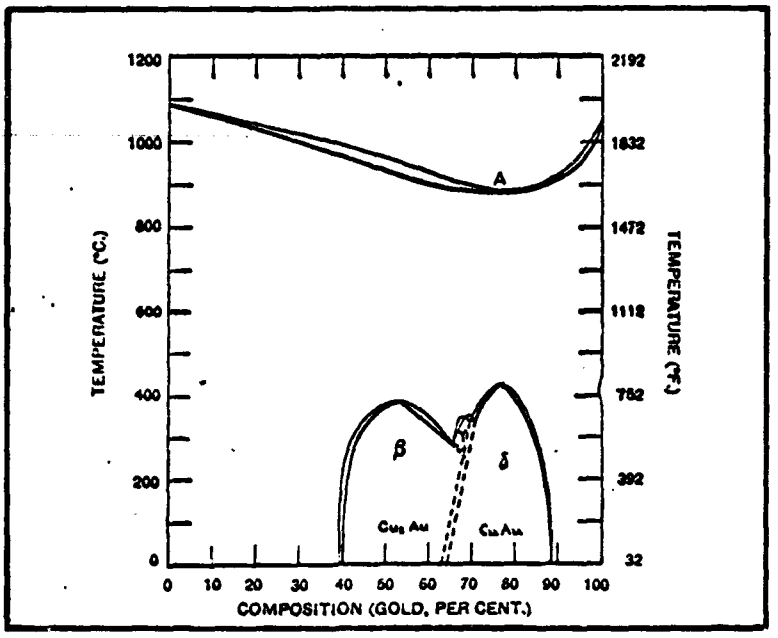

Figure 13. Phase Diagram of the Au-Cu Alloys (Ref 1)

metallic denture bases, complex partial denture structures, and certain types of bridgework. The liquidus temperature of this type of alloy varies between 1300 and 1500 °C; thus, making them difficult to cast, relative to the gold alloys. An advantage of these alloys is that they are lighter and stronger than the gold alloys; however, there is controversy over whether these advantages overcome the difficulties encountered in casting[1]. The approximate composition of the alloy investigated in this study was Ni-24.5Cr-24.5Pd-10.5Co.

Open-Circuit Corrosion Potentials

The open-circuit corrosion potentials (E_{corr}) of the six alloys, taken at 24-hour intervals prior to each test are given in Table III. There was no obvious trend in the change of these potentials with time; however, all of the

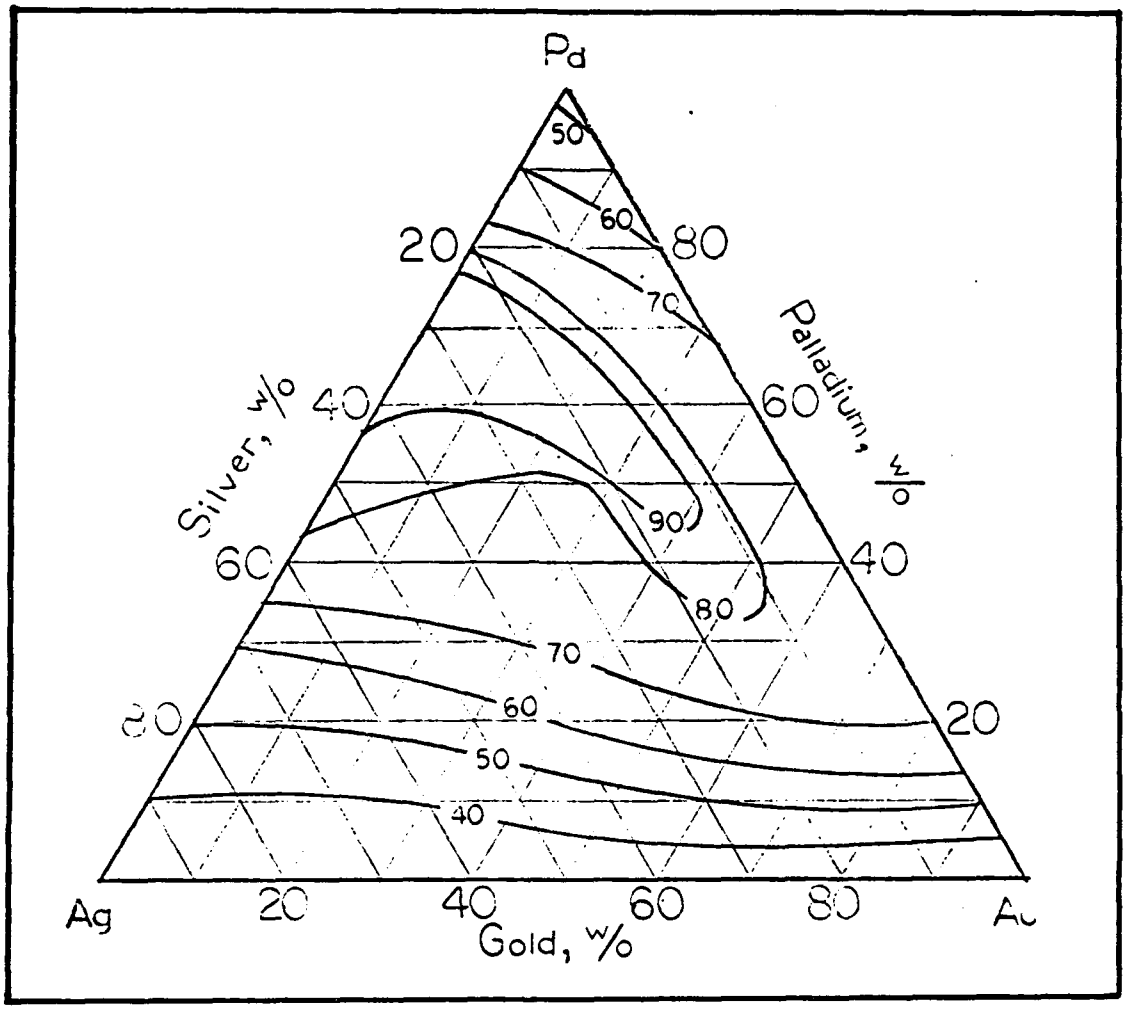

Figure 14. Ternary Diagram of the Au-Pd-Ag Alloy System Showing Vickers Hardness as a Function of Composition (Ref 23)

alloys approached reasonably stable values within 48 to 96 hours.

Results in Table III are for the tests where the surface finish of the specimen was ground with 4/0 emery paper. Similar results were obtained for the other two surface finishes investigated.

The effect of raising the electrolyte temperature to 98.6°F on the open-circuit corrosion potential of the two

alloys is also shown in Table III. In accordance with theoretical considerations, the potentials shifted slightly in the active direction when the temperature was increased.

Values of the steady-state open-circuit corrosion potentials for the Ag-Sn amalgam were somewhat more noble than the values obtained by other investigators(24). However, this may be attributed to the differences in the composition of the electrolyte. It is suspected that a predominate oxygen-reduction process occurred in the present investigation due to the use of aeration.

Linear-Polarization Curves

Galvanostatic, cathodic linear-polarization curves were determined within 15 mv of the open-circuit corrosion potential for the six dental alloys studied (Table I). Each of the curves (Figures 15-32) was obtained by testing in aerated synthetic saliva at 22 $\pm$1°C. Consecutive tests (conducted every 24 hours until steady-state conditions were established) for a given specimen and surface finish were plotted on the same figure to show the effect of time on the corrosion rate. Relative corrosion rates can be obtained from these figures (i.e., steeper slopes indicate lower corrosion rates).

The effect of time and surface finish on the corrosion current densities (i_{corr}) are summarized in Table IV. Values of i_{corr} were obtained using the polarization resistances ($\Delta E/\Delta i$), the Stern-Geary relationship, and the β_a values

Table III

Effect of Time on Open-Circuit Corrosion Potentials (Volt vs. S.C.E.)

for Dental Alloys in Aerated, Synthetic Saliva

Alloy	0 Hrs.	24 Hrs.	48 Hrs.	72 Hrs.	96 Hrs.	120 Hrs.
* Au-13Ag-9Cu	+0.009	+0.068	+0.079	+0.078	+0.073	+0.075
* Au-5Pd-1Ag	+0.022	+0.032	+0.037	+0.062	+0.071	+0.061
* Ni-16.5Cr-2.5Mo	-0.037	-0.022	-0.018	-0.010	-0.018	-0.011
** Ni-16.5Cr-2.5Mo	-0.057	-0.037	-0.025	-0.019	-0.023	-0.022
* Hg-30Ag-12Sn-2Zn	-0.044	-0.062	-0.065	-0.073	-0.074	-0.073
** Hg-30Ag-12Sn-2ZN	-0.101	-0.120	-0.131	-0.142	-0.145	-0.144
* Hg-34.5Cu	-0.107	-0.127	-0.105	-0.115	-0.113	-0.117
* Ni-24.5Cr-24.5Pd-10.5Co	-0.001	-0.005	-0.002	+0.010	+0.006	+0.007

* At 22°C
** At 37°C (98.6°F)

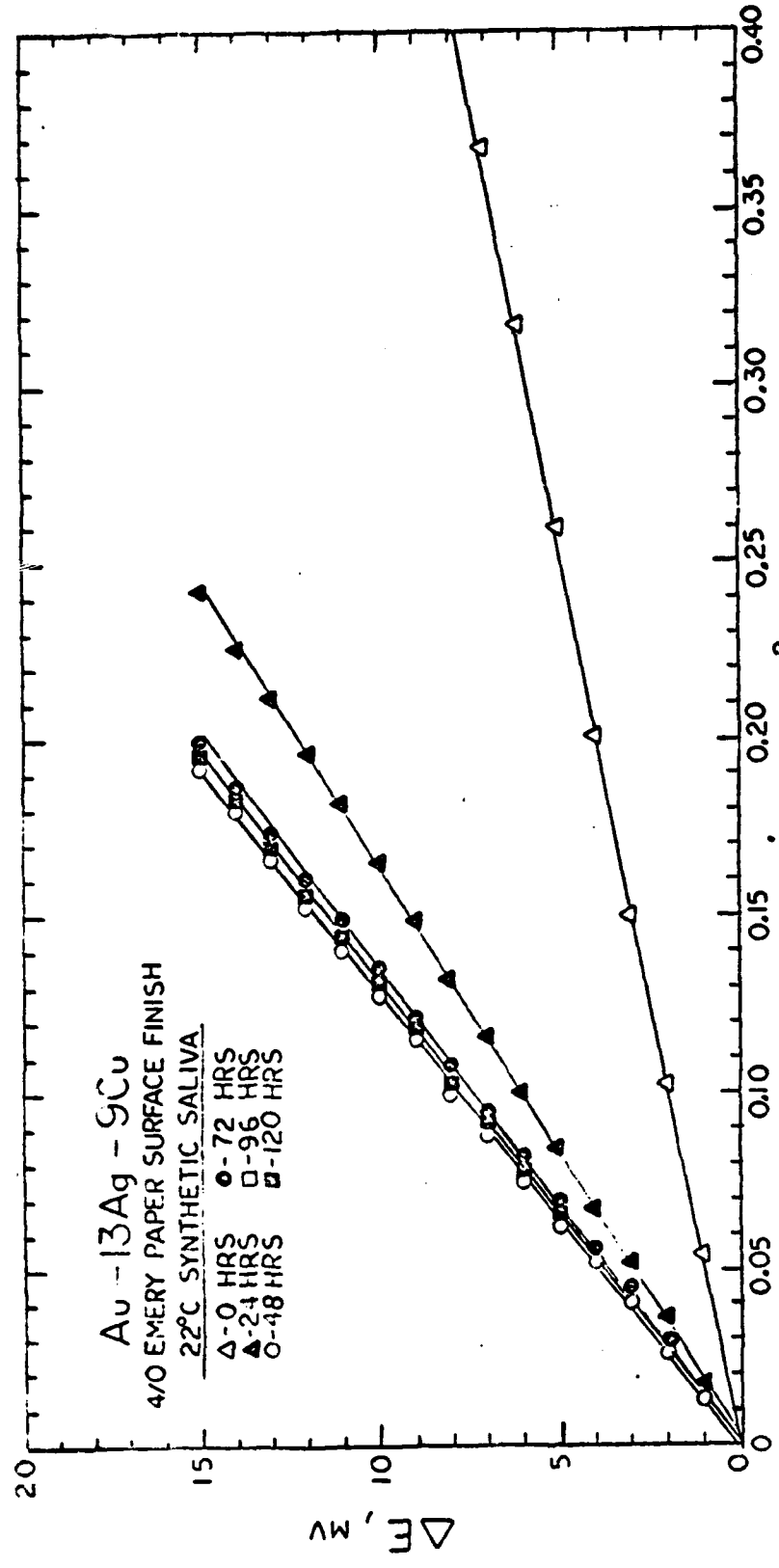

Figure 15. Effect of Time on the Galvanostatic Cathodic Linear-Polarization Curves for Au-13Ag-9Cu Dental Alloy in Aerated Synthetic Saliva at 22°C. Surface Finished with 4/0 Emery Paper.

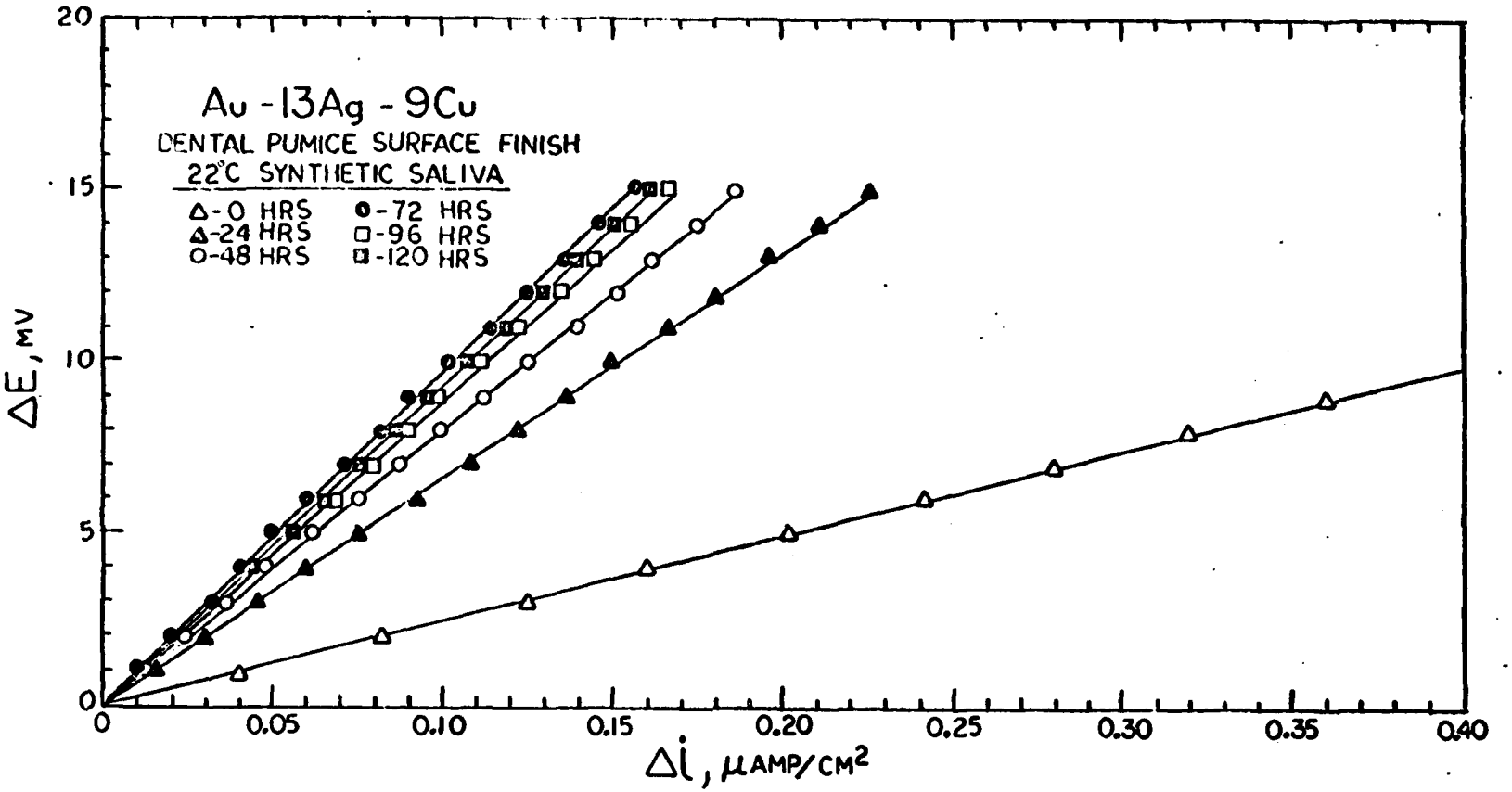

Figure 16. Effect of Time on the Galvanostatic Cathodic Linear-Polarization Curves for Au-13Ag-9Cu Dental Alloy in Aerated Synthetic Saliva at 22°C. Surface finished with Dental Pumice.

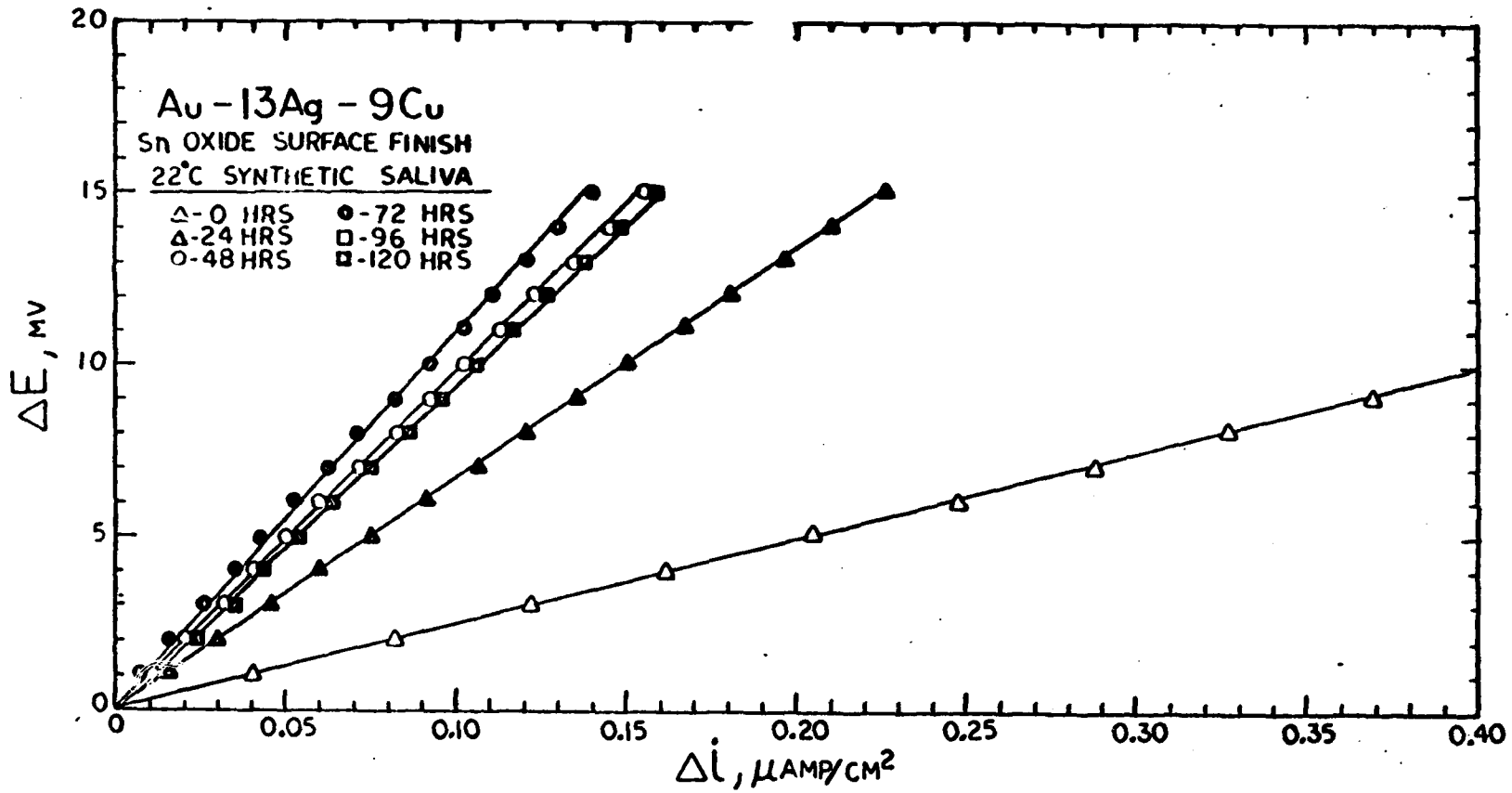

Figure 17. Effect of Time on the Galvanostatic Cathodic Linear-Polarization Curves for Au-13Ag-9Cu Dental Alloy in Aerated Synthetic Saliva at 22°C. Surface finished with Dental Tin-Oxide.

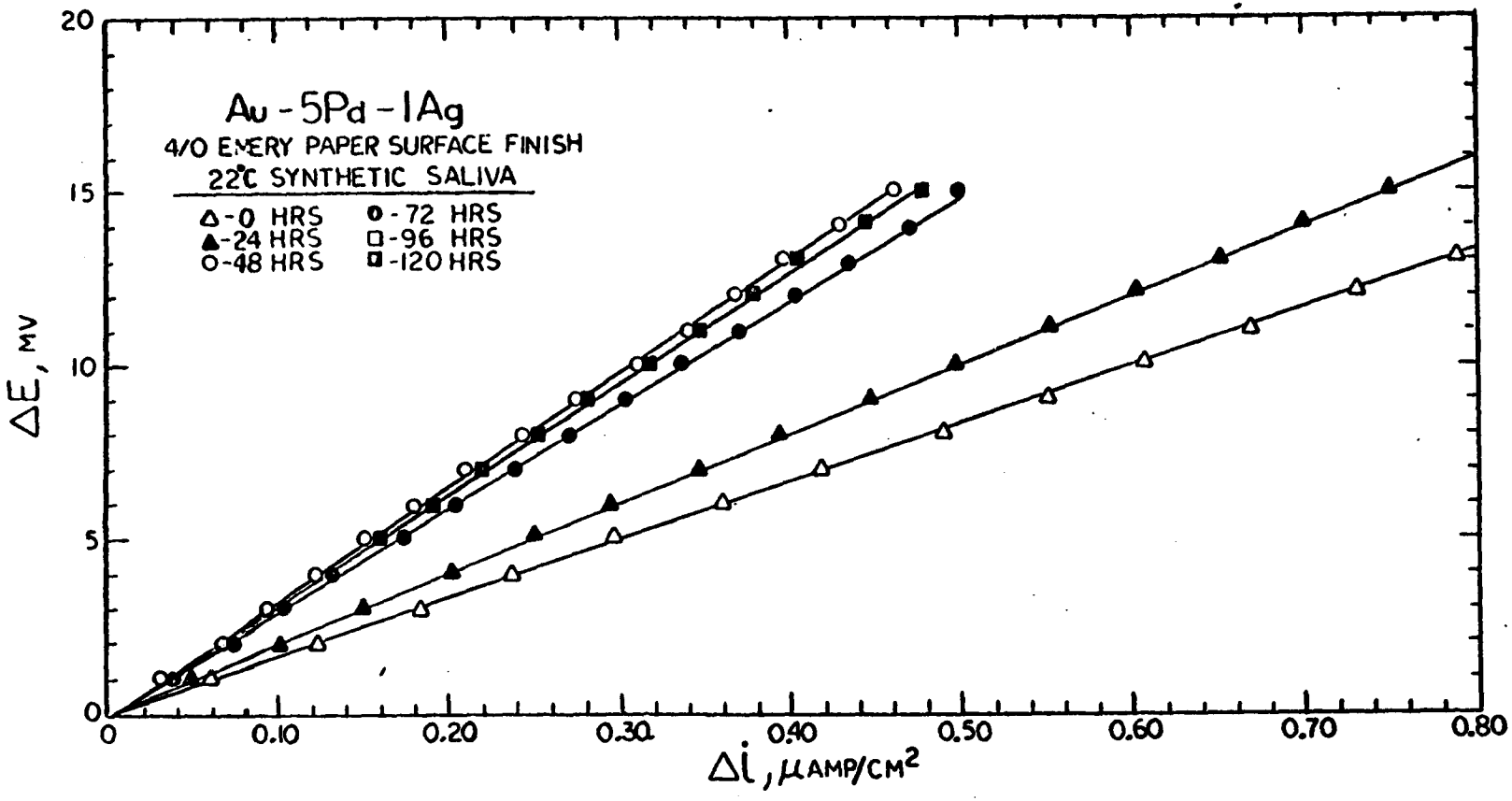

Figure 18. Effect of Time on the Galvanostatic Cathodic Linear-Polarization Curves for Au-5Pd-1Ag Dental Alloy in Aerated Synthetic Saliva at 22°C. Surface finished with 4/0 emery paper.

GAM/MC/71-11

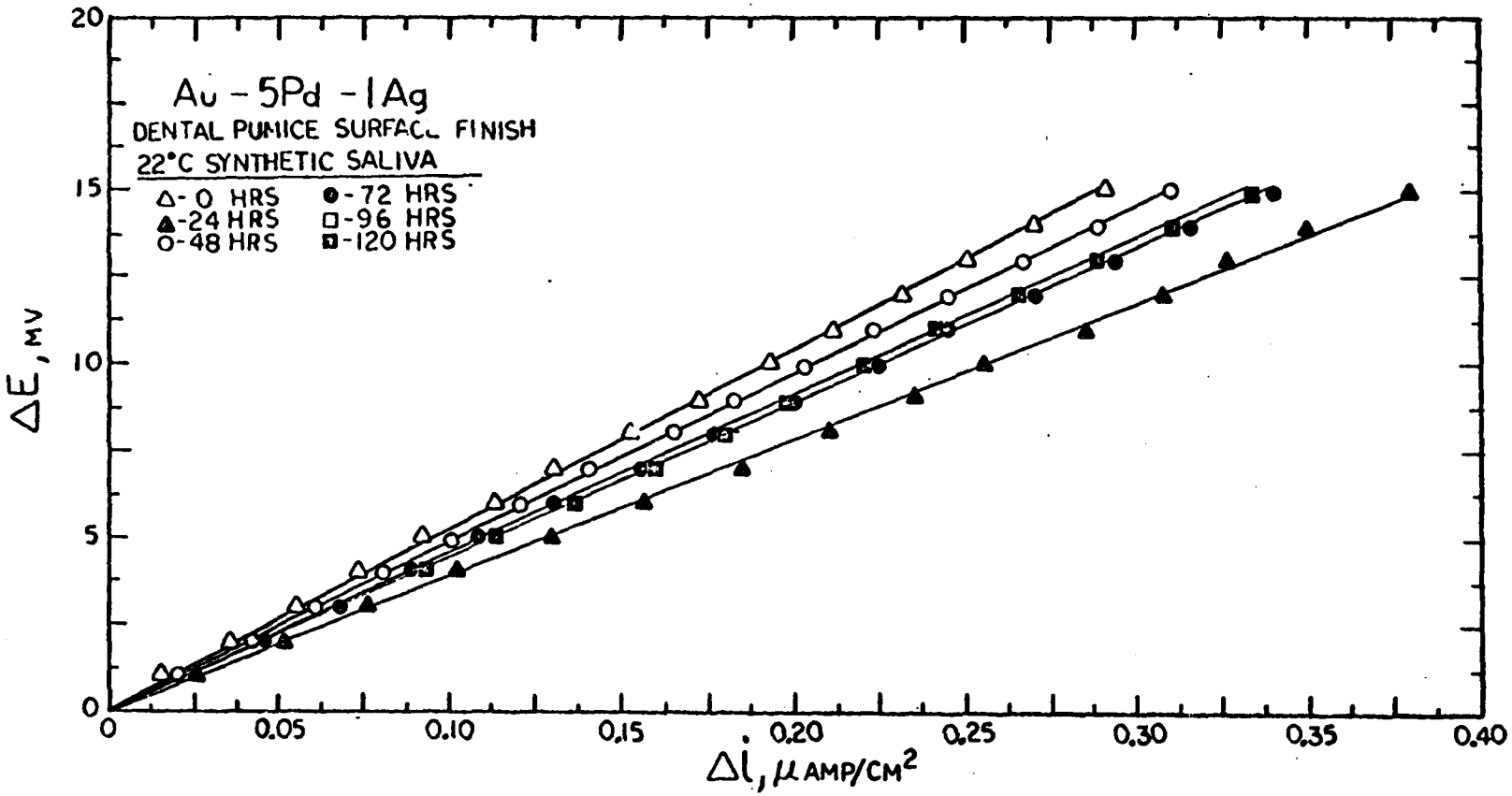

Figure 19. Effect of Time on the Galvanostatic Cathodic Linear-Polarization Curves for Au-5Pd-1Ag Dental Alloy in Aerated Synthetic Saliva at 22°C. Surface Finished with Dental Pumice.

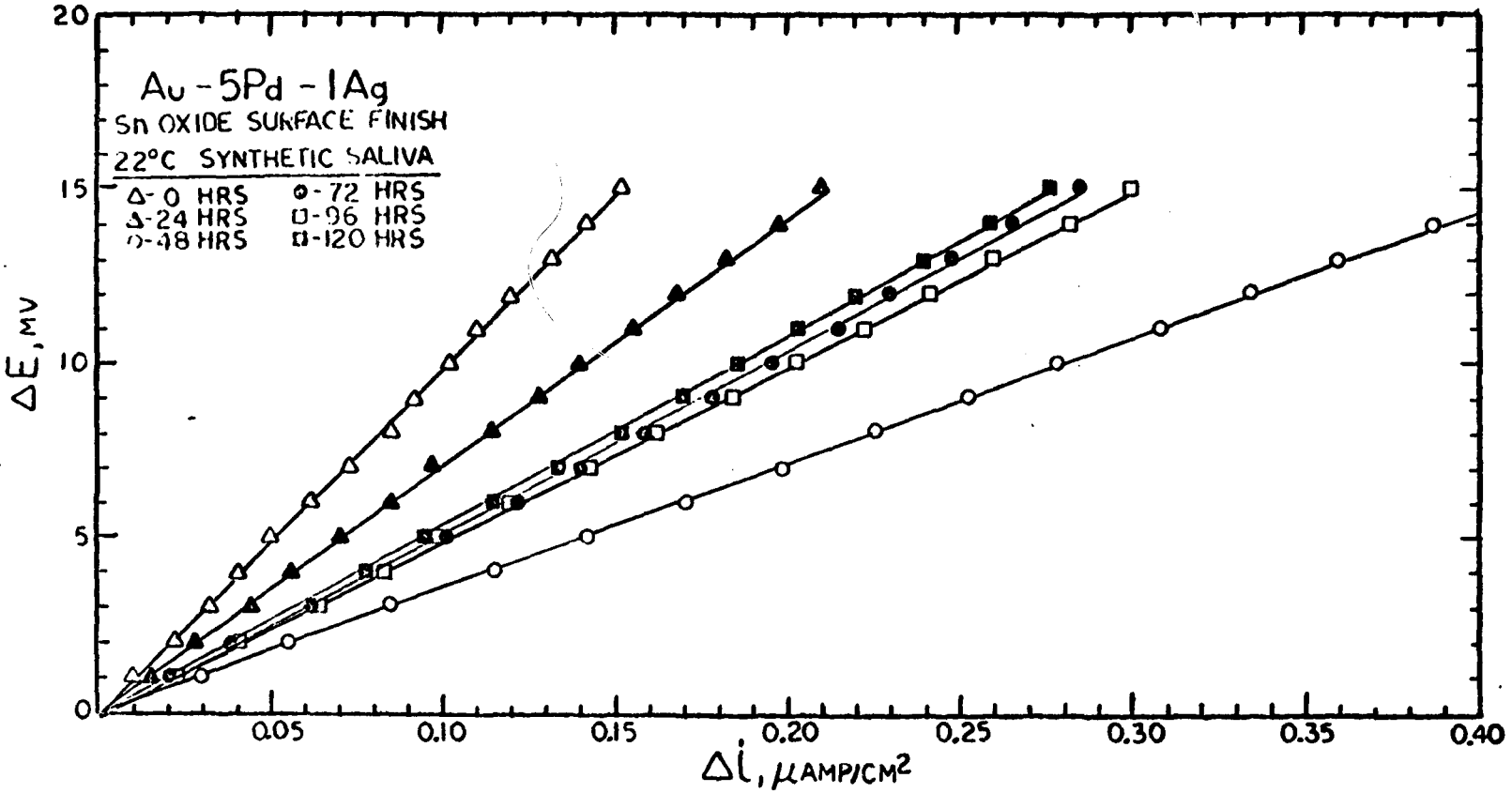

Figure 20. Effect of Time on the Galvanostatic Cathodic Linear-Polarization Curves for Au-5Pd-1Ag Dental Alloy in Aerated Synthetic Saliva at 22°C. Surface Finished with Dental Tin-Oxide.

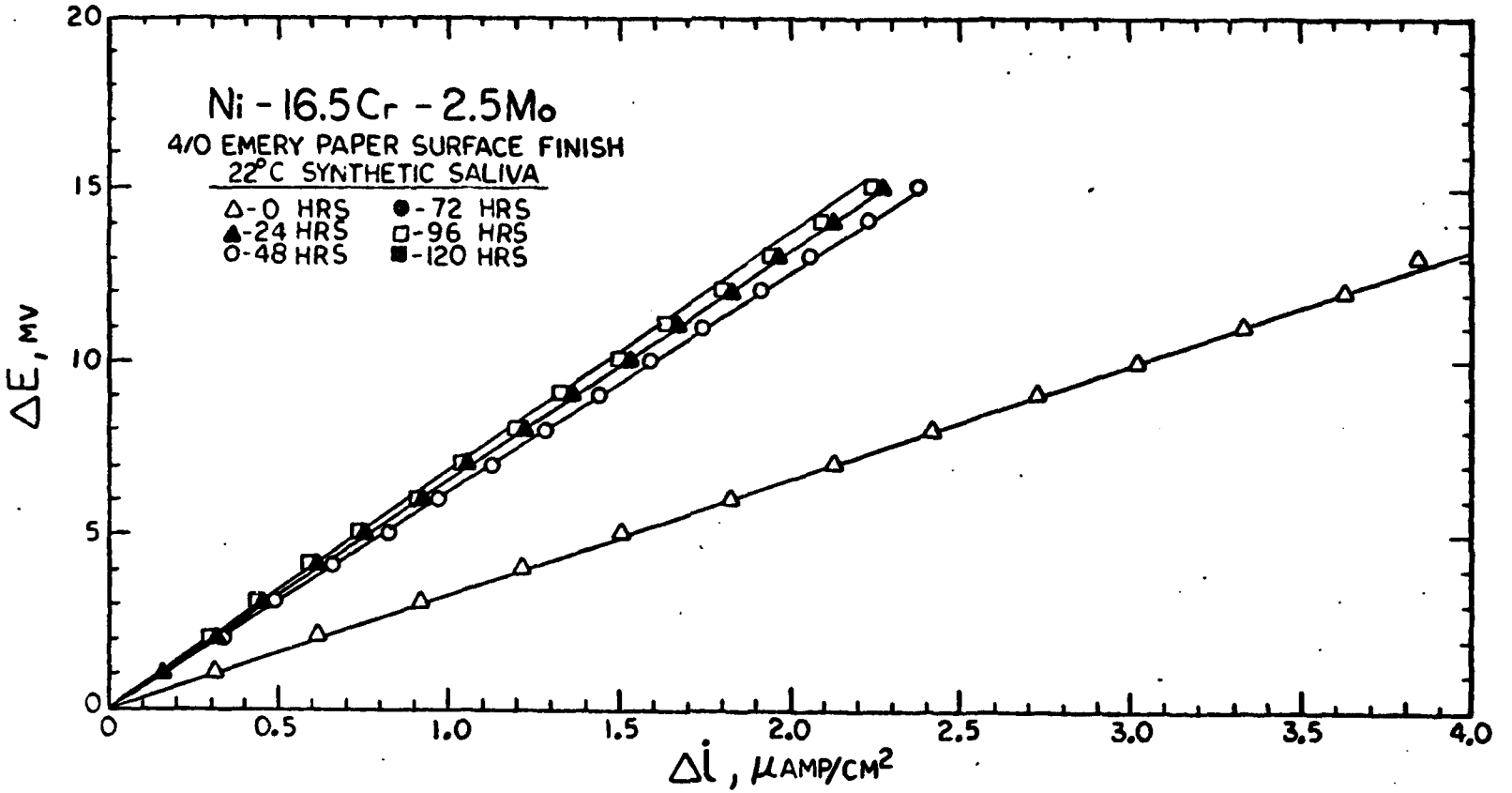

Figure 21. Effect of Time on the Galvanostatic Cathodic Linear-Polarization Curves for Ni-16.5Cr-2.5Mo Dental Alloy in Aerated Synthetic Saliva at 22°C. Surface Finished with 4/0 Emery Paper.

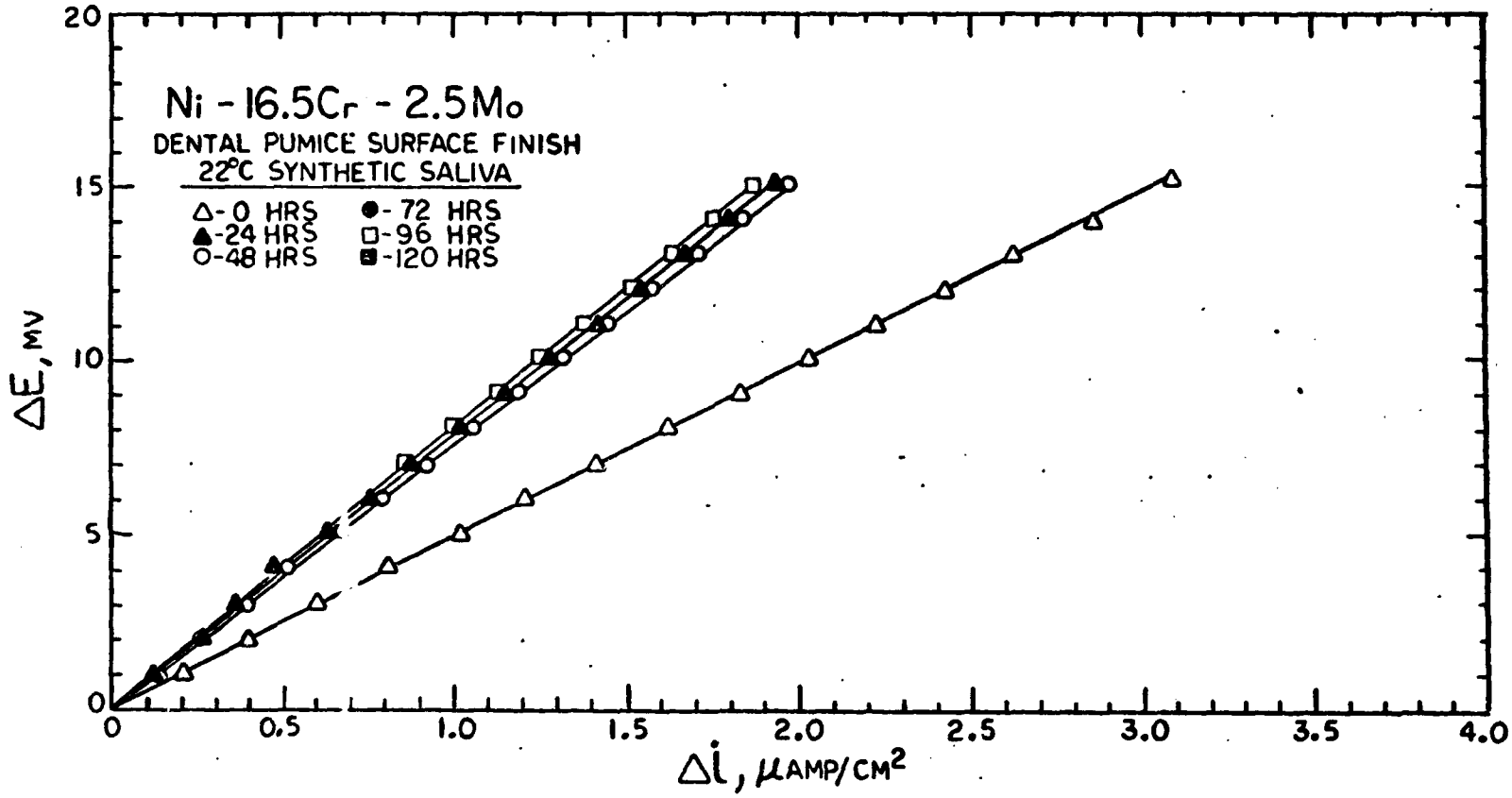

Figure 22. Effect of Time on the Galvanostatic Cathodic Linear-Polarization Curves for Ni-16.5Cr-2.5Mo Dental Alloy in Aerated Synthetic Saliva at 22°C. Surface Finished with Dental Pumice.

GAW/MC/71-11

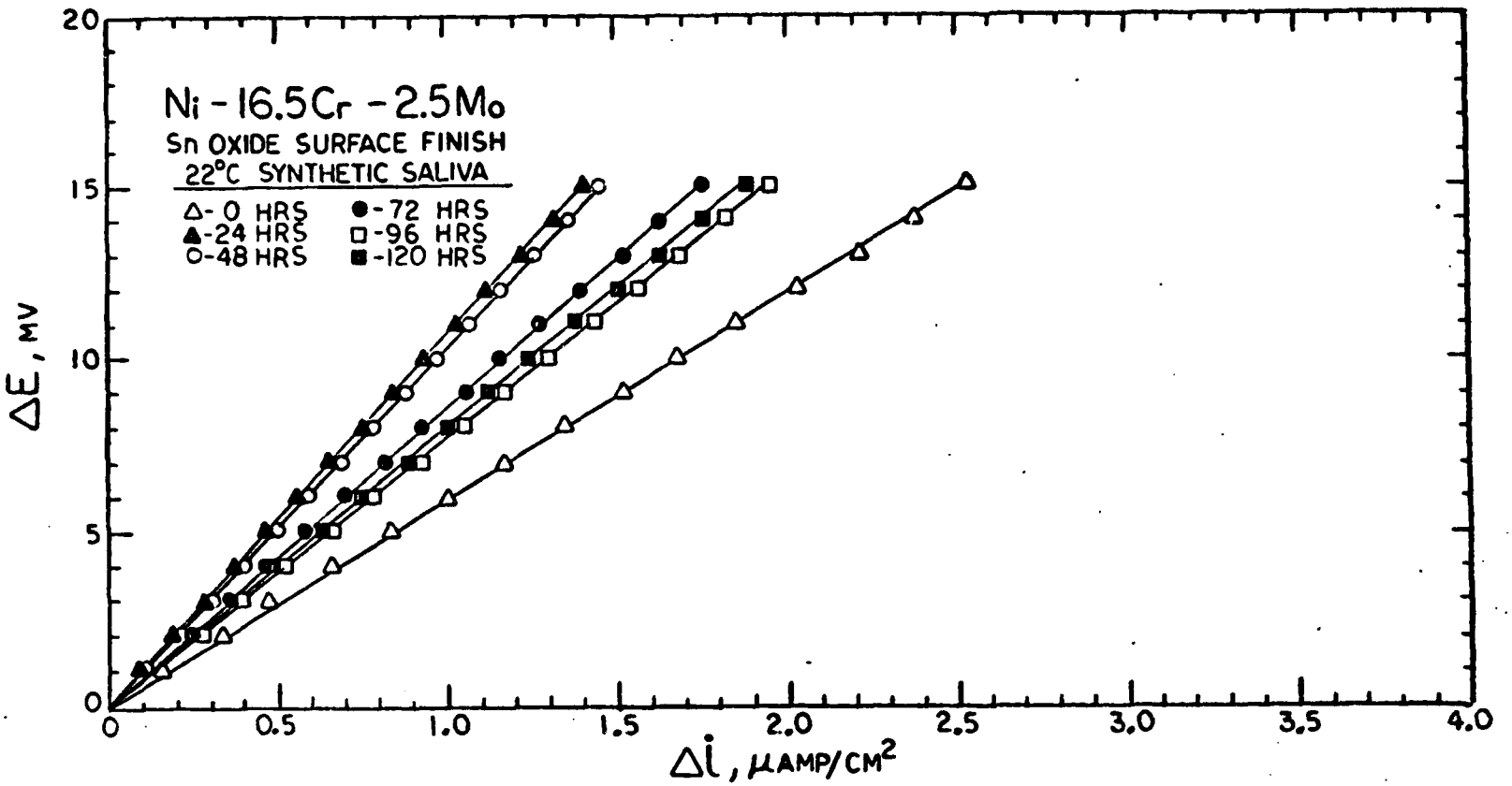

Figure 23. Effect of Time on the Galvanostatic Cathodic Linear-Polarization Curves for Ni-16.5Cr-2.5Mo Dental Alloy in Aerated Synthetic Saliva at 22°C. Surface finished with Dental Tin-Oxide.

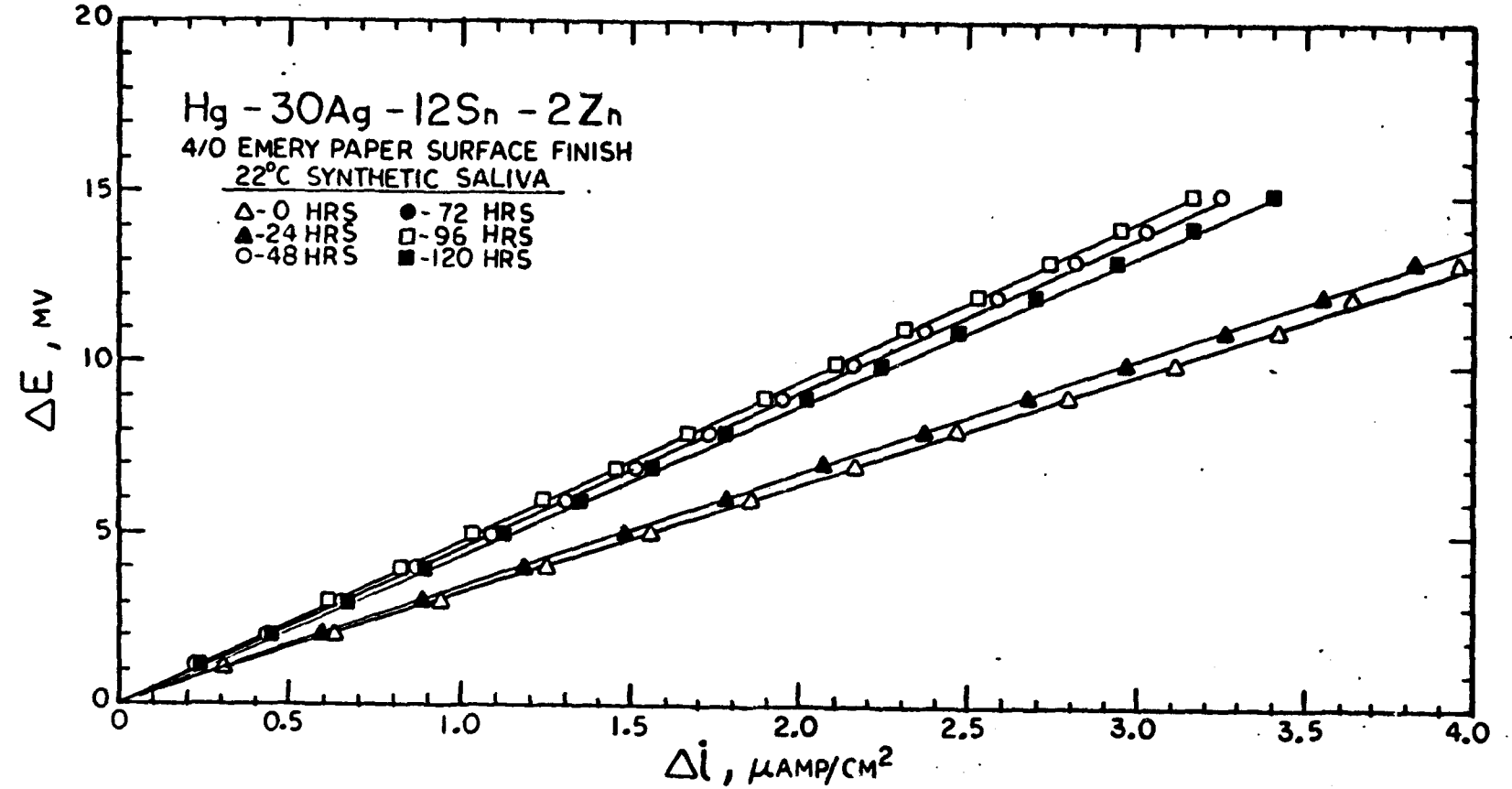

Figure 24. Effect of Time on the Galvanostatic Cathodic Linear-Polarization Curves for Hg-30Ag-12Sn-2Zn Dental Alloy in Aerated Synthetic Saliva at 22°C. Surface Finished with 4/0 Emery Paper.

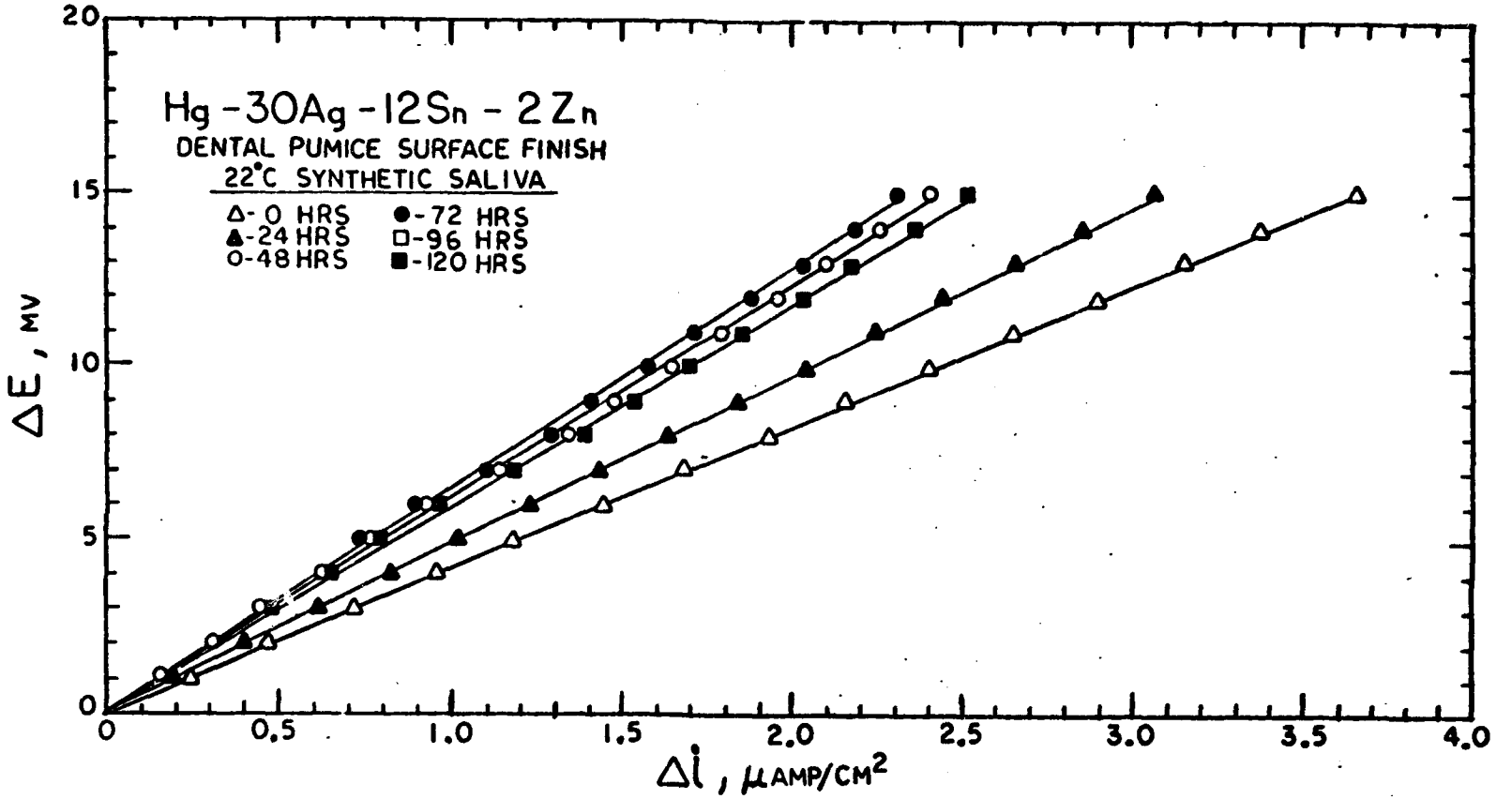

Figure 25. Effect of Time on the Galvanostatic Cathodic Linear-Polarization Curves for Hg-30Ag-12Sn-2Zn Dental Alloy in Aerated Synthetic Saliva at 22°C. Surface Finished with Dental Pumice.

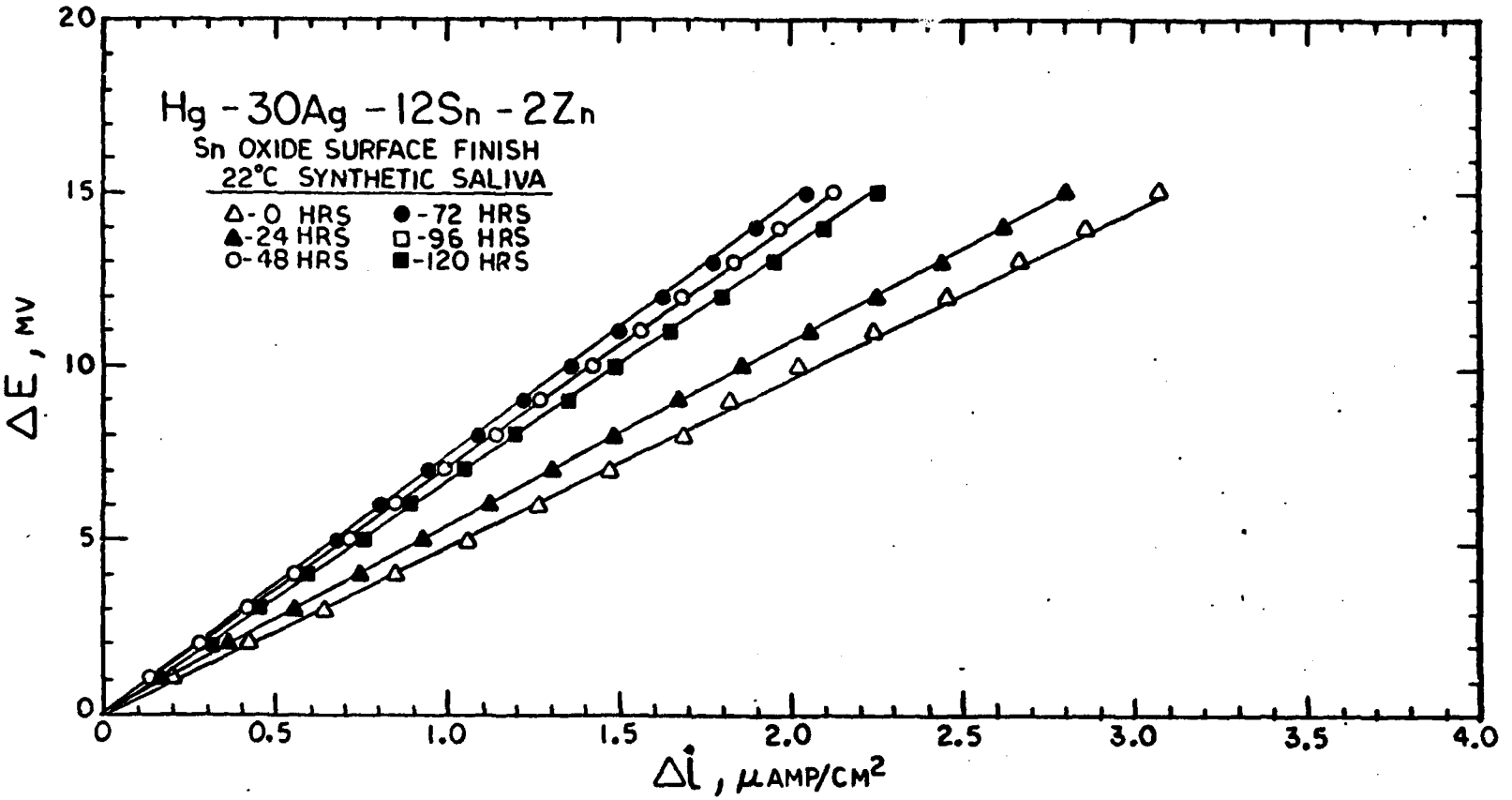

Figure 26. Effect of Time on the Galvanostatic Cathodic Linear-Polarization Curves for Hg-30Ag-12Sn-2Zn Dental Alloy in Aerated Synthetic Saliva at 22°C. Surface Finished with Dental Tin-Oxide.

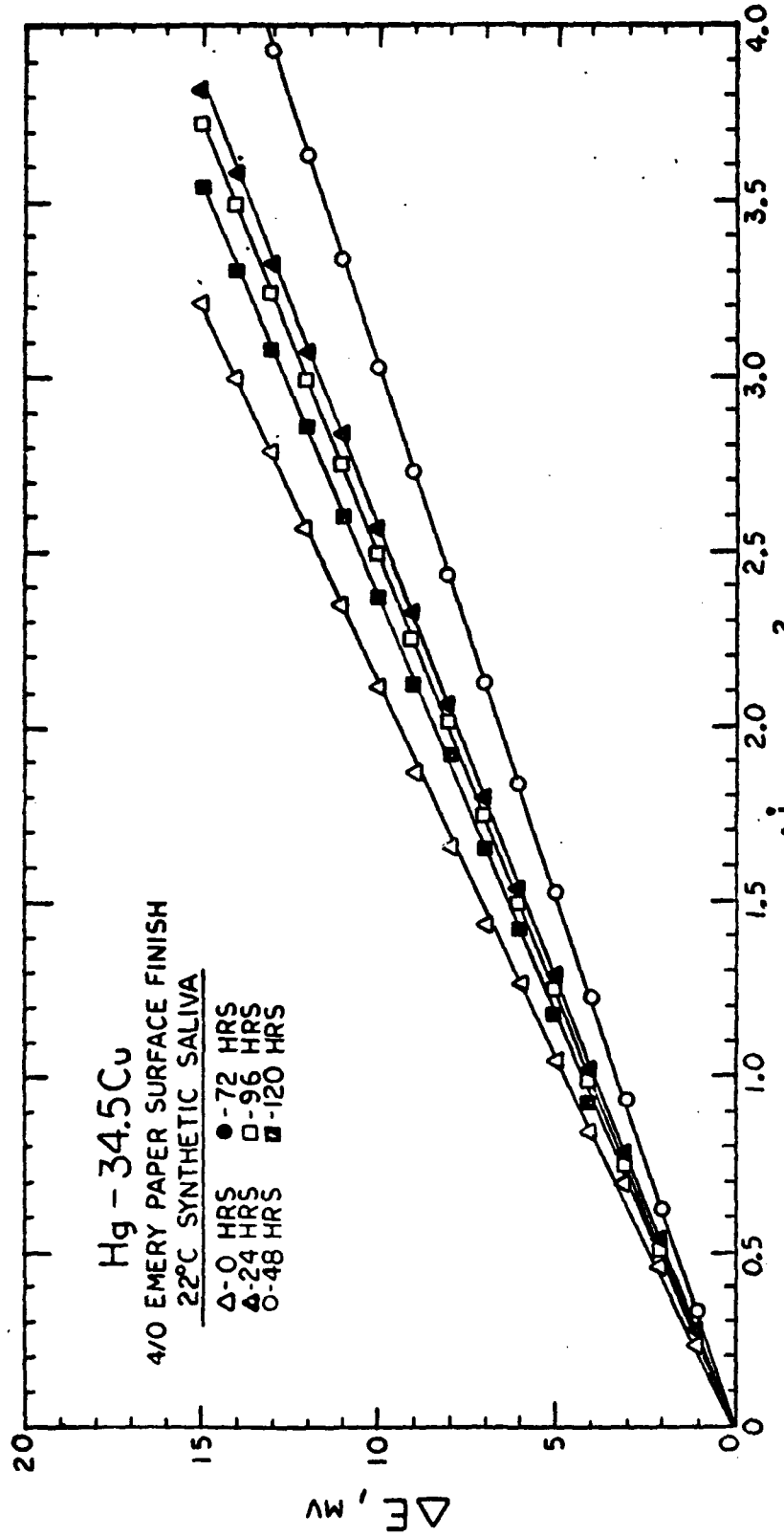

Figure 27. Effect of Time on the Galvanostatic Cathodic Linear-Polarization Curves for Hg-34.5Cu Dental Alloy in Aerated Synthetic Saliva at 22°C. Surface Finished with 4/0 Emery Paper.

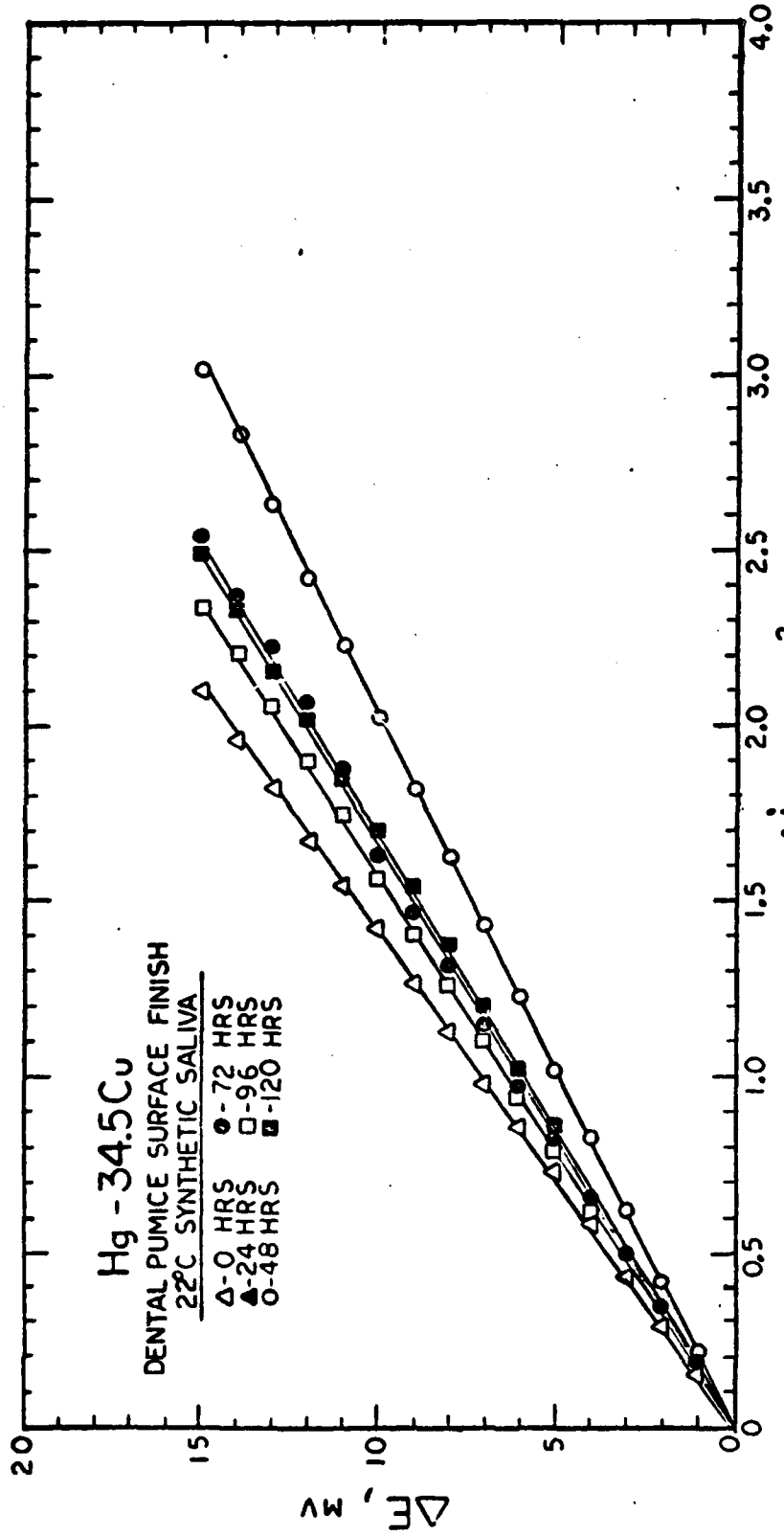

Figure 28. Effect of Time on the Galvanostatic Cathodic Linear-Polarization Curves for Hg-34.5Cu Dental Alloy in Aerated Synthetic Saliva at 22°C. Surface Finished with Dental Pumice.

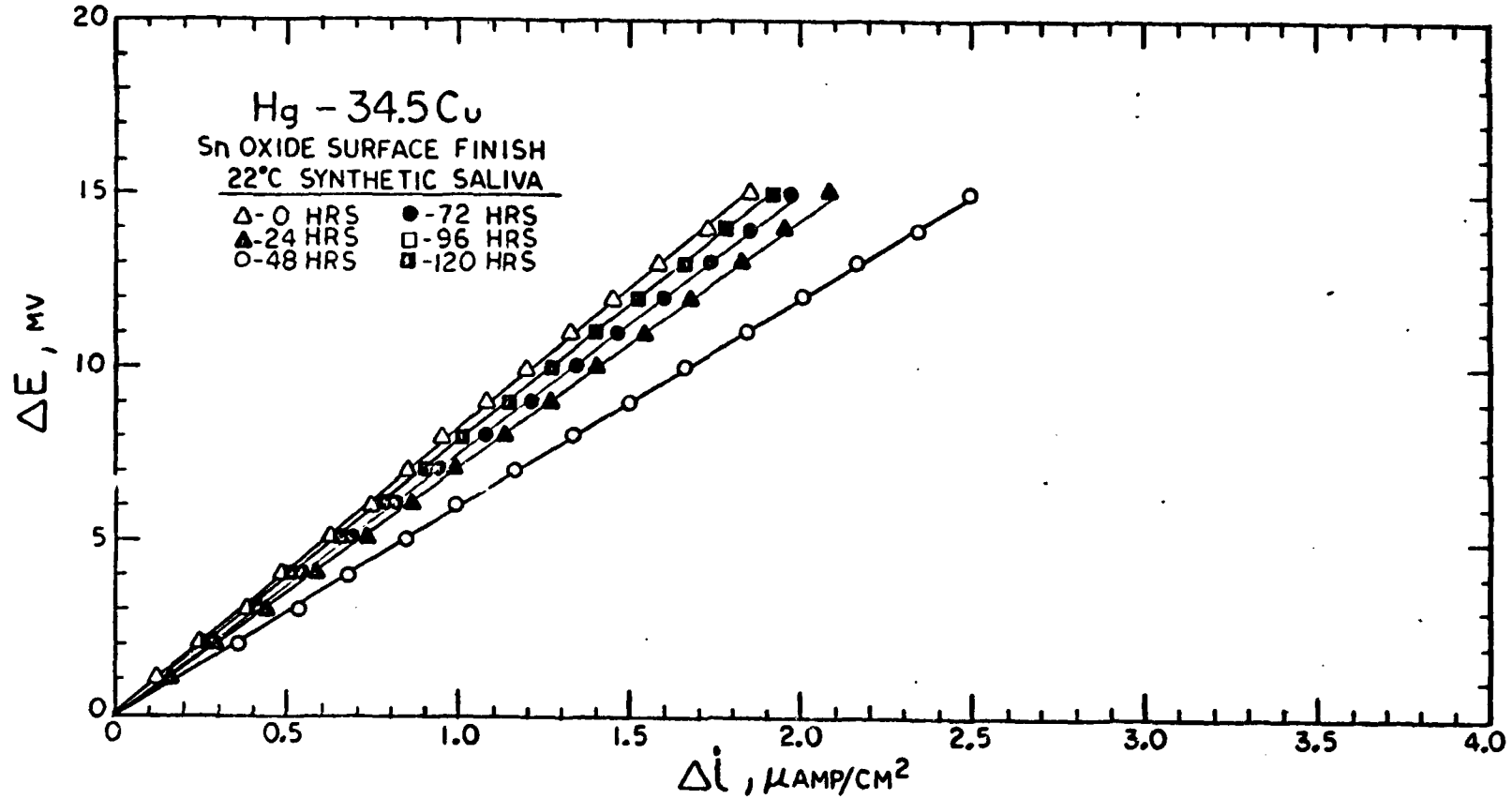

Figure 29. Effect of Time on the Galvanostatic Cathodic Linear-Polarization Curves for Hg-34.5Cu Dental Alloy in Aerated Synthetic Saliva at 22°C. Surface Finished with Dental Tin-Oxide.

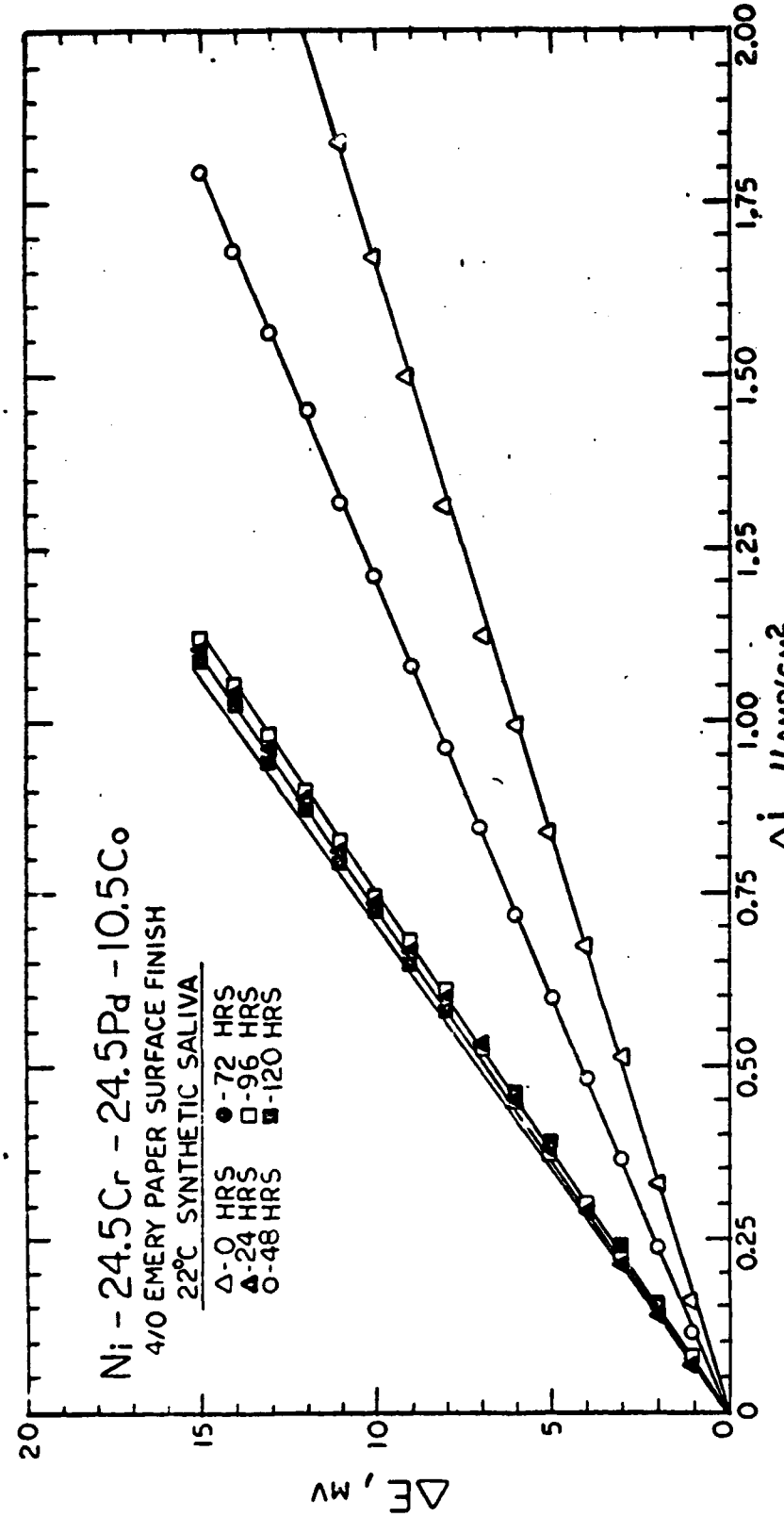

Figure 30. Effect of Time on the Galvanostatic Cathodic Linear-Polarization Curves for Ni-24.5Cr-24.5Pd-10.5Co Dental Alloy in Aerated Synthetic Saliva at 22°C. Surface Finished with 4/0 Emery Paper.

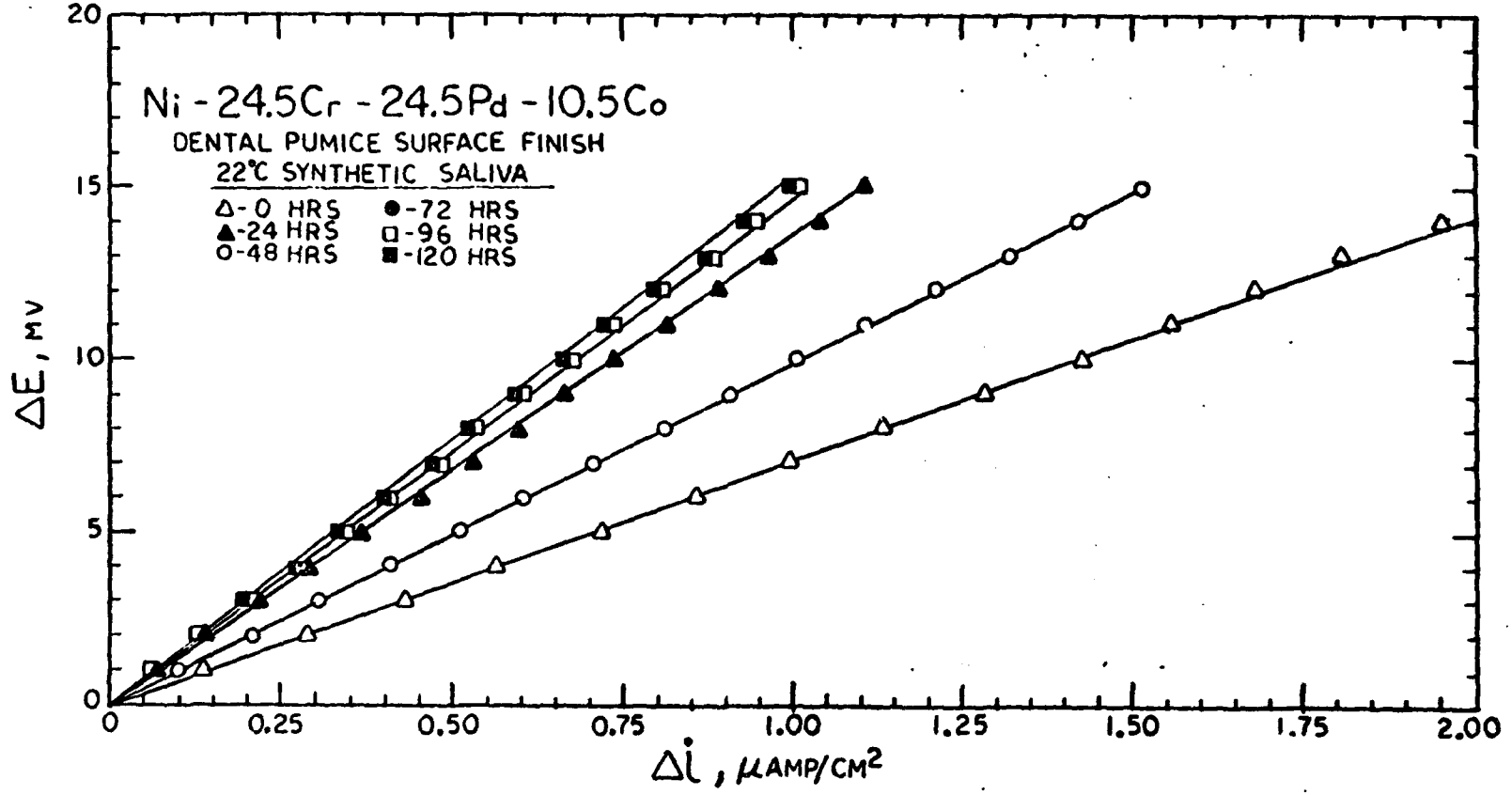

GAW/MC/71-11

Figure 31. Effect of Time on the Galvanostatic Cathodic Linear-Polarization Curves for Ni-24.5Cr-24.5Pd-10.5Co Dental Alloy in Aerated Synthetic Saliva at 22°C. Surface Finished with Dental Pumice.

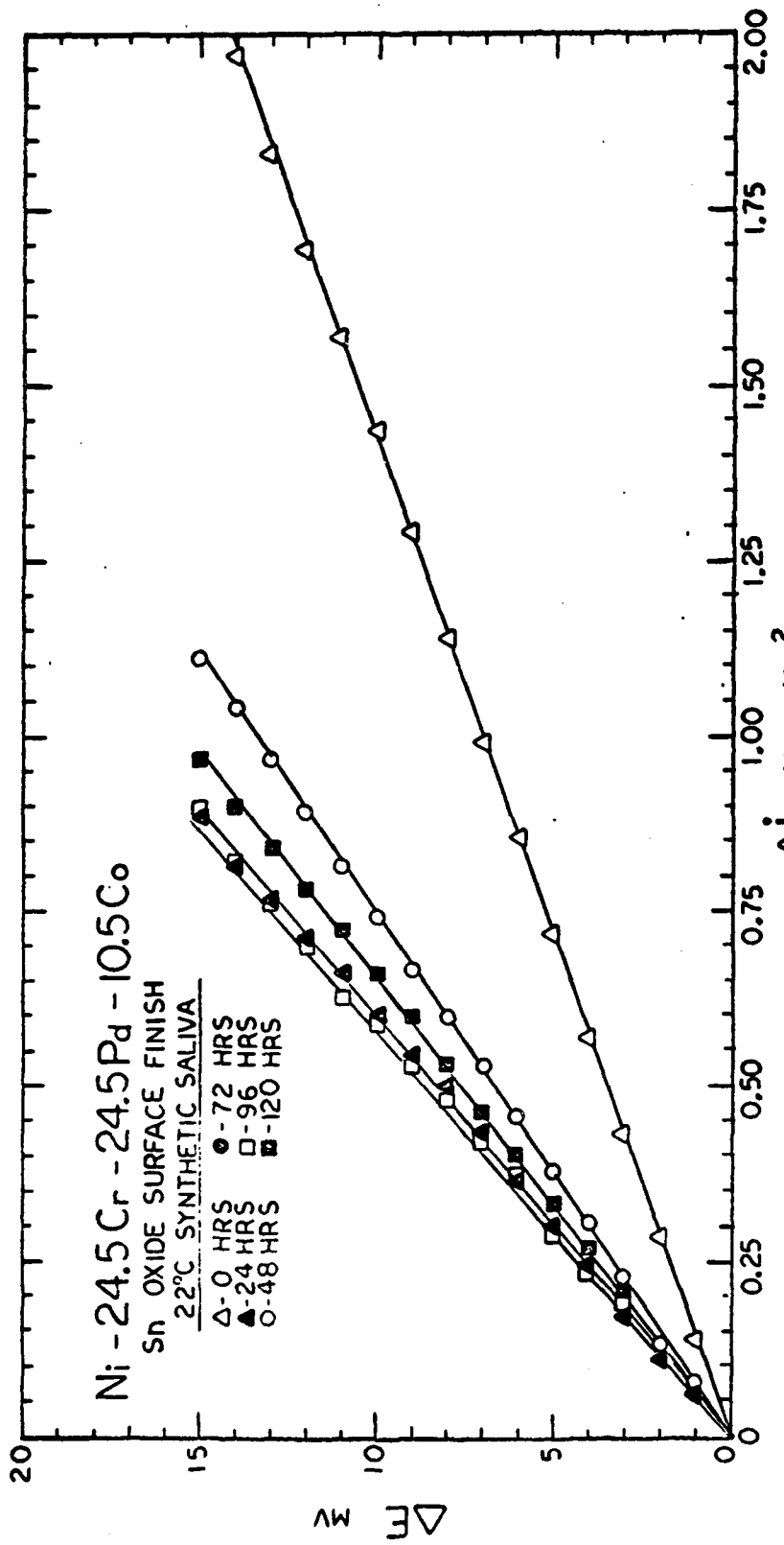

Figure 32. Effect of Time on the Galvanostatic Cathodic Linear-Polarization Curves for Ni-24.5Cr-24.5Pd-10.5Co Dental Alloy in Aerated Synthetic Saliva at 22°C. Surface Finished with Dental Tin-Oxide.

Table IV

Effect of Time and Surface Finish on Corrosion-Current Densities (ma/cm^2) for Dental Alloys in Aerated Synthetic Saliva at 22°C

Alloy	0 Hrs.	24 Hrs.	48 Hrs.	72 Hrs.	96 Hrs.	120 Hrs.
*Au-13Ag-9Cu	0.00147	0.00047	0.00036	0.00038	0.00037	0.00038
**Au-13Ag-9Cu	0.00114	0.00042	0.00036	0.00029	0.00030	0.00031
***Au-13Ag-9Cu	0.00116	0.00042	0.00029	0.00026	0.00027	0.00029
*Au-5Pd-1Ag	0.00184	0.00151	0.00095	0.00103	0.00095	0.00094
**Au-5Pd-1Ag	0.00061	0.00078	0.00061	0.00068	0.00068	0.00067
***Au-5Pd-1Ag	0.00031	0.00043	0.00085	0.00060	0.00061	0.00061
*Ni-16.5Cr-2.5Mo	0.00459	0.00231	0.00241	0.00231	0.00232	0.00233
**Ni-16.5Cr-2.5Mo	0.00307	0.00195	0.00198	0.00192	0.00200	0.00200
***Ni-16.5Cr-2.5Mo	0.00257	0.00142	0.00146	0.00177	0.00198	0.00190

*Surface finished with 4/0 Emery Paper
**Surface finished with Dental Pumice
***Surface finished with Dental Tin-Oxide

Table IV
(Cont.)

Alloy	0 Hrs.	24 Hrs.	48 Hrs.	72 Hrs.	96 Hrs.	120 Hrs.
*Hg-30Ag-12Sn-2Zn	0.01082	0.01034	0.00751	0.00720	0.00744	0.00755
**Hg-30Ag-12Sn-2Zn	0.00835	0.00708	0.00510	0.00573	0.00573	0.00574
***Hg-30Ag-12Sn-2Zn	0.00701	0.00648	0.00492	0.00494	0.00517	0.00518
*Hg-34.5Cu	0.00776	0.00998	0.01114	0.00930	0.00926	0.00928
**Hg-34.5Cu	0.00520	0.00599	0.00742	0.00602	0.00616	0.00618
***Hg-34.5Cu	0.00444	0.00519	0.00616	0.00527	0.00540	0.00534
*Ni-24.5Cr-24.5Pd-10.5Co	0.00254	0.00113	0.00184	0.00113	0.00113	0.00114
**Ni-24.5Cr-24.5Pd-10.5Co	0.00218	0.00113	0.00154	0.00102	0.00103	0.00102
***Ni-24.5Cr-24.5Pd-10.5Co	0.00218	0.00091	0.00113	0.00089	0.00091	0.00099

*Surface finished with 4/0 Emery Paper
**Surface finished with Dental Pumice
***Surface finished with Dental Tin-Oxide

obtained from the potentiostatic, anodic polarization curves (Figures 34-45). Calculations were performed on an IBM 1620 digital computer using the computer program described in Appendix A.

In general, it was observed that the corrosion-current densities decreased with increasing smoothness of the surface finish. The two amalgams had similar steady-state corrosion current densities. However, the variance with time of the corrosion-current densities were not similar. The steady-state corrosion-current density (7.5 μamp/cm^2) of the Ag-Sn amalgam (surface finished with 4/0 emery paper) compared well with the 9 μamp/cm^2 reported by earlier investigators[24] using the Tafel-slope extrapolation method.

Of the two nickel-base alloys, the alloy containing palladium and the higher chromium content exhibited lower corrosion-current densities for all test times. The two gold alloys exhibited the lowest corrosion-current densities of any alloy studied.

Occasionally, some of the tests were repeated to check data reproducibility. Reproducibility of the linear-polarization data was considered excellent. This is in agreement with the findings of other investigators[10,11,14]. It was also found that polarization data obtained on separate specimens of the same alloy were highly reproducible. Occasional checks on the polarization resistance ($\Delta E/\Delta i$) several days after testing showed that this value had not changed significantly from the previously recorded steady-state value.

The effect of raising the electrolyte temperature to 98.6°F (on corrosion-current densities and corrosion rates) was insignificant for the two alloys tested, and the data are not included in Table IV. However, the open-circuit corrosion potentials of these alloys did shift slightly to more active values (Table III).

Corrosion Rates

Corrosion rates were obtained using the i_{corr} values and Faraday's Law (Equation 3). Corrosion rates are given in Table V. The calculations were performed on an IBM 1620 digital computer using the computer program in Appendix A. For these calculations, all metal elements were assumed to go into solution in their most stable valence state.

There was no definite time dependent pattern for the corrosion rates of the six dental alloys tested; however, in most cases the steady-state corrosion rate was established within 48 to 96 hours and had a value lower than the initial (0 hour) corrosion rate. The lowest corrosion rates were exhibited by the gold alloys. However, the steady-state corrosion rate of the gold alloy having a high silver content was lower than that of the other gold alloy by almost a factor of two. Of the two nickel-base alloys, the alloy containing palladium and a higher chromium content had a lower steady-state corrosion rate by almost a factor of two.

The highest corrosion rates were exhibited by the two amalgam alloys. However, a surprising result was that the copper amalgam exhibited a slightly lower steady-state

Table V

Effect of Time and Surface Finish on

Corrosion Rates (microns per year) for Dental

Alloys in Aerated Synthetic Saliva at 22°C

Alloy	0 Hrs.	24 Hrs.	48 Hrs.	72 Hrs.	96 Hrs.	120 Hrs.
*Au-13Ag-9Cu	20.50	6.543	5.045	5.282	5.203	5.282
**Au-13Ag-9Cu	15.84	5.912	4.966	4.020	4.178	4.257
***Au-13Ag-9Cu	16.16	5.912	4.020	3.626	3.784	4.099
*Au-5Pd-1Ag	21.15	17.38	10.89	11.80	10.96	10.82
**Au-5Pd-1Ag	6.981	8.936	7.051	7.819	7.819	7.679
***Au-5Pd-1Ag	3.560	4.887	9.704	6.842	7.051	6.981
*Ni-16.5Cr-2.5Mo	47.03	23.70	24.69	23.62	23.77	23.84
**Ni-16.5Cr-2.5Mo	31.50	19.98	20.30	19.68	20.51	20.51
***Ni-16.5Cr-2.5Mo	26.39	14.53	14.92	18.17	20.32	19.49

*Surface finished with 4/0 emery paper
**Surface finished with Dental Pumice
***Surface finished with Dental Tin-Oxide

Table V
(Cont.)

Alloy	0 Hrs.	24 Hrs.	48 Hrs.	72 Hrs.	96 Hrs.	120 Hrs.
*Hg-30Ag-12Sn-2Zn	287.3	274.4	199.4	191.1	197.4	200.3
**Hg-30Ag-12Sn-2Zn	221.5	187.9	151.2	151.9	152.1	152.3
***Hg-30Ag-12Sn-2Zn	186.1	171.9	130.5	131.1	137.1	137.5
*Hg-34.5Cu	128.8	165.5	184.8	154.3	153.6	153.9
**Hg-34.5Cu	86.20	99.32	123.1	99.94	102.3	102.5
***Hg-34.5Cu	73.57	86.08	102.1	87.43	89.52	88.66
*Ni-24.5Cr-24.5Pd-10.5Co	27.06	11.98	19.61	12.01	12.04	12.11
**Ni-24.5Cr-24.5Pd-10.5Co.	23.14	12.01	16.22	10.81	10.97	10.84
***Ni-24.5Cr-24.5Pd-10.5Co.	23.14	9.710	11.98	9.484	9.710	10.65

*Surface finished with 4/0 emery paper
**Surface finished with Dental Pumice
***Surface finished with Dental Tin-Oxide

corrosion rate for all surface finishes tested. As mentioned earlier, clinical evidence has shown that copper amalgam has a higher corrosion rate in the oral cavity than the Ag-Sn amalgam. It is believed that the lower corrosion rates found for the copper amalgam in this investigation is the result of not heating, triturating, and condensing the amalgam as would be done in normal dental practices. Without performing those operations, the Hg content was higher than would be found in a dental restoration of this amalgam. Thus, with the higher Hg content, the percentage of the less-noble copper was lower. In addition, the higher percentage of the Hg caused the amalgam to have a higher density; this would tend to lower the results of the Faraday Law calculations.

The steady-state corrosion rate of the Ag-Sn amalgam with the surface finished with 4/0 emery paper was 200.3 microns/yr. This was in close agreement with the 9 mils/yr (220.5 microns/yr) obtained in previous investigations of this amalgam[24]. This corrosion rate is higher than could be tolerated in any type of dental restoration. It appears that the conditions of the test cell do not take into account the high resistance of the external corrosion circuit in the true oral environment[24]. It is believed that the open-circuit corrosion potentials of the Ag-Sn amalgam in this investigation are probably representative of the true oral environment; however, in agreement with Guthrow[24], the corrosion rates are probably not representative.

In general, it can be seen in Table V that the corrosion rates decrease as the surface finish becomes smoother. The alloys which were affected most by surface finish were the amalgams. Corrosion rates for these materials when polished with dental tin-oxide dropped to approximately 60% of the value of the corrosion rates, obtained when the surface was finished with 4/0 emery paper.

Comparison of Computer Calculations

Using various values of β_a and β_c, Stern and Weisert[11] found that a log-log plot of corrosion-current density versus polarization resistance such as Figure 33 could be obtained. This figure shows the limits within which the relation between corrosion-current density and polarization resistance applies for most corroding systems.

Figure 33 was used to compare the computer calculations of the corrosion current densities found in this investigation. If beta values and $\Delta E/\Delta i$ are known for a corroding system, the approximate value of i_{corr} can be obtained using Figure 33. For example, Ag-Sn amalgam (surface finished with 4/0 emery paper) had a steady-state $\Delta E/\Delta i$ of $4.6 \times (10)^3$ ohm-cm^2 and from the potentiostatic polarization studies of this investigation $\beta_a = 0.080$, $\beta_c = \infty$; the i_{corr} from Figure 33 is approximately 9 μamp/cm^2. The actual value calculated, using the computer program in Appendix A, was 7.55 μamp/cm^2 which demonstrates excellent agreement. Similar agreement was obtained for all of the alloys investigated.

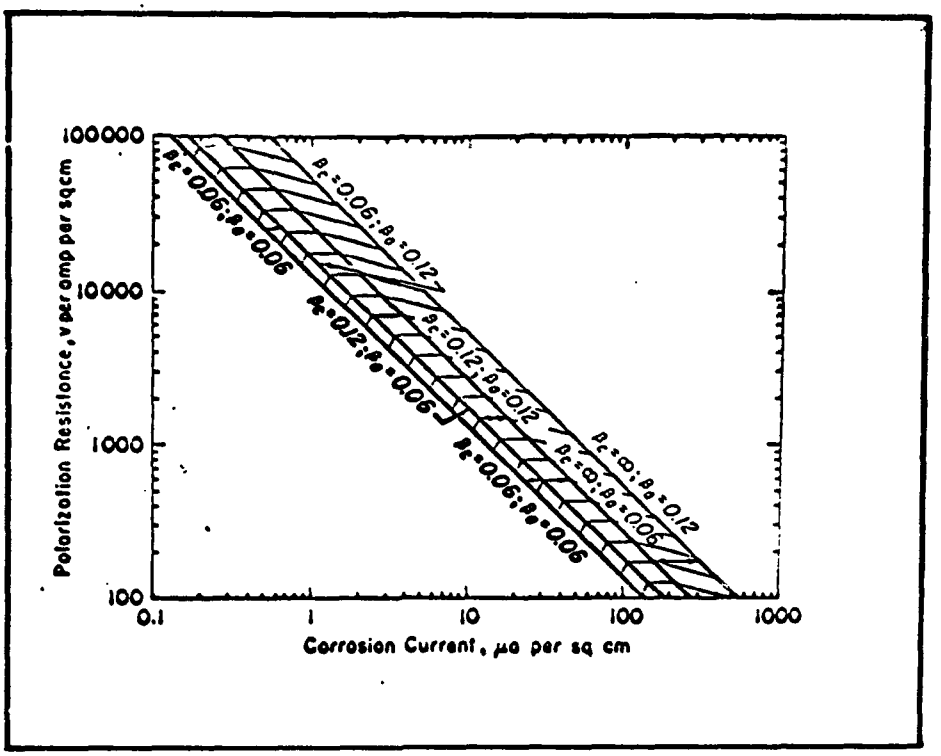

Figure 33. Limits Within Which the Relation Between Corrosion-Current Density and Polarization Resistance Applies for Most Real Systems (Ref 11)

Anodic and Cathodic Polarization Curves

Potentiostatic anodic and cathodic polarization curves (Figures 34 thru 45) were obtained for all of the specimens in aerated synthetic saliva at 22 ± 1°C. The only surface finish considered in these tests was that obtained by grinding with 4/0 emery paper. Reproducibility of curves for randomly-selected specimens was very good throughout the entire potential range. These consistent results can be attributed to the working electrode assembly (Figure 10) which places the surface of the specimen in a vertical plane. This prevented any accumulation of corrosion products (this

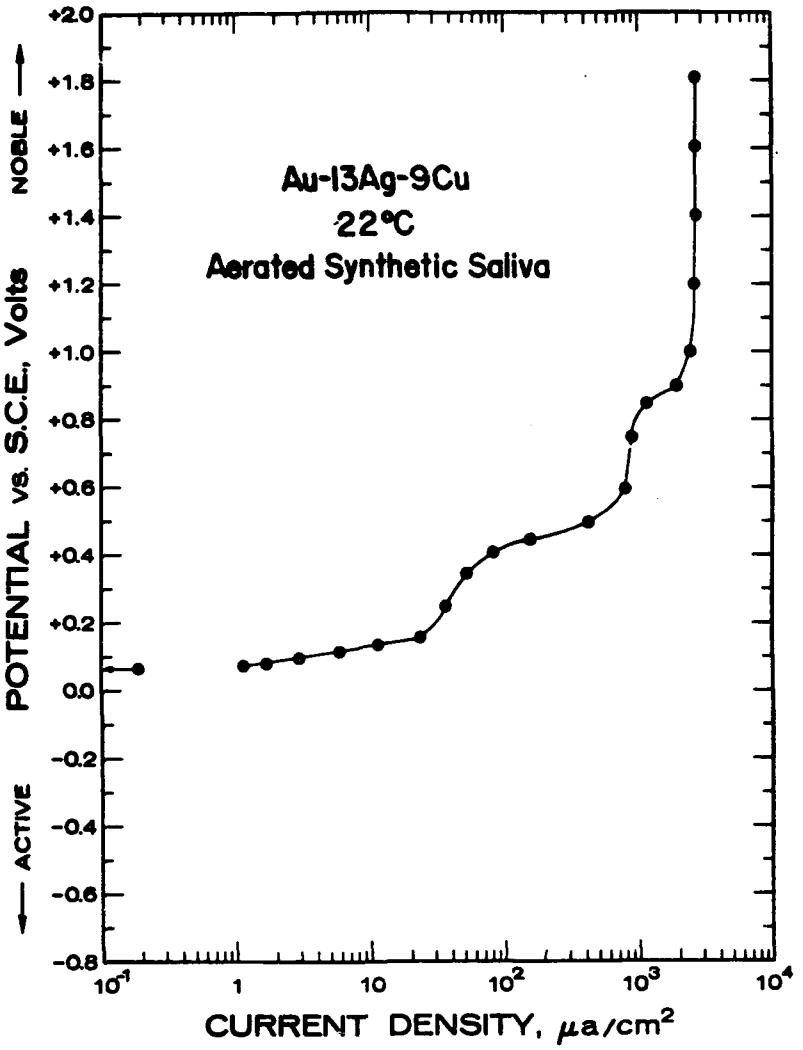

Figure 34. Potentiostatic Anodic Polarization Curve for Au-13Ag-9Cu Dental Alloy in Aerated Synthetic Saliva at 22° C.

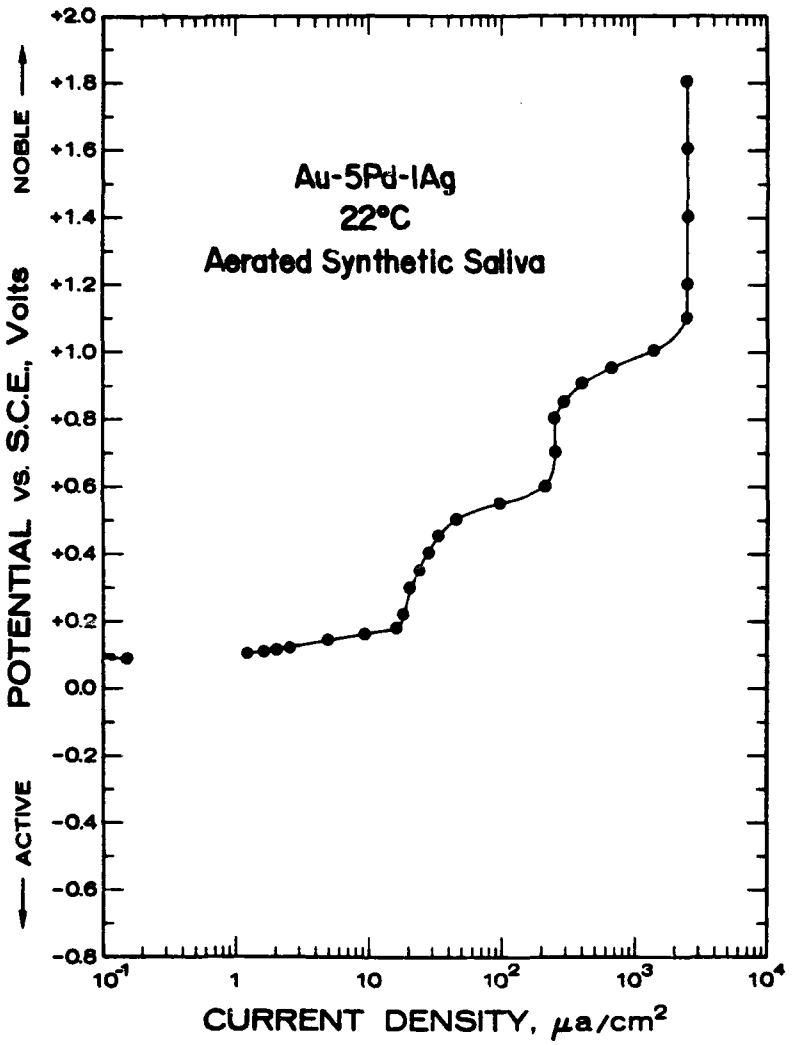

Figure 35. Potentiostatic Anodic Polarization Curve for Au-5Pd-1Ag Dental Alloy in Aerated Synthetic Saliva at 22°C.

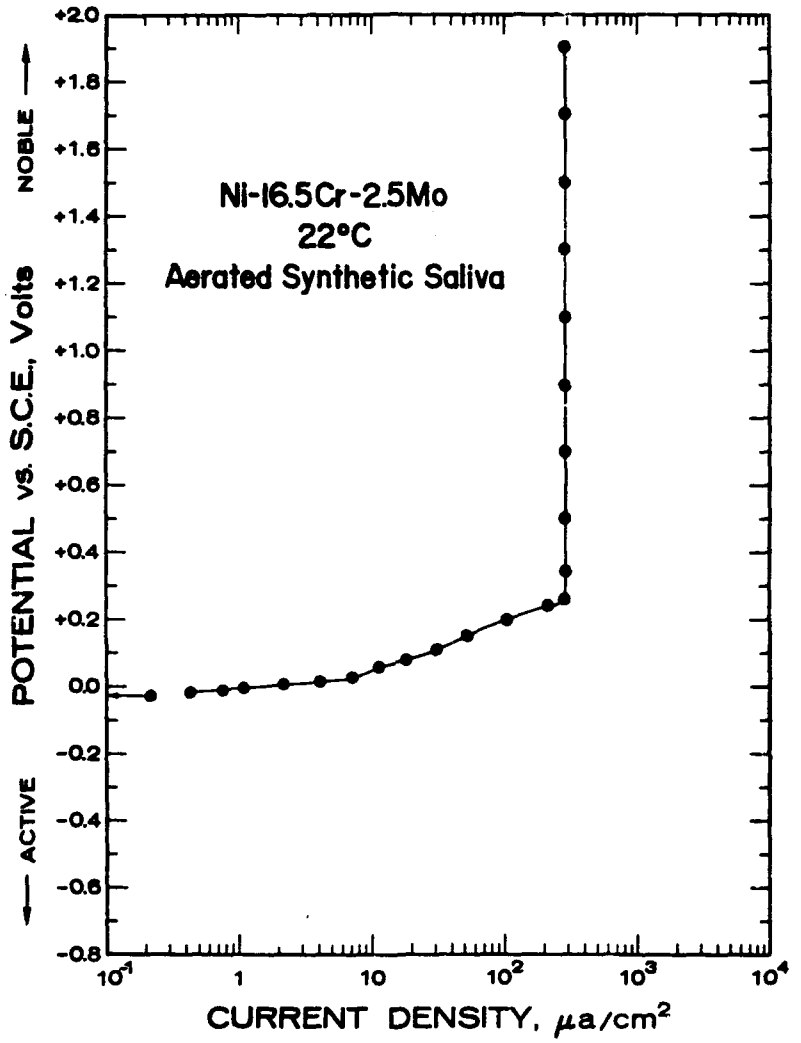

Figure 36. Potentiostatic Anodic Polarization Curve for Ni-16.5Cr-2.5Mo Dental Alloy in Aerated Synthetic Saliva at 22°C.

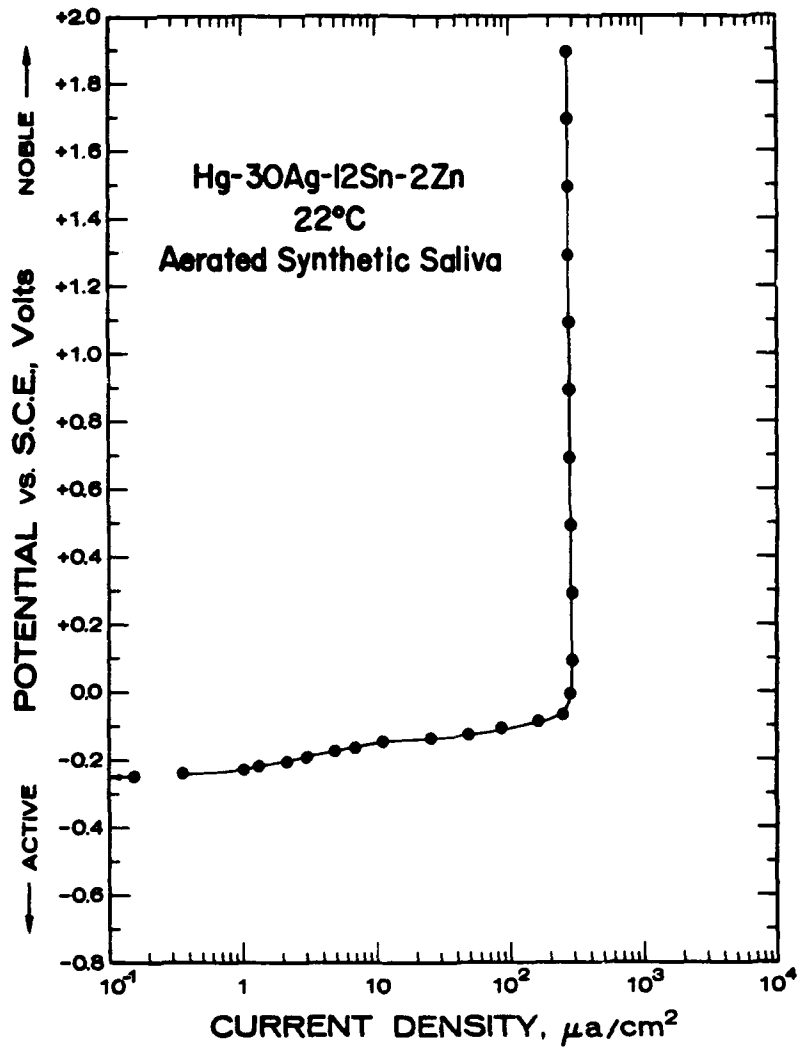

Figure 37. Potentiostatic Anodic Polarization Curve for Hg-30Ag-12Sn-2Zn Dental Alloy in Aerated Synthetic Saliva at 22°C.

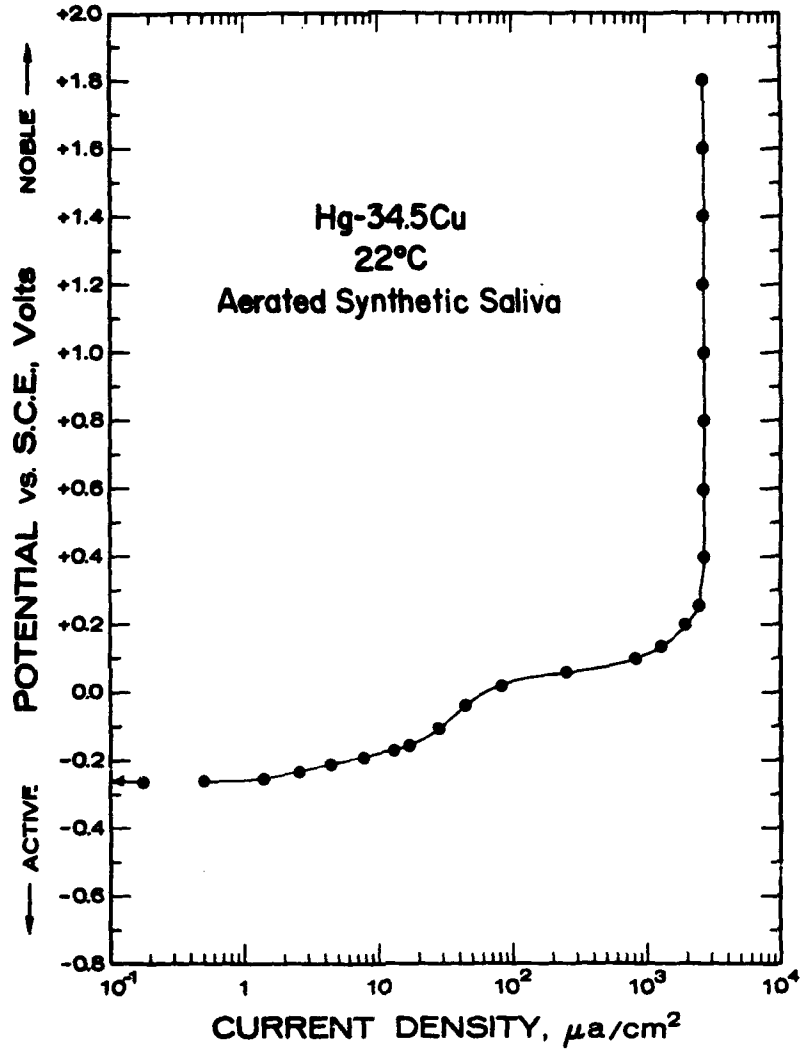

Figure 38. Potentiostatic Anodic Polarization Curve for Hg-34.5Cu Dental Alloy in Aerated Synthetic Saliva at 22° C.

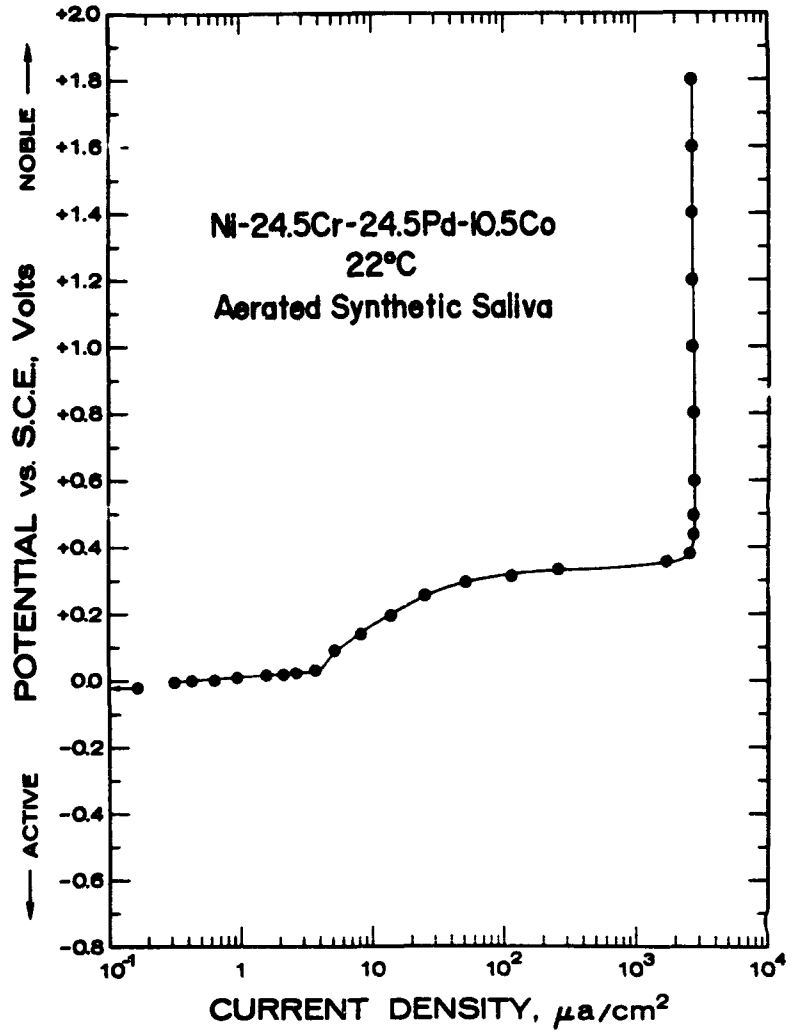

Figure 39. Potentiostatic Anodic Polarization Curve for Ni-24.5Cr-24.5Pd-10.5Co Dental Alloy in Aerated Synthetic Saliva at 22°C.

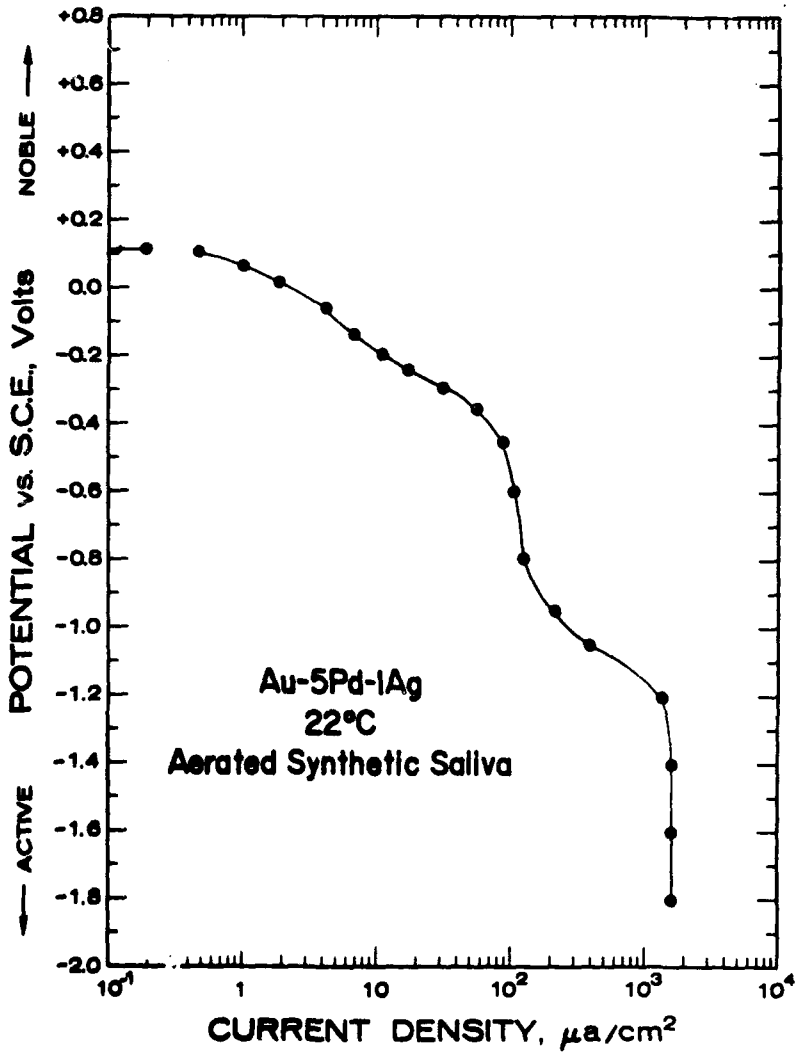

Figure 41. Potentiostatic Cathodic Polarization Curve for Au-5Pd-1Ag Dental Alloy in Aerated Synthetic Saliva at 22°C.

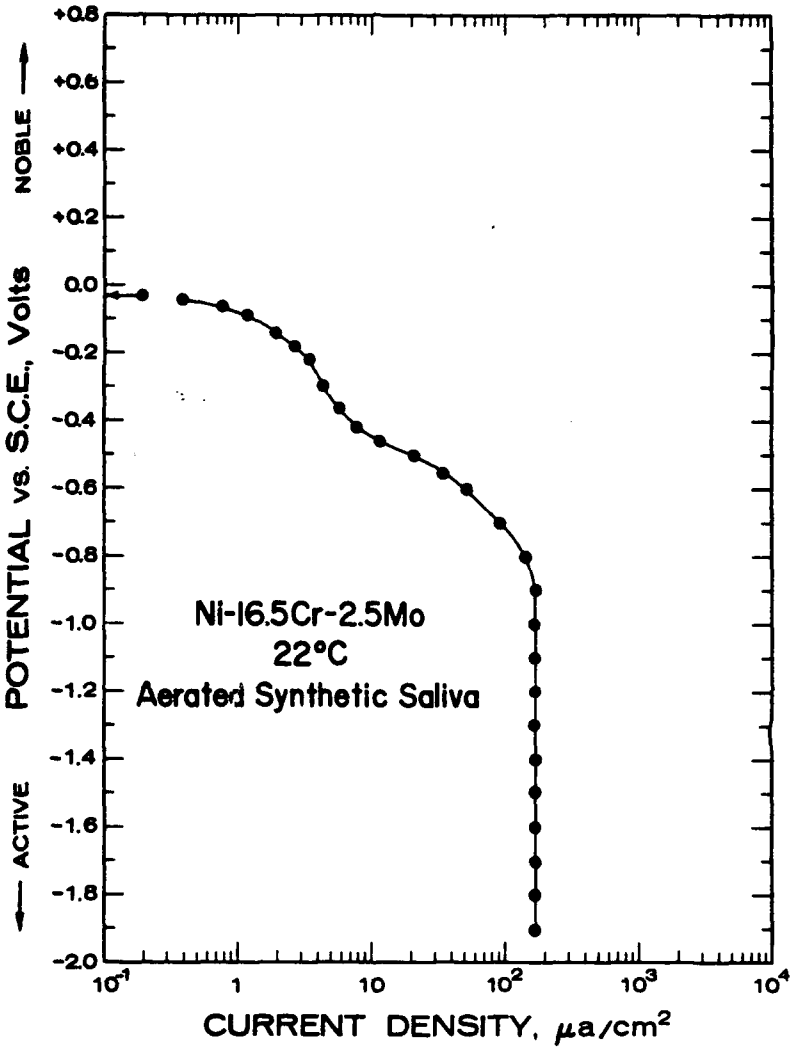

Figure 42. Potentiostatic Cathodic Polarization Curve for Ni-16.5Cr-2.5Mo Dental Alloy in Aerated Synthetic Saliva at 22°C.

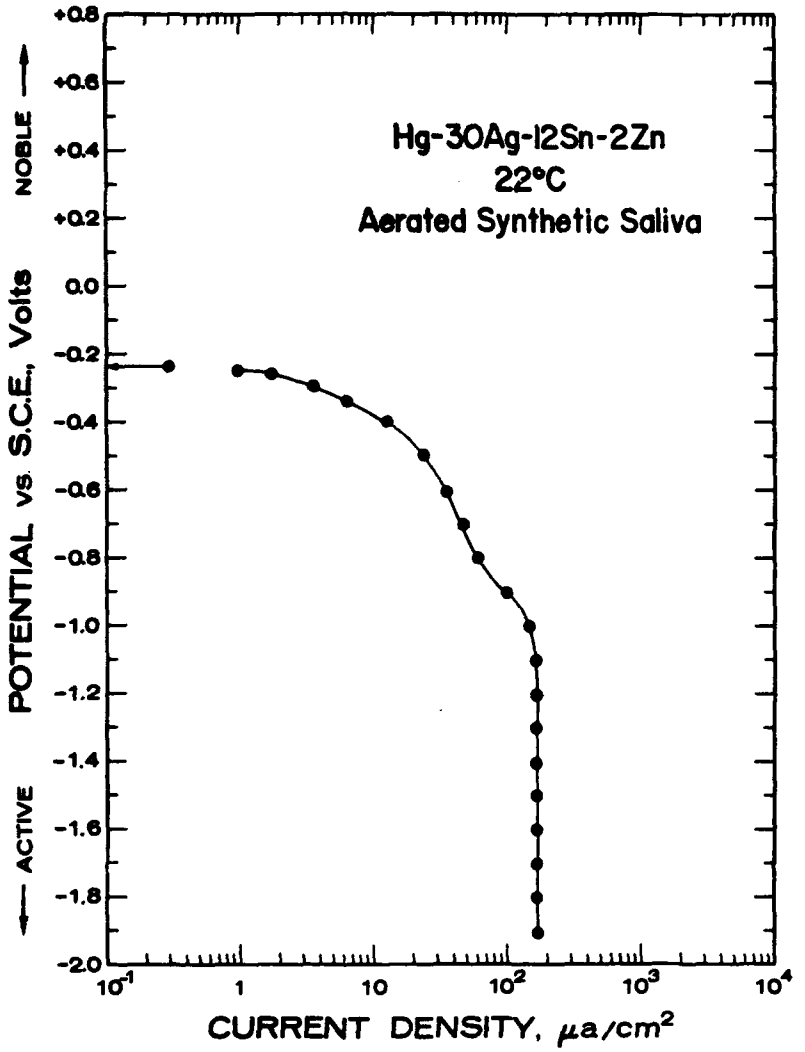

Figure 43. Potentiostatic Cathodic Polarization Curve for Hg-30Ag-12Sn-2Zn Dental Alloy in Aerated Synthetic Saliva at 22°C.

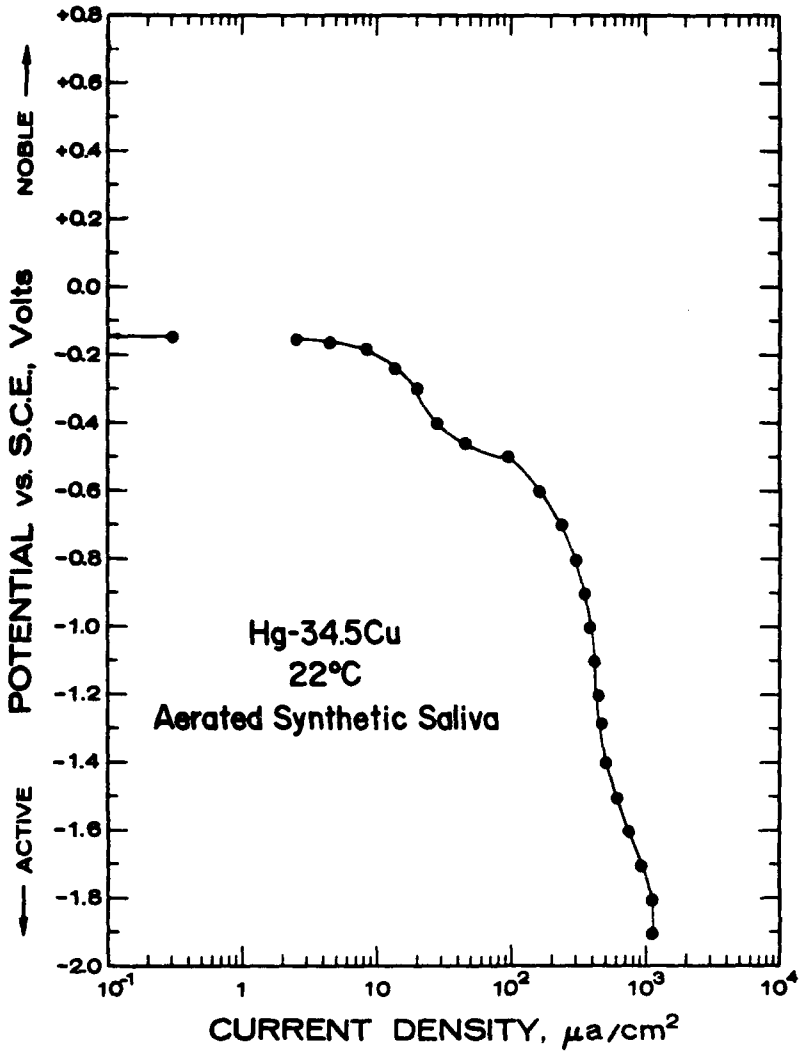

Figure 44. Potentiostatic Cathodic Polarization Curve for Hg-34.5Cu Dental Alloy in Aerated Synthetic Saliva at 22°C.

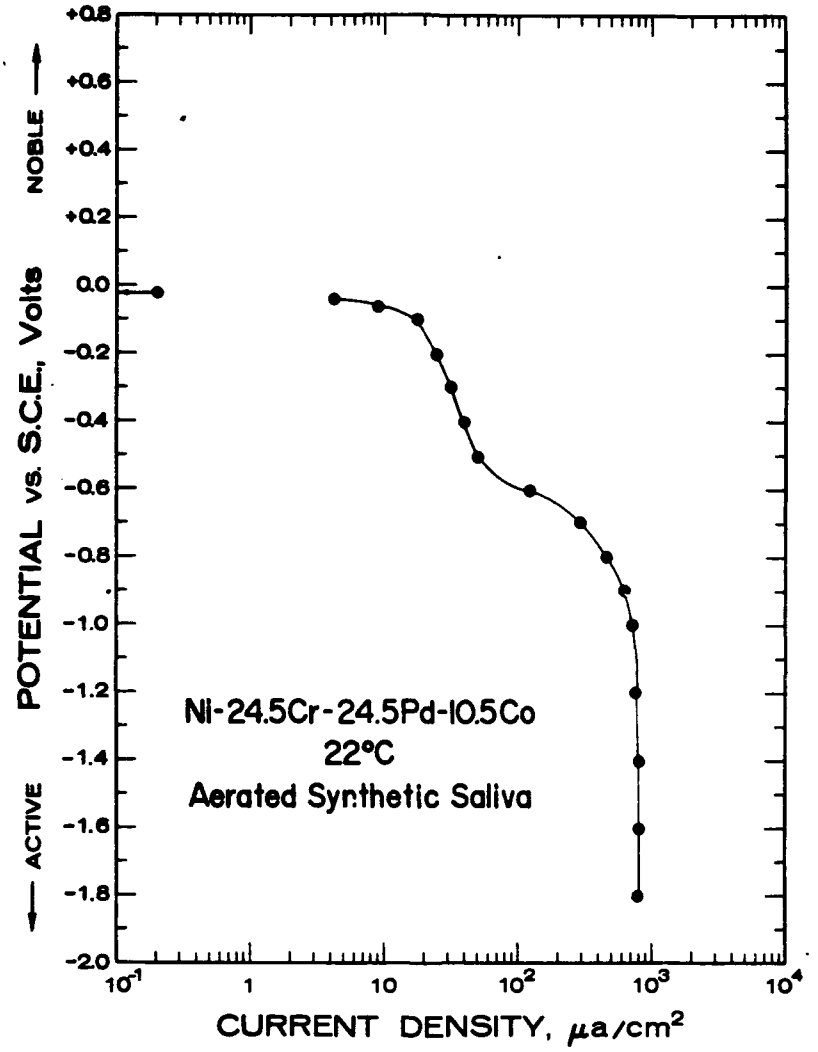

Figure 45. Potentiostatic Cathodic Polarization Curve for Ni-24.5Cr-24.5Pd-10.5Co Dental Alloy in Aerated Synthetic Saliva at 22°C.

is not possible for specimens that are positioned with their surfaces in a horizontal plane). Although the low corrosion rates of these dental alloys did not yield large accumulations of corrosion products; there was some evidence at the higher current densities of tarnish and drop-off of corrosion products for each of the specimens tested.

The anodic polarization curves exhibited distinct active regions, but passive and transpassive regions were not observed. A constant (limiting) current density was obtained for each specimen; there was no tendency for increases in current density even when the potential was increased to the limit of the potentiostat (+5.4 volts). This limiting current density may be attributed to a concentration build-up of OH ions at the cathode, thus preventing diffusion of O_2 to cathode surface. Tafel behavior for anodic dissolution (linear dependence of the logarithm of current density with applied potential) was observed for all specimens; however, this behavior was usually limited to a current-density range of one decade. The Tafel slopes for anodic dissolution (βa) varied from 0.035 to 0.085 volt/decade (Table VI). These Tafel slopes were used in the Stern-Geary relationship (equation 2) along with linear-polarization data to obtain the corrosion rates in Table V.

The basic alloying element of each of the alloys seemed to determine the general shape of the polarization curve. It was observed that there was a great similarity in the shapes of the anodic polarization curves of the two gold alloys.

Table VI

Tafel Slopes for Anodic Dissolution of Six Dental Alloys in Aerated Synthetic Saliva at 22°C

Type of Dental Alloy and Composition	Tafel Slope(βa), volts/decade
Dental Gold, Au-13Ag-9Cu	0.065
Dental Gold, Au-5Pd-1Ag	0.070
Dental Ag-Sn Amalgam, Hg-30Ag-12Sn-2Zn	0.080
Dental Copper Amalgam, Hg-34.5Cu	0.085
Dental Casting Alloy, Ni-16.5Cr-2.5Mo	0.035
Casting Alloy, Ni-24.5Cr-24.5Pd-10.5Mo	0.035

Likewise, the two amalgams had similar curves as did the two nickel-base alloys.

Cathodic polarization curves for the six dental alloys studied are given in Figures 40 thru 45. These cathodic polarization curves did not exhibit Tafel regions, even after repeated attempts. However, each specimen did reach a limiting current density. This was expected in the aerated electrolyte. The absence of Tafel behavior was also expected since the corrosion process in aerated solutions is usually under concentration polarization control[5]. Thus, a value of infinity was used for β_c and the modified Stern-Geary relationship (equation 2) was used for the corrosion-rate calculations[10].

Again, for the cathodic polarization curves, the major element in each alloy seemed to determine the general shape of the curve.

V. Conclusions and Recommendations

Conclusions

Using the results of this investigation on the corrosion characteristics of six dental alloys in aerated synthetic saliva, it can be concluded:

1. Steady-state corrosion rates were obtained within 48 to 96 hours.

2. All steady-state corrosion rates were exceptionally low: ranging from approximately 4 to 200 microns/yr. The gold alloys had the lowest corrosion rates, the amalgams had the highest.

3. As the smoothness of the surface finish increased, the corrosion rates decreased (i.e., alloys whose surfaces were finished with dental pumice and tin-oxide had lower corrosion rates than the same alloy whose surface was finished with 4/0 emery paper). The alloys whose corrosion rates showed the greatest dependence on surface finish were the amalgams.

4. The steady-state corrosion rate of 200.3 microns/yr for the Ag-Sn amalgam compared favorably with results of other investigators. However, this corrosion rate is higher than could be tolerated in dental applications and is probably not representative due to the inability to simulate the high resistance of the external corrosion circuit in the oral cavity.

5. Comparison of the calculated corrosion-current densities with those obtained from the generalized curves

of Stern and Weisert[11] showed excellent agreement for all alloys investigated.

6. In general, the linear-polarization technique was found to be an accurate and relatively fast method of predicting low corrosion rates.

7. Complete anodic polarization curves did not exhibit passive behavior; instead, each reached a constant (limiting) current density to the potential limit of the potentiostat (+5.4 volts). Each alloy exhibited Tafel behavior for anodic dissolution. Tafel slopes ranged from 0.035 to 0.085 volt/decade.

8. Complete cathodic polarization curves exhibited the effect of concentration polarization. Limiting current densities were obtained without cathodic Tafel behavior.

Recommendations

It is recommended that the following areas be considered for further study:

1. Further investigations of the corrosion characteristics of dental materials should be made with more realistic simulation of the external-circuit resistance found in the oral cavity.

2. Investigation of the localized corrosion rates in crevices at the tooth-alloy interface should be more meaningful than general corrosion rates; however, design and instrumentation of electrochemical apparatus could make this a difficult undertaking.

3. An investigation of corrosion rates of dental restorations *in vivo* would be of wide interest. These results would probably be more meaningful than those obtained in the laboratory. The linear-polarization technique has demonstrated that it can be adapted to *in vivo* investigations[15,16].

Bibliography

1. Skinner, E. W. and R. W. Phillips. The Science of Dental Materials (5th Edition). Philadelphia: W. B. Saunders Co., 1960.

2. Ross, T. K., et al. "A Potentiostatic Study of the Corrosion of Dental Silver-Tin Amalgam." Corrosion Science, 7: 373-376 (1967).

3. Jenkins, G. N. The Physiology of the Mouth. Oxford: Blackwell Co., 1961.

4. Stern, M. and A. L. Geary. "Electrochemical Polarization, I. A Theoretical Analysis of the Shape of Polarization Curves." Journal of the Electrochemical Society, 104: 56-63 (1957).

5. Fontana, M. G. and N. D. Greene. Corrosion Engineering. New York: McGraw-Hill Book Co., 1967.

6. Uhlig, H. H. Corrosion and Corrosion Control. New York: John Wiley and Sons, Inc., 1963.

7. Mottern, M. M. and J. R. Myers. "Polarization of Iron-Cobalt Alloys in Sulfuric Acid Solutions." Corrosion, 24: 197-205 (1968).

8. Haugen, W. J. An Evaluation of Corrosion Characteristics Utilizing the Linear-Polarization Technique. Unpublished Thesis, Wright-Patterson Air Force Base, Ohio: Air Force Institute of Technology, June 1970.

9. Steigerwald, R. F. "Electrochemistry of Corrosion." Corrosion, 24: 1-10 (1968).

10. Stern, M. "A Method for Determining the Corrosion Rates from Linear Polarization Data." Corrosion, 14: 440t-444t (1958).

11. Stern, M. and E. D. Weisert. "Experimental Observations on the Relation Between Polarization Resistance and the Corrosion Rate." Proceedings of the American Society for Testing Materials, 59: 1280-1291 (1959).

12. Roydhouse, R. H. Materials in Dentistry. Chicago: Year Book Medical Publishers, Inc., 1962.

13. Jones, D. A. and N. D. Greene. "Electrochemical Measurements of Low Corrosion Rates." Corrosion, 22: 198-205 (1966).

14. Legault, R. A. and M. S. Walker. "Linear Polarization Measurements in the Study of Corrosion Inhibition." Corrosion, 19: 222t-226t (1963).

15. Greene, N. D. and D. A. Jones. Corrosion of Surgical Implants, Paper A presented at ASTM-ASM Medical Materials Symposium, Detroit, Michigan, October 19, 1965.

16. Collangelo, V. J. et al. Corrosion Rate Measurements in Vivo, Paper presented at the National Association of Corrosion Engineers meeting, Los Angeles, California, 1967.

17. Smulczenski, L. A. Polarization Behavior of Ni-Cr-Al and Ni-Cr-Ti Alloys in Sufuric Acid. Unpublished Thesis, Wright-Patterson Air Force Base, Ohio: Air Force Institute of Technology, June 1968.

18. Kortum, G. and J. Bockris. Textbook of Electrochemistry. Amsterdam: Elsevier Publishing Co., 1951.

19. Barnartt, S. "Magnitude of IR Drop Corrections in Electrode Polarization Measurements Made with a Luggin-Haber Capillary." Journal of the Electrochemical Society, 108: 102-104 (1961).

20. Eisenberg, M. C. W. Tobias, and C. R. Wilke. "Application of Backside Capillaries in the Measurement of Non-Uniform Polarization." Journal of Electrochemical Society, 102: 415-419 (1955).

21. Myers, J. R., E. G. Gruenler, and L. A. Smulczenski. "Improved Working Electrode Assembly for Electrochemical Measurements." Corrosion, 24: 352-353 (1968).

22. Hansen, M. Constitution of Binary Alloys. New York: McGraw-Hill Book Co., 1958.

23. Crowell, Walter S. "Gold Alloys in Dentistry" Metals Handbook (8th Edition, Vol. 1). Metals Park, Ohio: American Society for Metals, 1961.

24. Guthrow, C. E., L. B. Johnson, and K. R. Lawless. "Corrosion of Dental Amalgam and its Component Phases." Journal of Dental Research, 46: 1372-1381 (1967).

Appendix A

Development of Computer Program for Determining Corrosion Rates from Linear-Polarization Data

This appendix contains the development, symbology, and discussion of the computer program which was used to determine the corrosion-current densities (i_{corr}) and corrosion rates of the alloys investigated. The program is general, and can be used for any alloy containing up to 6 elemental components. The program utilizes the polarization resistance ($\Delta E/\Delta i$) taken from a linear-polarization curve, the Stern-Geary relationship (in either its original or modified form), and Faraday's law (with necessary conversion factors) to calculate i_{corr} in ma/cm^2 and corrosion rates in microns/yr and mils/yr.

The following symbols were used for the inputs and variables used in the computer program (Figure A-1). Note that all variables are floating point:

W1 thru W6	Weight percent of elements in the alloy
DE	ΔE from linear-polarization in volts
DI	Δi from linear-polarization curve in amp/cm^2
BA	βa in volts/decade
BC	βc in volts/decade
TD1 thru TD6	Theoretical densities (gm/cm^3) of the elements in the alloy
N1 thru N6	Electrons transferred (valence number) in the oxidation of each metallic element

AW1 thru AW6 ..... Gram atomic weights (gms/gm atom) of elements in the alloy

SLOPE ..... $\Delta E/\Delta i$, ohm-cm^2

ICORR ..... i_{corr}, ma/cm^2

GMA1 thru GMA6 ..... Gram atoms of each element in the alloy

GMAT ..... Total gram atoms in the alloy

A1 thru A 6 ..... Atomic percent of elements in the alloy

EW1 thru EW6 ..... Equivalent weight (gms) of each element in the alloy

EWT ..... Equivalent weight of the alloy in gms

V1 thru V6 ..... Specific volume (cm^3/gm) of each element in the alloy

VT ..... Specific volume (cm^3/gm)of the alloy

DA ..... Density of the alloy (gm/cm^3)

C ..... Conversion factor used with Faraday's law to obtain corrosion rate in microns/yr

CR ..... Corrosion rate in microns/yr

CRM ..... Corrosion rate in mils/yr

The program with sample input and output data is on pages 89 thru 91 of this appendix. The format for the input data is as follows:

Card 1: Weight percents of elements in the alloy. Enter a value of 0.0 for elements that are not present.

Card 2: ΔE in volts, Δi in amps/cm^2, β_a in volt/decade, β_c in volt/decade. Enter value of 0.0 for β_c if concentration polarization is controlling the corrosion process.

Card 3: Theoretical densities of the elements in the alloy in gm/cm^3. Enter value of 1.0 for elements not present.

Card 4: Number of electrons (n) transferred (valence number) in the oxidation of each of the metallic elements in the alloy. Enter a value of 1.0 for elements not present.

Card 5: Gram atomic weights of each element in the alloy in gms/gm-atom. Enter a value of 1.0 for elements not present.

Information printed out is i_{corr} in ma/cm^2, corrosion rate in microns/yr and in mils/yr. The program with sample input and output data is on the remaining pages of this appendix.

```
C  C   CORROSION RATES FROM LINEAR POLARIZATION DATA
     1   READ,W1,W2,W3,W4,W5,W6
     2   READ,DE,D1,BA,BC
     3   READ,TD1,TD2,TD3,TD4,TD5,TD6
     4   READ,XN1,XN2,XN3,XN4,XN5,XN6
     5   READ,AW1,AW2,AW3,AW4,AW5,AW6
     6   FORMAT(1X,8HICORR = ,E10.4,2X,12HMA PER SQ CM)
     7   FORMAT(1X,17HCORROSION RATE = ,E10.4,2X,14HMICRONS PER YR)
     8   FORMAT(1X,17HCORROSION RATE = ,E10.4,2X,11HMILS PER YR)
         EWT=0.
         CRM=0.
         CR=0.
         C=0.
         SLOPE=0.
         SLOPE=DE/D1
         IF(BC-0.)10,10,2
     9   XICOR=((BA*BC)/(2.3*SLOPE*(BA+BC)))*1000.
         GO TO 11
    10   XICOR=(BA/(2.3*SLOPE))*1000.
    11   GMA1=W1/AW1
         GMA2=W2/AW2
         GMA3=W3/AW3
         GMA4=W4/AW4
         GMA5=W5/AW5
         GMA6=W6/AW6
    17   GMAT=GMA1+GMA2+GMA3+GMA4+GMA5+GMA6
         A1=(GMA1/GMAT)*100.
         A2=(GMA2/GMAT)*100.
         A3=(GMA3/GMAT)*100.
         A4=(GMA4/GMAT)*100.
         A5=(GMA5/GMAT)*100.
         A6=(GMA6/GMAT)*100.
```

Figure A-1. Computer Program for Calculating Corrosion Rates from Linear-Polarization Data

Reproduced from best available copy.

```
      EW1=(AW1*A1*.01)/XN1
      EW2=(AW2*A2*.01)/XN2
      EW3=(AW3*A3*.01)/XN3
      EW4=(AW4*A4*.01)/XN4
      EW5=(AW5*A5*.01)/XN5
      EW6=(AW6*A6*.01)/XN6
   31 EWT=EW1+EW2+EW3+EW4+EW5+EW6
      V1=(W1*.01)/TD1
      V2=(W2*.01)/TD2
      V3=(W3*.01)/TD3
      V4=(W4*.01)/TD4
      V5=(W5*.01)/TD5
      V6=(W6*.01)/TD6
      VT=V1+V2+V3+V4+V5+V6
      DA=1./VT
      C=(1350.*24.*365.)/965.
      CR=C*XICORRENT*(1./DA)
      CRR=CR*(0.1/2.54)
      PUNCH6,XICOR
      PUNCH7,CR
      PUNCH8,CRR
      STOP
      END

   78.0    13.25    4.29    1.01    0.    0.
   .010    .325-6    .065      0.
   19.3    10.5    8.65    12.0    1.    1.
   3.    1.    2.    1.    1.
   106.97    107.57    63.54    106.4    1.    1.

C  C  CORROSION RATES FROM LINEAR POLARIZATION DATA
 ICORR = 0.14706E-02  MA PER SQ CM
 CORROSION RATE = 0.33586E+02  MICRONS PER YR
 CORROSION RATE = 0.13220E+01  MILS PER YR
      STOP  END OF PROGRAM AT  STATEMENT 0043 + 00 LINES
```

Figure A-1. Computer Program for Calculating Corrosion Rates from Linear-Polarization Data (Continued)

Vita

Terry James Rickard was born on 29 August 1937 in Pontiac, Michigan, the son of Lawrence Charles and Virginia Ellen Rickard. In 1955 he graduated from Waterford Township High School, Waterford, Michigan and two years later enlisted in the USAF. After 8 years as a Military Public Health Specialist, he was accepted under the Airman Education and Commisioning Program for enrollment at Oklahoma State University, Stillwater, Oklahoma. He received a Bachelor of Science Degree in Mechanical Engineering (Aerospace Option) in 1966. That same year he was commissioned a Second Lieutenant in the USAF upon graduation from Officers Training School, Lackland AFB, Texas. Being assigned to Kelly AFB, Texas, he spent 3 years as a Project Engineer working with aircraft egress systems and aerial delivery equipment. In 1969 he was assigned to the Air Force Institute of Technology to pursue work toward a Master of Science Degree in Aerospace Engineering. He is a member of the Pi Tau Sigma and the American Society for Metals.

Permanent address: 3931 San Castle Blvd.
Lakeworth, Florida 33460

This thesis was typed by Mrs. Mary E. Batman